Third Annual Report for NSF EAR-0724958 entitled "Transformative Behavior of Water, Energy and Carbon in the Critical Zone: An Observatory to Quantify Linkages among Ecohydrology, Biogeochemistry, and Landscape Evolution" (Jemez-Santa Catalina CZO). August 31, 2013.

JRB-SCM CZO Team:

Principal investigators: Jon Chorover, Peter Troch, Paul Brooks, Jon Pelletier, Craig Rasmussen, Greg Barron-Gafford, David Breshears, Travis Huxman, Jennifer McIntosh, Thomas Meixner, Shirley Papuga, Marcel Schaap (University of Arizona). **Collaborators:** Enrique Vivoni (ASU), Marcy Litvak (UNM), Robert Parmenter (Valles Caldera National Preserve), Kathleen Lohse (ISU).

Postdoctoral scientists: Jason Field, Ciaran Harman, Adrian Harpold, Bhaskar Mitra, and Julia Perdrial.

Graduate Students (supported at least in part in fourth year of CZO): Kate Condon, Angelica Vazquez-Ortega, Ingo Heidbuechel, Jessica Driscoll, Kristine Nelson, Xavier Zapata-Rios, Courtney Porter, Clare Stielstra, Rebecca Lybrand, Caitlin Orem, Molly Holleran, Michael Pohlmann, David Huckle, Rachel Maxwell.

Data and Field Management Scientists: Matej Durcik, Nathan Abramson, Mark Losleben, Scott Compton, Betsy Schafer, Kate Condon.

Information included in the first, second and third annual reports are either not repeated or only briefly summarized here. The purpose of the current report is to provide an update on the more recent activities and findings during Year 4 of the Jemez-Santa Catalina CZO project.

1. Major Research and Education Activities. Project funding was initiated in September 2009. The UA portion of the CZO team, comprising 12 faculty, 4 postdoctoral scientists, 17 affiliated graduate students, two field technical staff, and a data management specialist, derive from five departments at the University of Arizona. This group meets weekly to discuss research and education progress toward building a CZO that has two observatory locations: The Jemez River Basin NM (JRB) and the Santa Catalina Mountains AZ (SCM).

We hypothesize that *effective energy and mass transfer* (EEMT, MJ m^{-2} y^{-1}) quantifies climatic forcing that shapes the co-evolution of vegetation, soils and landscapes in the critical zone (Rasmussen et al., 2010; Pelletier et al., 2013). Testing of this hypothesis occurs across EEMT gradients in the JRB-SCM CZO that also span granite, rhyolite and schist rock types. We expect that gradients in EEMT and lithology will predict key aspects of CZ structure formation from molecular to grain to pedon to watershed scales.

Rock types include granite and schist in SCM, and rhyolite in JRB. In the SCM, instrumented ZOBs have been installed at low (ca. 1100 m) intermediate (ca. 2100 m) and high (ca. 2400 m) elevations. In the JRB, a high elevation ZOB (ca. 3000 m) was instrumented in spring, summer and fall of 2010. Following the Las Conchas wildfire of June-July 2011 (for details see second year annual report), a fire-disturbed ZOB was installed in a similar (but burned) mixed conifer vegetation type (see third year annual report). Instrumentation across sites includes selected sites for Eddy flux towers, meteorological stations, precipitation collectors, soil moisture, potential and temperature probes, soil solution samplers, piezometers, flumes, pressure transducers and ISCO samplers. In June 2013, a second wildfire during the CZO grant period (Thompson Ridge Fire) burned intensely through a previously unburned portion of the

JRB CZO, including the "unburned" mixed conifer ZOB and flux tower sites, which were subjected to stand replacing wildfire. The burn perimeters pertaining to the Las Conchas and Thompson Ridge Fires are shown on a map of the complete Valles Caldera National Preserve (VCNP) in Figure 1.

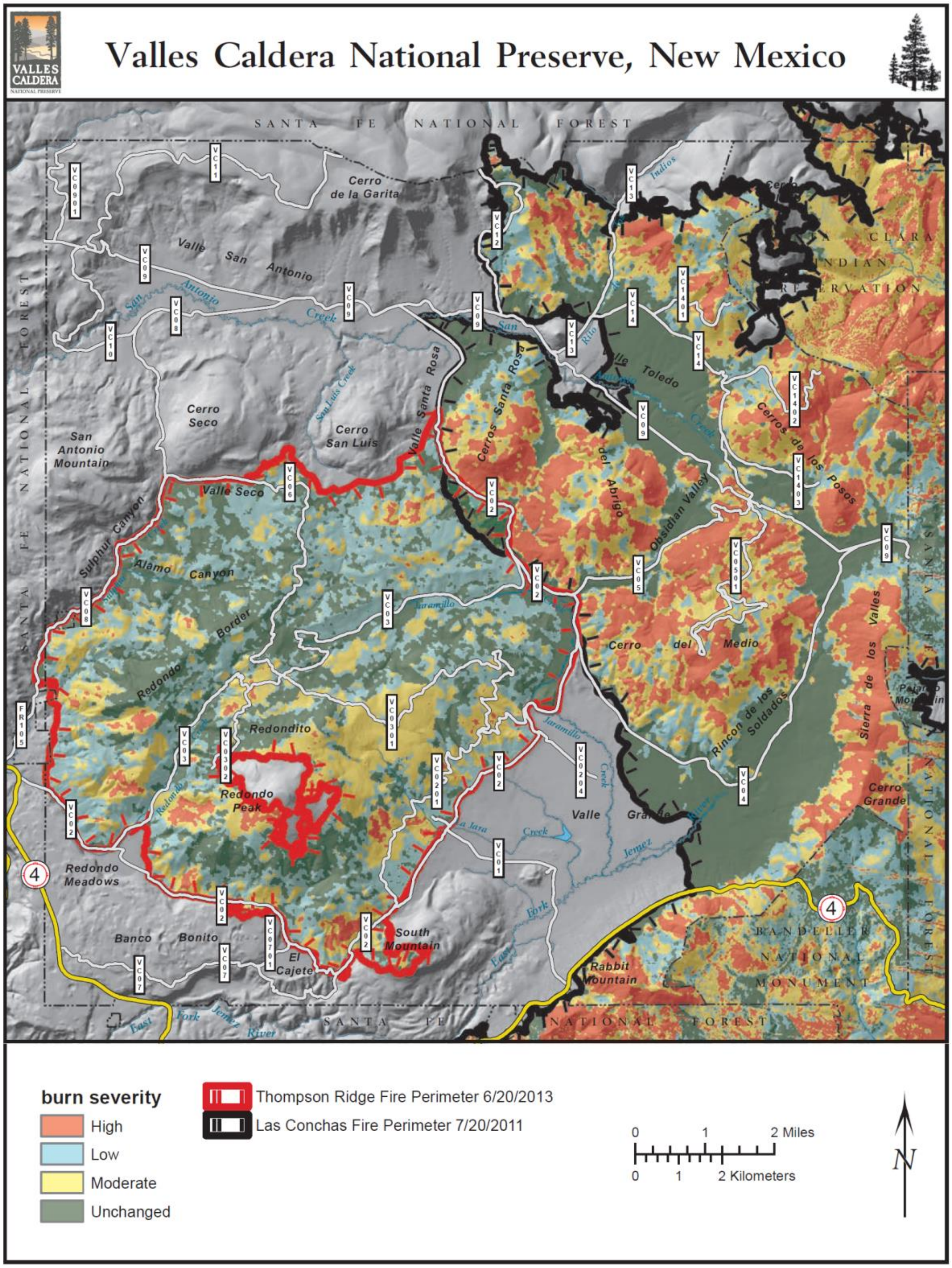

Figure 1. Burn severity map of VCNP showing both Las Conchas and Thompson Ridge Fire perimeters.

The Thompson Ridge fire of June 2013 burned ca. 24,000 acres, dominantly within the Valles Caldera National Preserve, which is the focal point of JRB CZO operations. As with the Las Conchas fire, ignition resulted from a tree collapsing into a power line, in this case in Sulfur Canyon. The fire burned up and over Thompson Ridge before ascending the western slope of Redondo Mountain, whereafter it progressed eastward to the boundary of the Las Conchas fire perimeter and the Valles Grande (Figure 1).

Soon after ignition, a crew of seven CZO and VCNP personnel extracted equipment from the MC ZOB and MC flux tower locations of the CZO prior to the area being burned severely (Figure 2). Direct effects of the fire on CZO infrastructure were nonetheless significant, since not all equipment could be removed from the site within the allowable time frame. In particular, repairs are underway in the MC ZOB and flux tower sites to get sensors and samplers back into functioning order, with replacements being made when necessary.

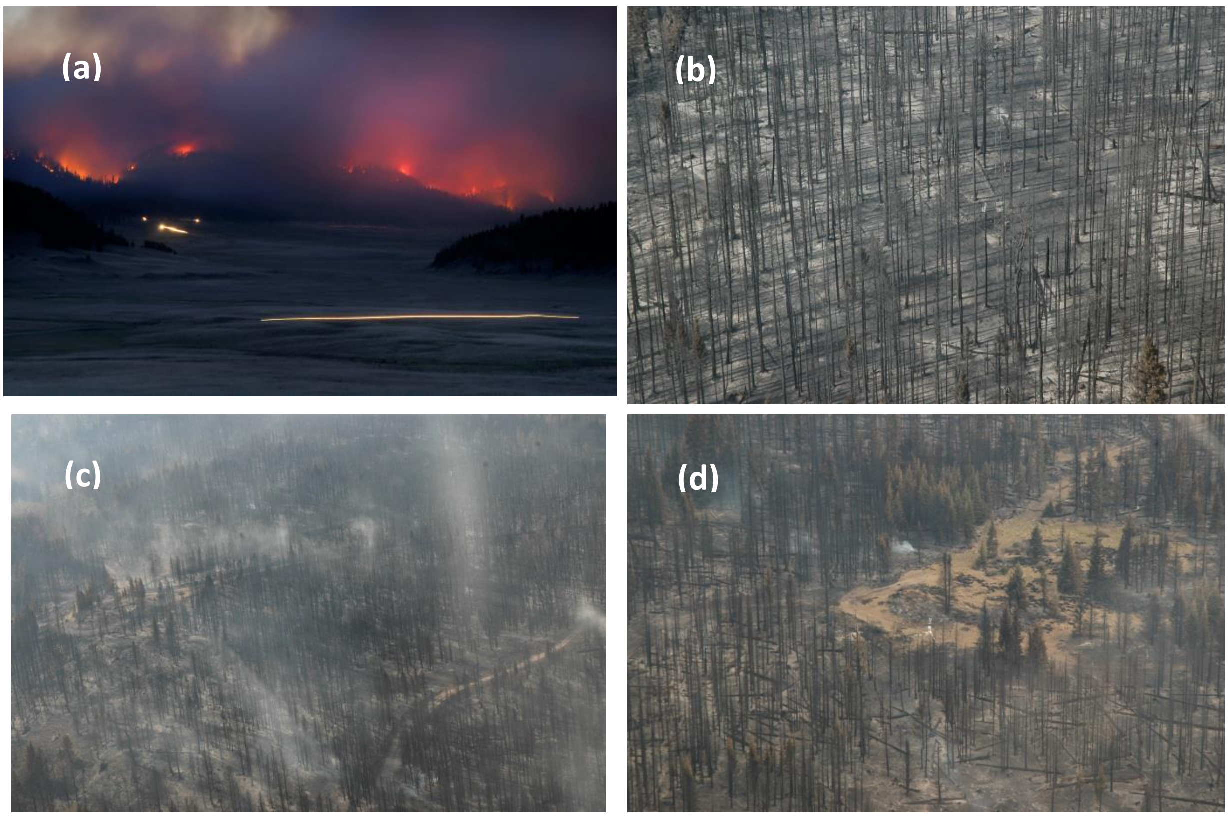

Figure 2. (a) Night view over VCNP 6-5-13, (b) JRB CZO Mixed Conifer Eddy Flux tower site 6-8-13 (c) Upper La Jara Drainage near the MC ZOB site 6-8-13, (d) Redondito Met station 6-8-13 (photos courtesy of Bob Parmenter, Science Director, VCNP).

New CZO infrastructure: Immediately following the burn, as soon as CZO personnel were permitted access, soil CO_2 and O_2 probes were installed at four depths in each of the six instrumented pedons in the MC ZOB to enable continuous monitoring soil gas concentrations, with a particular interest in capturing any postburn responses. Dust samplers were also installed in the MC ZOB to measure airborne translocation of material resulting from the disturbance.

2. Activities in each of the JRB-SCM Science Themes.

The JRB-SCM CZO is designed to quantify contemporary fluxes of energy, water, carbon and other solutes in the CZ in order to better predict long term CZ evolution and structure in semi-arid southwestern environments. Research is conducted in conjunction with the four, cross-cutting scientific "themes" of EHP, SSB, SWD and LSE.

1. ***Ecohydrology and Hydrologic Partitioning*** (EHP)
2. ***Subsurface Biogeochemistry*** (SSB)
3. ***Surface Water Dynamics*** (SWD)
4. ***Landscape Evolution*** (LSE)

Work in each of these themes proceeds through development of complementary research lines that probe common ground with a variety of disciplines and techniques. For example, while our LSE theme investigates how long term EEMT forcing of rock weathering and ecosystem change drives soil production and erosion over millennia, EHP, SSB and SWD also have the goal of quantifying contemporary rates of water-, carbon- and weathering-driven processes. Contemporary rates of carbon, water and weathering flux constrain an evolving LSE model that strives for a predictive understanding of long term effects on landscape evolution (Pelletier et al., 2013).

Nested locations within the larger CZO watershed (e.g., vegetation stands, hillslopes, ZOBs) represent narrow windows in geologic time and EEMT space. These are ideal locations for detailed studies of coupled processes as they occur at the current phase of CZ evolution. Coupled surface Earth processes are being probed through sensor and sampler installations. To expand the EEMT and geologic parameter space that might otherwise not be explored, we are focusing our installations on small basins that occur along a gradient in climate or disturbance (with/without recent fire). By focusing on ZOBs situated in a range of climates within a common larger river basin, we seek to (i) quantify climate effects on CZO process coupling (via collocation of measurements of EHP, SSB, SWD and LSE), and (ii) scale up process-level understanding to resolve the dynamics of catchment aggregates and larger watershed systems (e.g., Santa Cruz and Jemez River Basins). These river basins – that capture essential water resources for growing human populations in the Southwest and that are expected to become hotter and drier with climate change – are likely to be dramatically affected by up-gradient changes in climate forcing.

2.1 *Activities:* Ecohydrology and Hydrologic Partitioning (EHP) Theme

The EHP group works closely with the other thematic groups (LSE, SWD, SSB), via weekly meetings, to address the following **three hypotheses**:

Energy: Hydrologic partitioning is uniquely related to effective energy;

Water: Vegetation controls pedon-scale water transit time; geomorphology controls catchment-scale water transit time;

Carbon: Hydrologic partitioning and water transit time control NEE, DOC and DIC input to subsurface, and biogeochemical export in streamflow.

EHP research efforts are focused on **two overarching questions** that guide installations and observations.

(i) *How do* ***temporal changes in vegetation structure and activity (e.g., mortality, phenology, seasonality****) affect hydrologic partitioning and the resultant transfer of water and carbon to subsurface and streamflow?*

(ii) *How does spatial variability in **vegetation composition and structure** reflect or control patterns in **hydrologic partitioning** over the last 1 – 100 yrs?*

Major efforts during the current reporting year include continued operation of major hydrometeorological, ecohydrological, phenological, and eddy covariance observatory infrastructure; focused efforts designed to capture the ecohydrological response of CZ structure and function to the Las Conchas fire that burned in 2011; reinstrumentation and new observations to capture the ecohydrological response to the Thompson Ridge fire in 2013; and targeted field sampling campaigns.

Specific activities during the current project year include:

CZ Structure Measurements:

• **Climatic controls on tree mortality:** We explored the role of atmospheric drought, in terms of vapor pressure deficit, as well as soil moisture drought, in triggering tree mortality. We specifically evaluated how changes in VPD, not just associated changes in temperature, affect tree health and could exacerbate tree mortality and die-off. We developed a progression of relationships related to VPD (Breshears et al. 2013 in press – Frontiers in Plant Science*), evaluated relationships of pinyon pine mortality on the Jemez Mountains Pajarito Plateau and through a gradient farther south (Clifford et al. 2013 in press New Phytologist*), and in collaboration with colleagues in Australia used the SPA model to disaggregate the effects of warmer temperature vs. changes in VPD on tree health (Eamus et al. 2013, Ecology and Evolution). We also further evaluated how non-structural carbohydrate dynamics relate to tree mortality (Adams et al. 2013)

• **Continuous observations of vegetation dynamics:** Continued quality control and data processing on the CZO phenocams (16 total, with hourly images) and meteorological stations (6 total) in both JRB and SCM. This includes using MATLAB for obtaining snow depth and greenness indices from the phenocam images. Full meteorological datasets and metadata are provided on the CZO website for years 2010 – 2012. Data for year 2013 continues to be updated. Additionally, images have been archived on the UA CZO server. Development of metadata and preparation of greenness and snow data from phenocams for provision to CZO website. In Fall 2012, the ten phenocams in the burned area from the Las Conchas fire were removed to be repaired; only three of the cameras were recoverable. In Summer 2013, the three phenocams in the Jemez Mixed Conifer site were removed prior to the Thompson Ridge Fire. These six cameras were installed at the recovered meteorological stations in the newly burned Mixed Conifer ZOB (3 in the southeast aspect, 3 in the southwest aspect).

• **Vegetation Structure:** ALSM data from multiple flights were combined with ground survey to develop distributed above ground biomass maps in the JRB Valles Caldera sites.

• **Vegetation recovery following fire:** We are currently analyzing the phenocam images from the Las Conchas fire burned ZOBs to determine a method to quantify the understory growth in these ecosystems. Additional ground based surveys and TLS scanning in coordination with LSE theme are placing this continuous point observations in an explicit spatial context.

• **Near-ground-wind prediction:** We are assessing an approach for improving prediction of near ground wind patterns using hemispherical photography. We are assessing calibration data obtained with Kestrel portable weather stations placed in a field of solid objects with known volume. We have obtained equipment to install an array of microclimate measurements that include near-ground anemometers that will be used in association with further assessment to see if such data can aide in predictions around the footprints of our flux towers.

CZ Function Measurements:

• **Quantifying species-specific water use:** We installed a sap flow system within two mixed-conifer study sites of the Jemez River Basin – Santa Catalina Mountains Critical Zone Observatory (JRB – SCM CZO) to better understand the direct role of vegetation in modulating transpiration in these water limited systems. At both sites, we identified the dominant tree species and installed sap flow sensors on healthy representatives for each of those species. At the JRB CZO site, sap sensors were installed in fir (4) and spruce (4) trees; at the SCM CZO site, sap sensors were installed at white fir (4) and maple (4) and one dead tree.

• **Forest disturbance and snowpack partitioning:** Analyses were completed and results published from extensive snow surveys in paired burned and unburned forested catchments on Rabbit Mountain that quantified changes in net snow water inputs following fire. These are among the first direct observations of stand and watershed-scale snowpack processes following high-intensity fire. Specifically, we are testing two hypotheses with potentially competing effects on net snowpack accumulation in unburned and post-burned forests: (1) reduced interception losses result in greater inputs to the snowpack; and (2) increased winter-season ablation from the snowpack surface results in reduced peak accumulation.

• **Water transit time:** EHP coordinated closely with SWD colleagues to understand how spatial variability in catchment hydrologic residence times was related to climate, and subsequently plant available water. More detail can be found in SWD section.

• **Plant physiological controls on water and carbon flux:** We have conducted measures of leaf-level carbon and water flux with the overstory trees across the upper SCM CZO sites, including the Mt. Bigelow eddy covariance tower and Marshall Gulch Granite and Schist sites. Quantifying rates of photosynthetic carbon uptake and transpirational water loss within numerous species and across multiple seasons (1) yielded insights into the influence of community composition on seasonal NEE and ET dynamics and (2) aided in partitioning among vegetative and soil components of the vertical fluxes of water and carbon.

• **Integrating flux tower and physiological observations with predictive modeling:** We began seasonal measures of various parameters necessary in applying a widely used ecosystem model to the upper SCM CZO sites. This work represents our first efforts towards coupling plant ecophysiological measurements within a carbon-water model. Within all species, we quantified light use efficiency, light saturation point, carboxylation efficiency, rates of electron transport within the leaves, relative stomatal limitation to carbon uptake, leaf water potential, and water use efficiency. We will continue these measurements within the coming post-monsoon, fall, and winter seasons, and then we will begin parameterizing the SIPNET (Simple Photosynthesis Evapo-Transpiration) process-based model to boost performance in this snow and summer rain driven ecosystem. Ultimately, model development will enable us to (1) better estimate ecosystem fluxes in other upper elevation CZO sites that have climate forcing monitoring but lack eddy covariance measurements and (2) forward-cast ecosystem fluxes for these systems under various projected climate scenarios.

• **Physiological underpinnings of vegetation response to drought:** We quantified ecophysiological responses to moisture and temperature stress within the footprint of the Mt. Bigelow Eddy Covariance Tower. In measuring a series of key parameters indicative of carbon and water fluxes within the dominant species across pre-monsoon and monsoon conditions we were able to develop a broader understanding of what abiotic drivers are most restrictive to plant performance in this ecosystem. We completed a year-long effort to quantify these seasonal dynamics, drivers, and feedbacks of thermal sensitivity of the overstory. We hypothesize that (1) there is substantial interspecific variation within each ecosystem, which may buffer against short-term periods of anomalously cold or warm temperatures, (2) species at the more southern extent of their range are likely more sensitive to high temperatures than species more adapted to warmer conditions, and (3) monsoon moisture modulates these temperature constraints on productivity. Results were presented at the 2012 Annual Meeting of the American Geophysical Union by an NSF-funded Research Experiences for Undergraduates (REU) student. Now that a full annual cycle of measurements has been completed, a manuscript is in preparation.

• Integrating biotic and abiotic controls on carbon uptake: We analyzed several potential drivers of photosynthetic temperature sensitivity within the SCM Marshall Gulch sites, including differences in soil parent material, aspect, and seasonality within a suite of species. Each of these variables captures a different physical driver: (i) soil parent material (granite vs. schist) influences water holding capacity of the soil; (ii) aspect influences how incoming energy drives evaporative loss of soil water, creating warmer and drier environments on south/east faces; and (iii) seasonality captures temporal patterns of soil moisture recharge. We used leaf-level gas exchange measurements on 24 trees across a range of temperatures to quantify this plant temperature sensitivity during the dry pre-monsoon and wet monsoon seasons.

• **Understanding endogenous (e.g., aboveground carbon dynamics via photosynthesis) and exogenous (e.g., temperature and soil moisture) Controls on NEE:** We collected data on leaf-level photosynthesis (Asat) and soil respiration (Rsoil) in different microhabitats (under shrubs vs. bunchgrasses) lower elevation sites. We evaluated time-scales over which endogenous and exogenous factors control Rsoil by analyzing our data in the context of a semi-mechanistic temperature-response model of Rsoil that incorporated effects of antecedent exogenous (soil water) and endogenous (Asat) conditions.

• Seasonal controls on soil respiration: Our two year study evaluating the influence of snow cover duration on soil evaporation and respiration in the SCM mixed conifer ecosystem has been accepted for publication in the peer-reviewed journal Ecohydrology (Nelson et al., 2013). Influence of snow cover duration on soil evaporation and respiration efflux in mixed-conifer ecosystems. Krystine Nelson was a CZO funded graduate student and Grace John was an undergraduate student funded through the Biosphere 2 REU Program.

• **Cross-site comparison of controls on soil respiration:** We completed a two-year study to quantify the interactions between climate and soil type on soil respiration at sites in both the SCM and JRB. A manuscript led by CZO MS student and recent graduate Stielstra is in review at Biogeochemistry.

• **Integrated carbon balance in catchment-ecosystems:** We quantified current C fluxes (net ecosystem exchange [NEE] and dissolved & particulate stream and ground water fluxes) and pools (above and below ground biomass, [AGB, BGB], soil C) in three catchments of the Jemez River Basin Critical Zone Observatory.

• **Critical zone goods and services:** We began to consider how our findings can be integrated into a framework for Critical Zone Goods and Services. We are building on recently developed frameworks (Breshears et al. 2011, Ambio; Lopez-Hoffman et al. 2010, Frontiers in Ecology and the Environment) specific to ecosystem goods and services and are considering how and in what ways are Critical Zone Goods and Services similar to or different from ecosystem goods and services, and integrating these insights into how they are impacted by disturbance such as die-off and wildfire.

2.2 *Activities:* Subsurface Biogeochemistry (SSB) Theme

The SSB group works closely with the other thematic groups via weekly meetings to address the following **three hypotheses**:

Energy: Mineral weathering rate/transformation increases with EEMT resulting in concurrent changes in soil C stabilization.

Water: Ratio of inorganic carbon to organic carbon flux increases with increasing water transit time.

Carbon: Wet/dry cycles promote CO_2 production, enhancing mineral weathering and thereby promoting greater soil C stabilization.

The SSB research efforts focus on **two overarching questions**:

(i) How does the critical zone partition total rock weathering into components of:
- *(a) chemical denudation (elemental mass loss at pedon/hillslope scales);*
- *(b) primary to secondary mineral transformation (element retention in thermodynamically stable forms).*

(ii) *In the subsurface, how is net ecosystem exchange partitioned into:*
- *(i) DOC/POC, DIC export;*
- *(ii) stable soil C pools;*
- *(iii) physical erosion of soil C.*

Specific activities during the current project year include:

- **Quantifying dynamics of rare earth elements and yttrium (REY) at a range of spatial scales in the JRB CZO** in order to: determine REY patterns and mass balances to quantify the relative contributions of biological weathering; identify mineral and organic phases controlling the transport and fate of REY in soils with topographically controlled variation in water and DOC fluxes; resolve depth dependent trends in Eu and Ce anomalies in soil profiles.

- **Soil solution time series:** Soil pore water was collected from ZOBs in the JRB and SCM using vacuum-imposed tension and passive capillary samplers on a weekly (SCM) to ca. biweekly (JRB) basis when available, and subjected to thorough isotopic and aqueous geochemical analysis.

- **Quantifying total catchment carbon budgets for watersheds surrounding Redondo Dome in the JRB.** This was accomplished by combining datasets from Eddy flux tower (net ecosystem exchange), catchment effluxes (DOC, DIC, POC), with quantification of soil and vegetation pools from sampling and LiDAR.

- **Measuring the influence of burn intensity and vegetation type on temporal dynamics of soil nitrogen pools and processes and microbial communities**.

- **Quantification and spatial modeling of soil physical and chemical properties in the JRB MC-ZOB.**

- **Quantification of bulk elemental chemistry and mineralogy and microscale weathering patterns of soils from convergent and divergent landscape positions from five ecosystems across the SCM gradient.**

- **Quantifying the physical distribution and mean residence time organic carbon across the various ecosystems and landscape positions in the SCM.**

- **High resolution spatial characterization of subsurface structure, mineralogy, and chemistry of the high elevation mixed conifer ZOB in the SCM.**

- **Uranium-series isotopes were analyzed on soil samples from ZOB soil pits 1,3,4, and 6 in order to investigate the behavior of U-series isotopes in the complex volcanic terrain of the VCNP.**

- **A sequential extraction experiment was performed on soil horizons from ZOB soil pits 1 and 3 to analysis U concentrations in different mineral phases.**

2.3 *Activities:* Surface Water Dynamics (SWD) Theme

The SWD group works closely with the other thematic groups (LSE, EHP, SSB), via weekly meetings, to address the following set of research questions as part of our CZO efforts:

(i) How does carbon and nutrient cycling vary as a function of EEMT, bedrock lithology, and water transit times?
(ii) How do chemical denudation rates vary as a function of EEMT, bedrock lithology, and water transit times?

Specific activities during the current project year include:

- **Stream water samples were collected at the seven flumes (where continuous discharge is measured) surrounding Redondo Peak and the newly installed burned catchment in the Valles Caldera Preserve on a daily to weekly basis during snowmelt, and bi-weekly to monthly during the summer, fall and winter.** Spring samples from each catchment, and longitudinal samples from La Jara and History Grove streams were collected periodically throughout the year. Grab samples of surface water were also collected from the outlet of the burned ZOB when flowing. Water samples were analyzed for major ion and trace metal chemistry, nutrients (N, P), stable isotopes (^{18}O, ^{2}H, ^{13}C), and rare earth elements. Carbon characteristics, including DOC, DIC, UVvis absorbance, and PARAFAC-quantified fluorescence spectra, were also analyzed. Select samples were analyzed for tritium. Particulate samples were preserved for analysis of POC, C/N ratios and stable isotopes (C, N).

• **Water samples were collected at La Jara springs and along La Jara stream during May snowmelt and November dry season in 2012.** Samples were analyzed for ($^{234}U/^{238}U$) of dissolved U.

• **Debris flows were analyzed for particulate C and N translocation.** Post-fire organic carbon and nitrogen fluxes in 4 ZOBs (~0.1 km2) and two larger catchments (~1.3 km2) were measured in debris fans resulting from the Las Conchas fire in the JRB CZO and compared to background fluxes from three, undisturbed catchments.

• **Rainfall samples were collected during the summer monsoons using two ISCO auto samplers at the Lower La Jara and lower Upper Jaramillo catchments.** In addition, rainfall chemistry and isotope samples were collected from six bulk samplers (3 with and 3 without mineral oil) in lower La Jara, Upper La Jara (MCZOB) and Upper Jaramillo.

• **ISCO autosamplers installed:** Two ISCO autosamplers were installed on South Spring in La Jara catchment and Upper Jaramillo spring in Upper Jaramillo catchment.

• **Post fire water quality analyses:** Following the Thompson Ridge fire in May-June 2013, grab samples from fire-impacted catchment outlets around Redondo Peak were collected as soon as our field personnel could gain access to the sites. An ISCO autosampler was installed on the East Fork of the Jemez River near the New Mexico EPSCOR continuous probes for comparison to capture the hydrograph during monsoon storm events draining the north and east sides of Redondo Peak and the Valles Grande. We are currently reinstalling ISCO autosamplers on the other catchments (e.g. La Jara, History Grove and Upper Jaramillo), and expect to reinstall the flumes that were destroyed by debri flows following the fire as soon as possible.

• **Stream water sample collections:** Grab samples were collected on a weekly basis from two ZOBs at high elevation (Marshall Gulch) and one ZOB at mid-elevation (Oracle Ridge) in the SCM CZO, starting in 2006 and 2011, respectively. Snowmelt samples were collected in snowmelt lysimeters in the two high elevation ZOBs during April-May, and rainfall samples were collected with and without mineral oil for isotopes and chemistry. Water samples were collected from the low elevation B2 Desert site when present (especially during monsoon rains). Water samples were analyzed for major and trace metal chemistry, rare earth elements, nutrients and water stable isotopes. Particulate samples were preserved for analysis of POC, C/N ratios and stable isotopes (C, N).

• **Measurement of emerging contaminant attenuation in the critical zone.** Discharge of the Summerhaven wastewater treatment plant by spray irrigation into the Oracle Ridge catchment enabled the measurement emerging contaminant attenuation during reactive transport through CZO soils.

• **Quantification of hydrograph-specific geochemistry:** Time-series samples were collected during several monsoon rainfall events at the outlet of Marshall Gulch catchment to measure colloidal and particulate organic carbon (filtered for variable sizes) and metal fluxes across the hydrograph.

2.4 *Activities:* Landscape Evolution (LSE) Theme

Students and faculty in the landscape evolution theme are currently focused primarily on quantifying flooding and erosion in fire-prone, semi-arid landscapes of the JRB. The LSE group also serves the other three themes. For example, PI Pelletier is working to quantify variations in regolith thickness above bedrock around Redondo Mountain in JRB using seismic refraction. The goal of the seismic work is to quantify and understand the topographic and climatic controls on regolith thickness, which, in turn, play a significant role in controlling water residence times and streamwater effluent chemistry.

Principal LSE theme activities in the fourth year of the CZO project included:

- **Quantifying how post-fire sediment yields are controlled by burn severity, slope and drainage area.** Student Caitlin Orem and PI Jon Pelletier are leading the effort to quantify the geomorphic effects of the Las Conchas (2011) and the Thompson Ridge (2013) fires. Caitlin has been monitoring erosion in non-fire affected regions and she has found that the amount of erosion that has occurred in one year following the fire is orders of magnitude larger than the "background" erosion rate of non-fire-affected catchments. This raises the possibility that the vast majority of all the erosion that occurs in forested landscapes occurs in the few years following a high severity fire. In 2013 she collected and analyzed 10Be cosmogenic samples from stream sediments. This work will enable Caitlin to place constraints on erosion rates over millennial time scales. Data collected and analyzed in previous years provided erosion rates in fire-affected and non-fire-affected drainage basins at time scales of ~1yr and ~ 106 yr.

- **Quantifying the export of C and N in fire-affected drainage basins.** As a compliment to the work of Orem and Pelletier, graduate student Kate Condon and Prof. Paul Brooks quantified post-fire organic carbon and nitrogen fluxes in four zobs (approximately 0.1 km2) and two larger catchments (approximately 1.3 km2) debris following the Las Conchas fire and compared these amounts to background fluxes from three, undisturbed catchments.

3. Findings in each of the JRB-SCM Science Themes.

3.1 *Findings*: Ecohydrology and Hydrologic Partitioning (EHP) Theme

• **Vegetation Dynamics and Trace Gas Exchange:** At the Fall 2012 AGU Meeting, we presented our two year study: Influence of understory greenness on trace gas and energy exchange in forested ecosystems (Jessica Swetish, Shirley A. Papuga, Marcy Litvak, Greg Barron-Gafford, and Bhaskar Mitra). Jessica Swetish was a CZO funded undergraduate student. In this study, using a combination of phenocam, eddy covariance, and remotely sensed satellite data we showed that in the JRB mixed conifer ecosystem: (1) the green up of the understory vegetation is tightly coupled with the carbon uptake, while the overstory is not and (2) the time series of NDVI is coupled with the overstory vegetation, while the understory is not. This suggests that the use of NDVI for understanding carbon dynamics in subalpine mixed conifer ecosystems may be problematic because it does not capture the understory vegetation dynamics. This work was also presented and awarded the 1st Place Student Poster at the Fall 2012 USA National Phenology Network (USA-NPN) & SW Region, American Society for Photogrammetry & Remote Sensing (SW-ASPRS) Sixth Annual Phenology Research and Observations of Southwest Ecosystems (PROSE) Symposium. This work is currently in preparation to be submitted for publication in Geophysical Research Letters.

• **Tree Species Effects on Transpiration Flux:** At the Fall 2012 AGU Meeting, we presented our two year study: Toward an improved understanding of the role of transpiration in critical zone dynamics (Bhaskar Mitra and Shirley A. Papuga). Understanding transpiration is critical for accurate assessment of catchment water balance and for understanding of the processes that govern the complex dynamics across critical zone. The interaction between transpiration and plant vegetation not only modulates soil water balance but also influences water transit time and hydrochemical flux - key factors in our understanding of how the critical evolves and responds. Unlike an eddy covariance system which provides only an integrated evapotranspiration flux from an ecosystem, a sap flow system can provide an estimate of the transpiration flux from the ecosystem. By isolating transpiration, the ecohydrological drivers of this major water loss from the critical zone can be identified. Still, the species composition of mixed-conifer ecosystems vary and the drivers of transpiration associated with each species are expected to be different. Therefore, accurate quantification of transpiration from a mixed-conifer requires knowledge of the unique transpiration dynamics of each of the tree species. In this study, we used sap flow systems within our two JRB-SCM CZO mixed-conifer study sites. Analysis of two years of sap flux rate shows that the environmental drivers of fir, spruce, and maple are different and also vary throughout the year. For JRB fir, during the snowmelt period, soil temperature was the primary control on the sap flux rate, while during the dry and monsoon periods the sap flux rate appeared to be sensitive only to net radiation. For JRB spruce, a combination of soil temperature and air temperature were the dominant drivers of sap flux rate during the snowmelt period while during the monsoon period, net radiation was the dominant driver. For SCM maple, during the dry period, soil moisture was the primary driver of the sap flux rate with the strength of the correlation with the soil moisture control on sap flux rate drastically dropping into the monsoon period. For SCM fir, soil moisture was a weak control on sap flux rate during the dry and monsoon periods. This study highlights the importance of species-specific information for understanding the role of transpiration in critical zone processes. Specifically, unique environmental drivers that vary throughout the year for different vegetation types complicate the assessment of both catchment-scale water and carbon balances and for understanding of the processes that govern the complex dynamics across the critical zone. Species-specific allometric equation for each species from the two aspects at Jemez is shown in Figure XX.

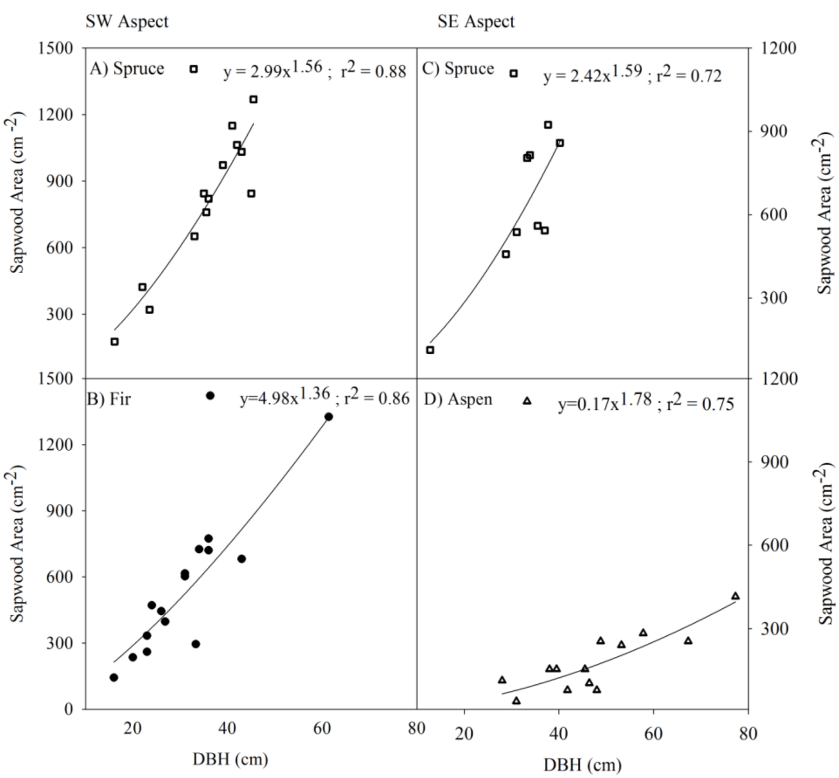

Figure 3. Stem diameter (DBH) versus sapwood area of the sampled tree species from the Jemez South East (SE) and Jemez south west (SW) aspects of the MCZOB. The tree species are collocated with the sap stations located at both the aspects.

• Integrated Carbon Balance in Catchment-Ecosystems:
Estimates revealed that study systems are dominated by gaseous fluxes (ranging from 3,200 to 3,900 kg ha^{-1} yr^{-1} over three years) with only small losses to streams as dissolved or particulate C (5 to 30 kg ha^{-1} yr^{-1}) or groundwater (1-6 kg ha^{-1} yr^{-1}) rendering these systems substantial sinks for atmospheric C. Estimates for biomass (20,000 – 240,000 kg ha^{-1}) and soil C (80.000 and 160.000 kg ha^{-1}) are comparable to stocks of similar soil and vegetation types (Lal 2005; North et al. 2009) and at current uptake rates only ~ 50-100 years are necessary for accumulation. Since old soil C accumulated over a longer period of time (10^2-10^3 yr), current uptake rates are either higher than in the past and/or disturbances reduced the stocks accumulated in the past. The effects of periodic disturbance due to logging and wildfire suggest that recurring wildfires strongly impact the C-balance of seasonally

snow-covered forests in the SW US leading to their oscillation between serving as sources versus sinks for atmospheric carbon.

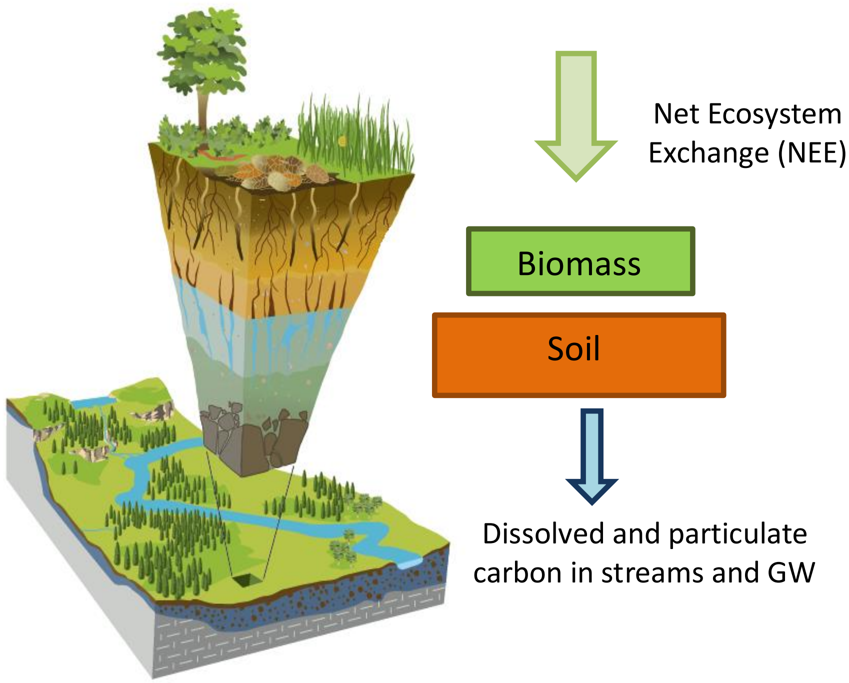

Figure 4. Annual NEE is negative and losses to streams and ground water are small. Biomass and soils constitute stocks for C.

• Physiological controls on carbon uptake: Preliminary results show that maximum photosynthetic rate was 51% higher during the monsoon than pre-monsoon season. Optimal photosynthetic temperature decreased 25% while the span of functional temperatures was 21% higher following the onset of monsoon rains. During the rainy season, soil parent material became an important factor. The greater water holding capacity of schist soils yielded greater maximum photosynthesis and reduced tree sensitivity to higher temperatures. More detailed analysis will allow us to examine the relative influence of each abiotic variable in driving this photosynthetic response, which impacts a suite of downgradient critical zone processes. An NSF-funded REU student will present these results at the 2013 Annual Meeting of the Society for the Advancement of Chicano and Native American Students (SACNAS) in October and at the 2013 Annual Meeting of the American Geophysical Union.

• **Endogenous and exogenous controls on components of NEE:** Across both microhabitats, antecedent soil water and antecedent Asat significantly affected Rsoil, but Rsoil under shrubs was more sensitive to Asat compared to under bunchgrasses. Photosynthetic rates one and three days prior to the Rsoil measurement were most important in determining current-day Rsoil under bunchgrasses and shrubs, respectively, indicating a significantly lag effect.

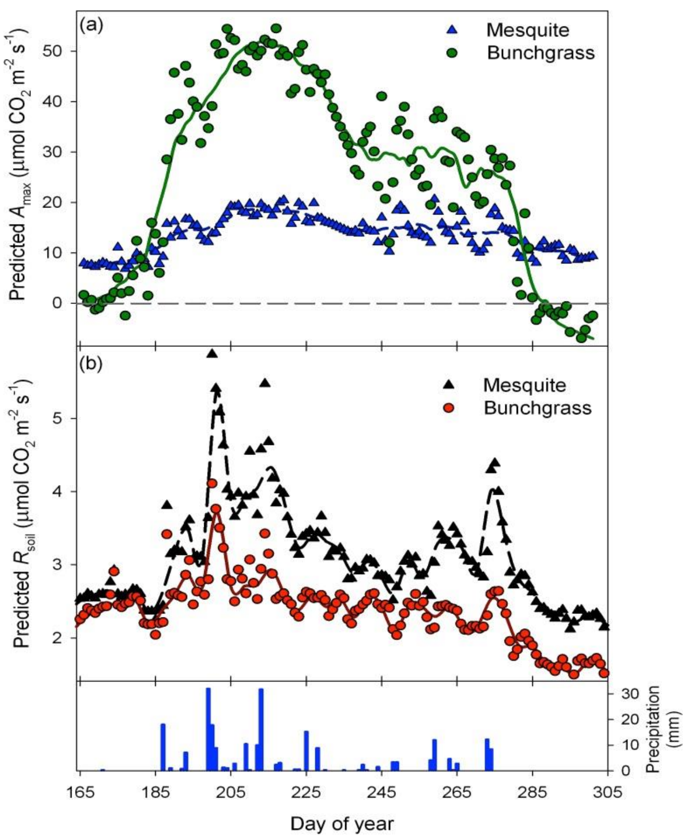

Figure 5. Precipitation sensitivity of plant carbon uptake (top) and soil respiration (bottom).

• **Fire and snow water partitioning**: Our work showed that despite increased new snowfall reaching the ground surface due to less interception in the burned forest, there was less water stored in the snowpack at peak accumulation (Fig. 6). These results suggest that increased winter season sublimation due to increases in radiation or turbulence compensated for reduced interception.

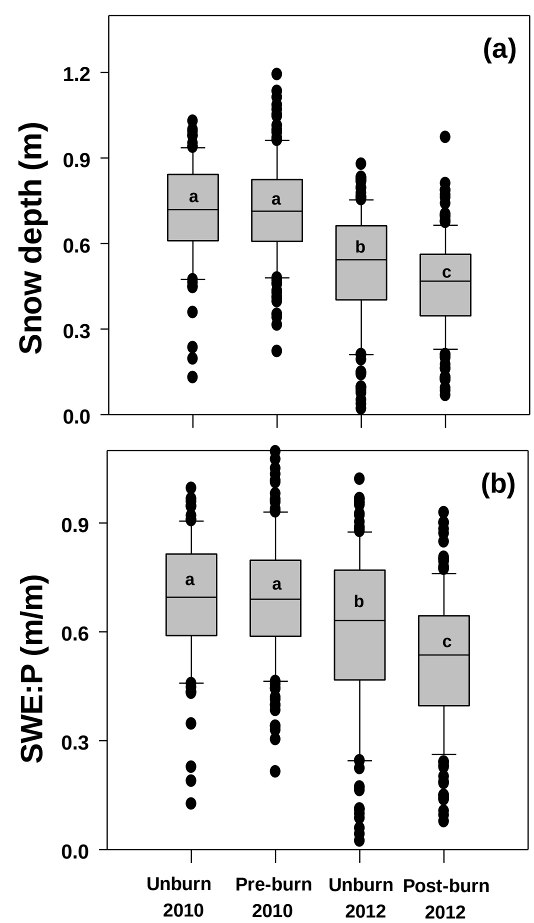

Figure 6. Snow surveys in 2012 demonstrate that the amount of snow depth (SWE is similar but not shown) and the fraction of winter precipitation in the snowpack at maximum accumulation are lower following fire, presumably due to increased sublimation from the snowpack surface once the canopy has been removed by fire.

• Cross-site comparison of soil respiration: Two years of distributed soil respiration measurements demonstrated that soil moisture was a stronger control on soil CO_2 fluxes than temperature in forested, seasonally snow covered sites in both SCM and JRB (Fig. 7). This was true both for winter and summer fluxes, and perhaps most interestingly, respiration rates were always higher in schist derived soils than granitic soils, presumably due to the greater water holding capacity of the fine grained schist soils that remained significantly wetter over the course of the study.

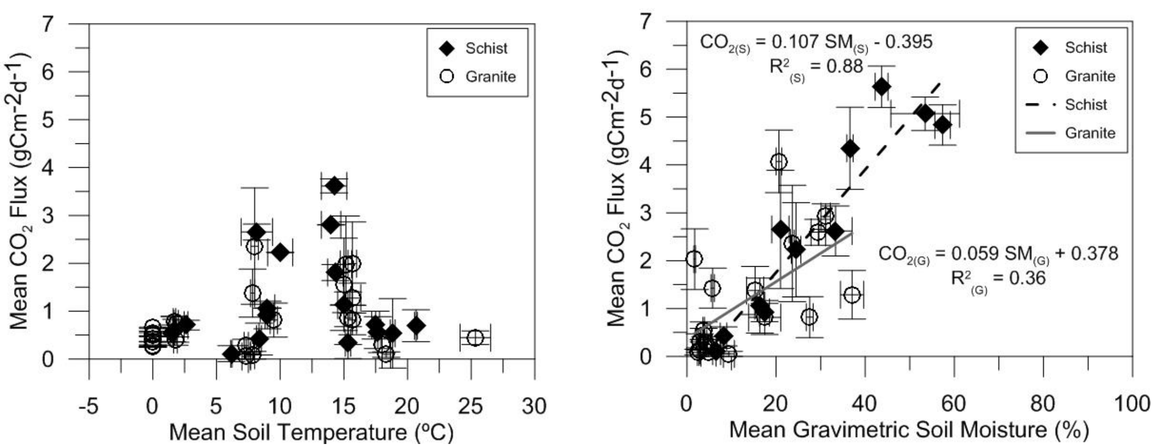

Figure 7. Relationships between CO_2 efflux and soil temperature (left) and soil moisture (right) demonstrate that respiration is primarily related to water availability even in high elevation forests of the Santa Catalina Mountains. Additionally, schist soils having higher water holding capacity and consequently higher soil carbon efflux than paired sites with granitic soils.

• Species-specific patterns of chlorophyll fluorescence drive phenology of function: At the Fall 2012 AGU Meeting, we presented our study: Species-specific and seasonal differences in chlorophyll fluorescence and photosynthetic light response among three evergreen species in a Madrean sky island mixed conifer forest (Daniel L. Potts, Rebecca L. Minor, Zev Braun, Greg A. Barron-Gafford). Zev Braun was an NSF-funded REU undergraduate student. In this study, we measured pre-dawn and light-adapted chlorophyll fluorescence as well as photosynthetic light response in southwestern white pine (*Pinus strobiformis*), ponderosa pine (*Pinus ponderosa*), and Douglas fir (*Pseudotsuga menziesii*) at the SCM Mt. Bigelow mixed conifer eddy covariance tower. Specifically, we quantified two parameters important in a plant's ability to dissipate excessive sunlight energy under periods of stress: photochemical quenching (qP), an indicator of the proportion of open PSII reaction centers, and non-photochemical quenching (qN), an indicator of heat dissipation ability. Non-photochemical quenching (NPQ) is induced under conditions when the photosynthetic apparatus cannot use all absorbed light energy for photochemistry, which can occur at quite low light intensity even under optimum conditions for photosynthesis. Stressful conditions, such as high light intensity, low internal CO_2 concentration due to drought, or low temperature, markedly promote NPQ. Therefore, the amount of NPQ is an indicator of stress severity. The qp values were greatest in *P. strobiformis* and smallest in *P. menziesiii*, and qp increased in response to monsoon rains. In contrast, qN was greatest in P. ponderosa and least in *P. menziesii*, but did not change in response to monsoon onset. These results suggest that *P. menziesii* were under the greatest stress during dry periods and that summer rains did not significantly ease this stress. Such patterns may reflect phenological differences or may be related to physiological trade-offs associated with cool- versus warm-season performance. In turn, these patterns may shape latitudinal and elevational range distributions of these species.

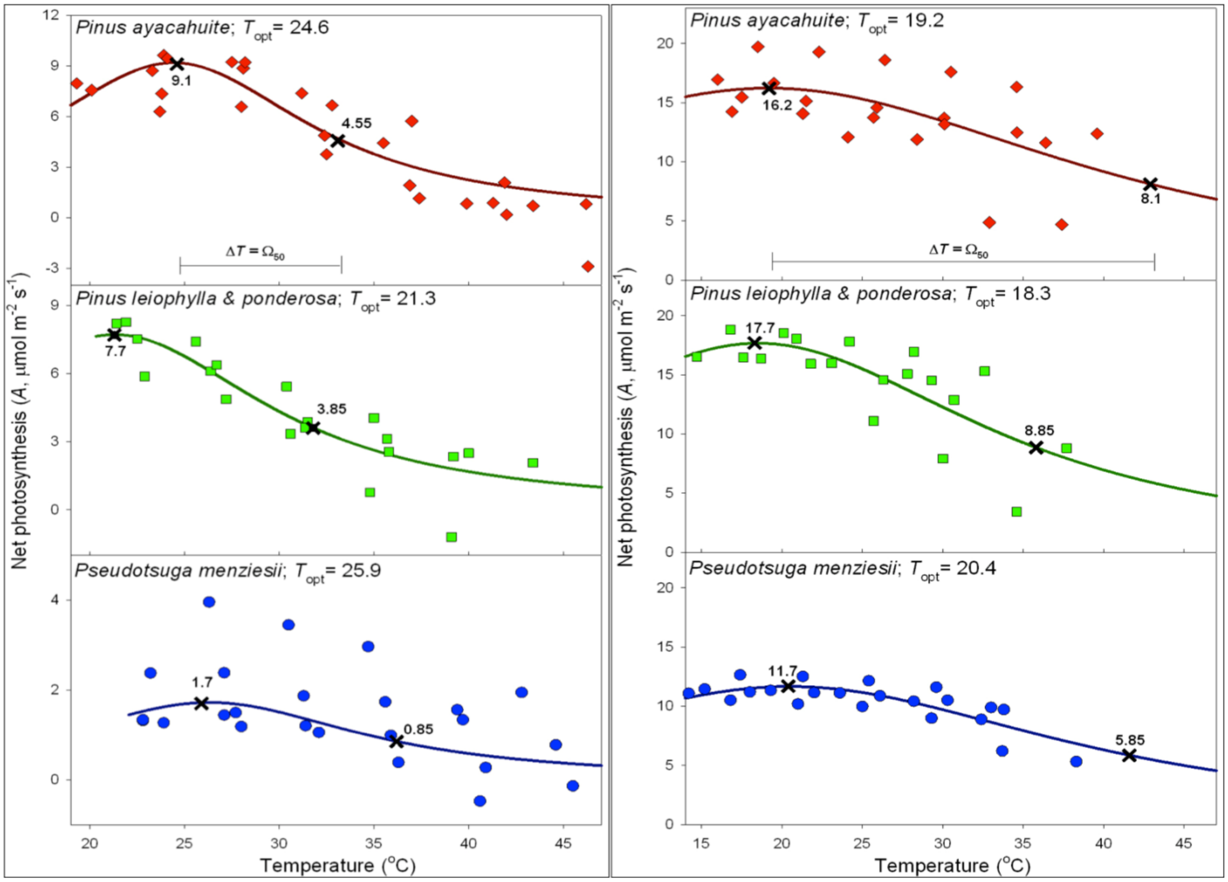

Figure 8. Species specific relationships between temperature and photosynthetic carbon uptake suggest marked differences associated in how major tree species will respond to both temperature and moisture variability.

Thermal constraints on vegetative carbon and water fluxes: At the Fall 2012 AGU Meeting, we presented our study: Quantifying thermal constraints on carbon and water fluxes in a mixed-conifer Sky Island ecosystem (Zev Braun, Rebecca L. Minor, Daniel L. Potts, Greg A. Barron-Gafford). Zev Braun was an NSF-funded REU undergraduate student. We quantified ecophysiological responses to moisture and temperature stress in ponderosa pine (*Pinus ponderosa*), southwestern white pine (*Pinus strobiformis*), and Douglas fir (*Pseudotsuga menziesii*) at the SCM Mt. Bigelow mixed conifer eddy covariance tower. In measuring a series of key parameters indicative of carbon and water fluxes within the dominant species across pre-monsoon and monsoon conditions we were able to develop a broader understanding of what abiotic drivers are most restrictive to plant performance in this ecosystem. Increased soil moisture from the summer monsoon positively influenced maximum photosynthetic rates (A_{max}) and reduced temperature sensitivities, but differentially so across the species (Fig. 8). In particular, wet conditions enhanced Amax most dramatically for *P. menziesii*, elevating photosynthesis by 590%. However, the range of temperatures across which a tree could conduct near-maximal photosynthesis grew most substantially (by 180%) for *P. ayacahuite*. Carbon sequestration decreased under high temperatures (>30°C) among all tree species, regardless of soil moisture status. Interspecific differences in temperature optima elucidated possible species dominance predictions for seasonal and gradual temperature changes, suggesting that *P. menziesii* may out-perform *P. ayacahuite* in the event that temperatures rise. However, if temperature increases are couple with reduced monsoon rains, *P. menziesii* may remain at subsistence levels of functioning.

3.2 *Findings*: Subsurface Biogeochemistry (SSB) Theme

• **Quantifying dynamics of rare earth elements and yttrium (REY) in the JRB MC-ZOB**: The objectives of this work were to: 1) employ REY mass balances and fractionation patterns to quantify the relative contributions of "biological weathering"; 2) identify mineral and organic phases that are controlling the transport and fate of REY in soils with topographically-induced variation in water and DOC fluxes; 3) resolve previously observed depth-dependent trends in europium and cerium anomalies. Results from objective 1 indicated significant relationships between the amount of reduced carbon fluxed in soil water and REY solution concentrations. In addition, the patterns of water, carbon and REY flux varied with landscape position, e.g., convergent versus planar landscape forms (Fig. 9).

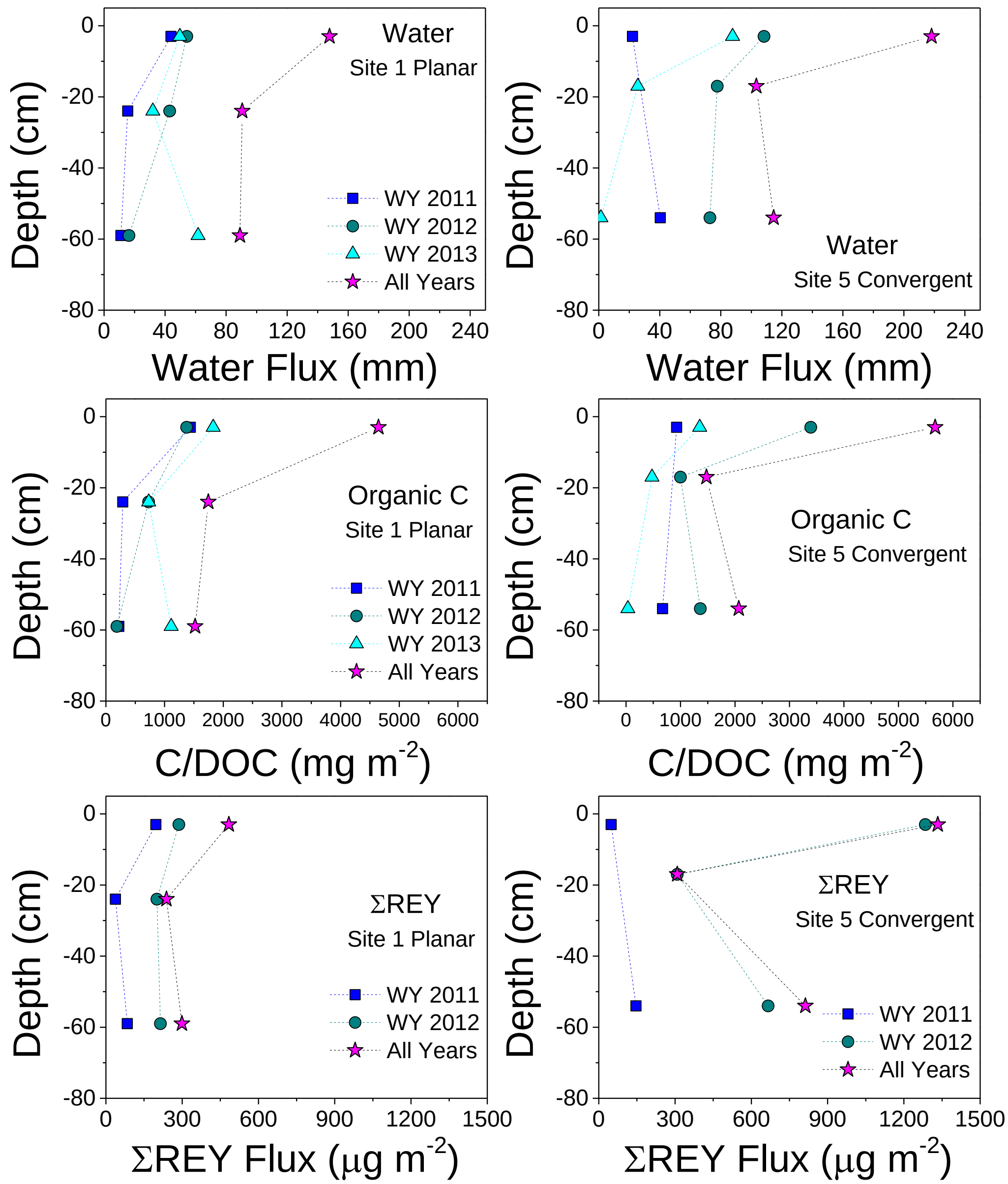

Figure 9. Data for planar and convergent landscape positions in the JRB MC-ZOB. Higher reduced organic carbon and water fluxes at depth in the convergent site were observed across all sampling dates over the water years

2011, 2012, and 2013 (only snowmelt period), resulting in higher REY transport (determined from ∑REY fluxes) relative to the planar site.

To address Objective 2 and a sequential chemical extraction procedure was employed to quantify the mass fraction of REY incorporated into soils as adsorbed (and exchangeable) species in planar and convergent landscape positions characterized by distinct water and reduced OC fluxes as well as for distinct bulk soil OC to elucidate the secondary weathering products that sequester REY. Results indicated an important role for both organo-metal complexes and short-range-order materials in sequestering REY. In particular the convergent location that is enriched in OC exhibited a much greater partitioning of REY into organo-metal complexes/colloids (Fig. 15).

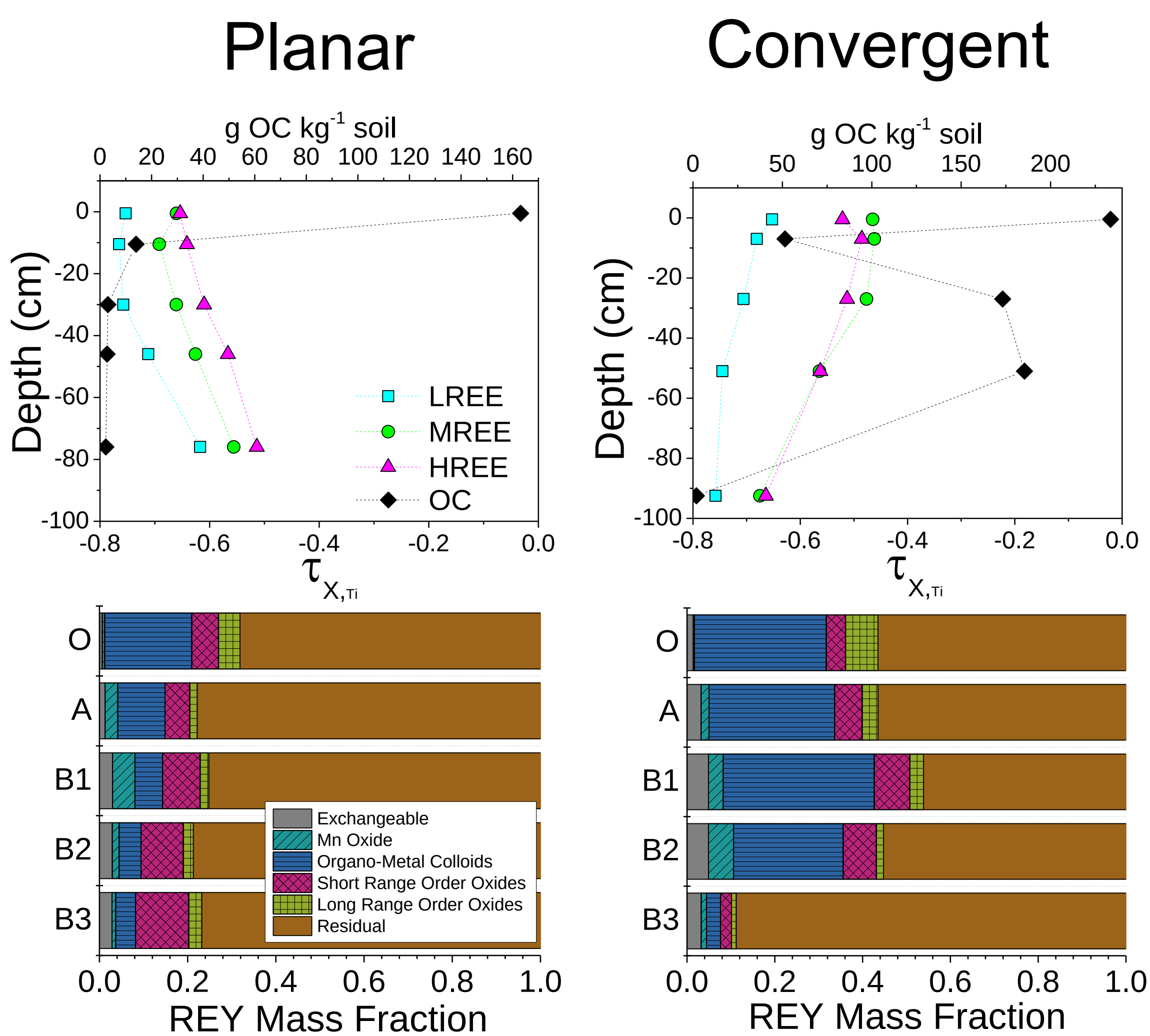

Figure 10. The depth distribution of bulk soil OC and relative depletion in REY as separated into light (LREE), medium (MREE), and heavy (HREE) components for a planar and convergent landscape position. Also shown is the relative partitioning of REY into exchangeable, Mn-oxide, organo-metal colloids, short-range order oxides, long-range order oxides, and residual materials.

Additionally, in the convergent profile it appears that greater abundance of OC and organo-metal complexes/colloids promotes greater REY fractionation; specifically, the LREE demonstrated greater depletion with depth than MREE or HREE.

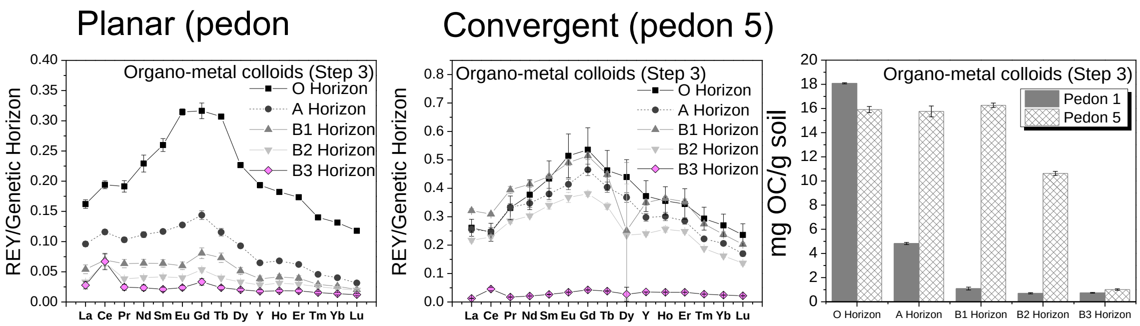

Figure 11. MREE downward concavity was observed in REY fractionation patterns in organo-metal complex/colloidal fraction. Preferential MREE transfers from primary to secondary phases. Apparent stability constants of REE with humic substance complexes induces preferential complexation with MREE.

● **Application of uranium isotopes to resolve weathering processes and soil age:** U-series trends in JRB MC ZOB soil profiles do not follow trends observed in typical weathering profiles. U-series results show evidence of potential mixing with volcanic ash and atmospheric dust sources. U-series isotopes in pedon 3 showed evidence U addition to soils from ^{234}U-enriched soilwater (Fig. 12). U-series models to calculate soil formation rates which assume uniform parent material and constant inputs of U-series isotopes over time were deemed inappropriate for application in the VCNP. Sequential extraction results show high U concentrations in exchangeable and organo-metal colloid mineral phases in Pit 3 in conjunction with enriched (^{234}U/^{238}U), supporting hypothesis of U addition to soils via adsorption to organic matter or U precipitation into Fe-oxyhydroxide minerals (Fig. 13).

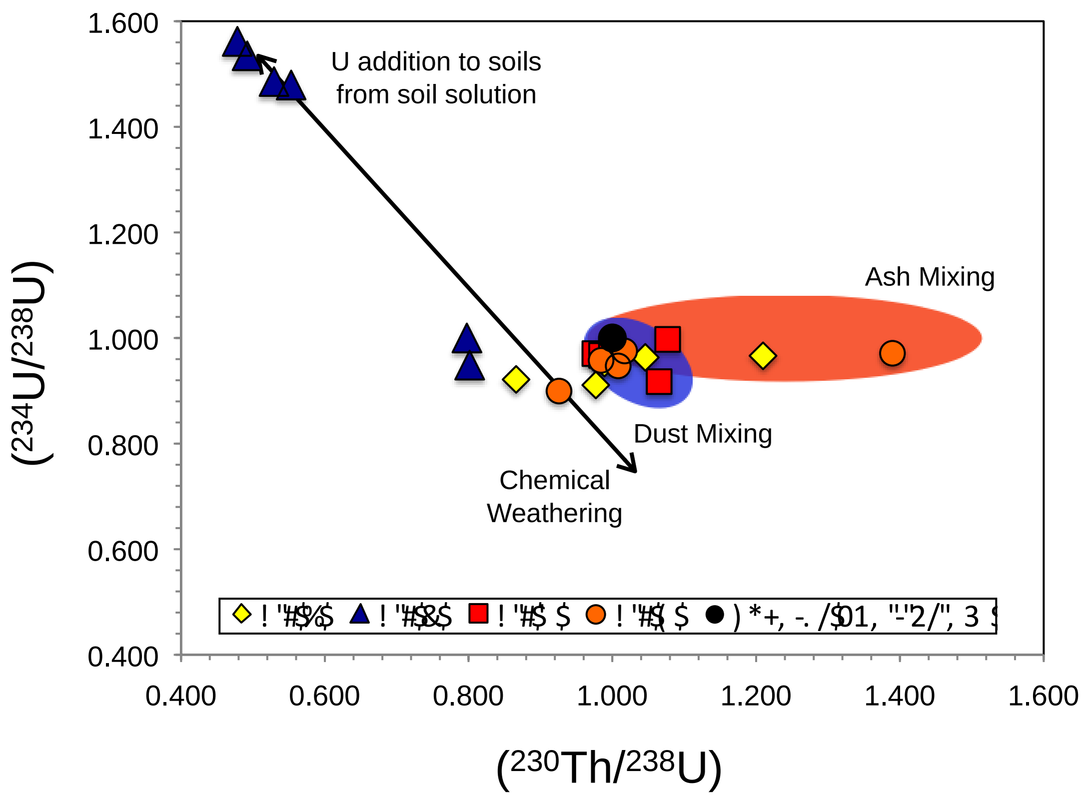

Figure 12. (^{230}Th/^{238}U) vs. (^{234}U/^{238}U) on ZOB soil samples. Enrichment in (^{230}Th/^{238}U) in conjunction with (^{234}U/^{238}U) close to unity was interpreted as evidence mixing with 230Th-enriched volcanic ash. Significant (^{234}U/^{238}U) enrichment in soils from Pit 3 was interpreted as evidence of U addition to soils from a ^{234}U-enriched soil solution.

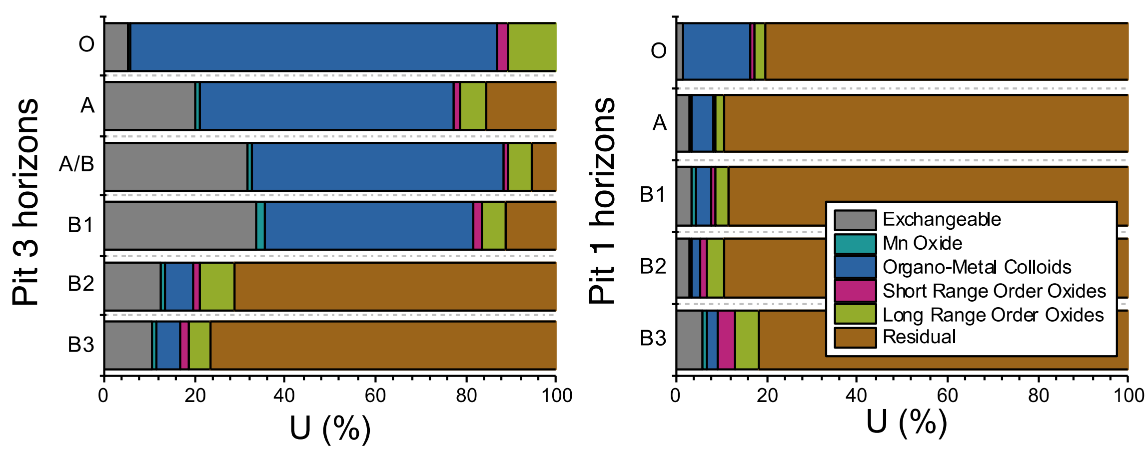

Figure 13. U mass balance from sequential extraction analysis on soil horizons from pits 1 and 3. U% is shown in each of the targeted phases in the extraction. In pit 1, most of the U is held in the residual solid phase, whereas in the upper horizons of pit 3 most of the U is held in the organo-metal colloid phase and the exchangeable phase, indicative of external U addition processes.

• Influence of burn intensity and vegetation type on temporal dynamics of soil nitrogen pools and processes: Fire frequency and spatial extent are increasing dramatically in the Western United States and represent an important critical zone loss term at larger spatial and longer temporal scales for net ecosystem carbon and nitrogen (N) balance. Fire strongly affects N cycling and losses through volatilization, leaching and erosion. Because N is often a limiting nutrient in terrestrial ecosystems, more intense fires may exacerbate N limitation and thus play an important role in post-fire recovery of ecosystem functions. We examined the soil N cycling and retention processes in response to varying burn intensities in different vegetation types in the Valles Caldera, NM. We measured soil pH, moisture, N pools and transformation rates, and total C and N pools in the organic and mineral horizons of ponderosa pine, mixed conifer and aspen stands 2 days, three months, 9 months and 1 year after containment of the Las Conchas Fire in the Valles Caldera, NM. Three randomized, replicated plots were selected within each of the burn and vegetation types.

Results showed that N pools and processes rates varied significantly with time and as a function of vegetation types and burn intensities (RMANOVA, $p<0.05$). Soil ammonium pools were quite high immediately following the fire (range 1-100 ug N/g dry soil) and were significantly higher in the ponderosa pine forest compared aspen and mixed conifer forests immediately following the fire in the organic horizon. In contrast, ammonium concentrations were lower but elevated across vegetation types in the mineral horizon. Soil nitrate lagged behind ammonium in both horizons and peaked one year following the fire and was highest in the aspen sites compared to the other vegetation types. Three weeks after the fire, severely burned sites in mixed conifer stands had higher rates of net N mineralization than unburned sites. In that same time frame, inorganic N was immobilized more rapidly in severely burned sites compared to unburned sites in ponderosa pine stands. Soil pH was high immediately following the fire in all vegetation types (range 6.09-7.89) and sustained in the mixed conifer that may help to explain lower rates of nitrification than in the other sites. Soil carbon to nitrogen (C:N) ratios decreased significantly in the ponderosa and aspen high and low burns but did not decrease in the low mixed conifer forest. Variable temperatures of burn reflected in the $\partial^{15}N$ values across the vegetation types may help to explain these variable responses as well as recovery of the microbial populations. Findings from our study suggest differences in fire intensity and vegetation can have profound effects on the spatial and temporal distribution of soil N pools and processes in the organic and mineral horizons.

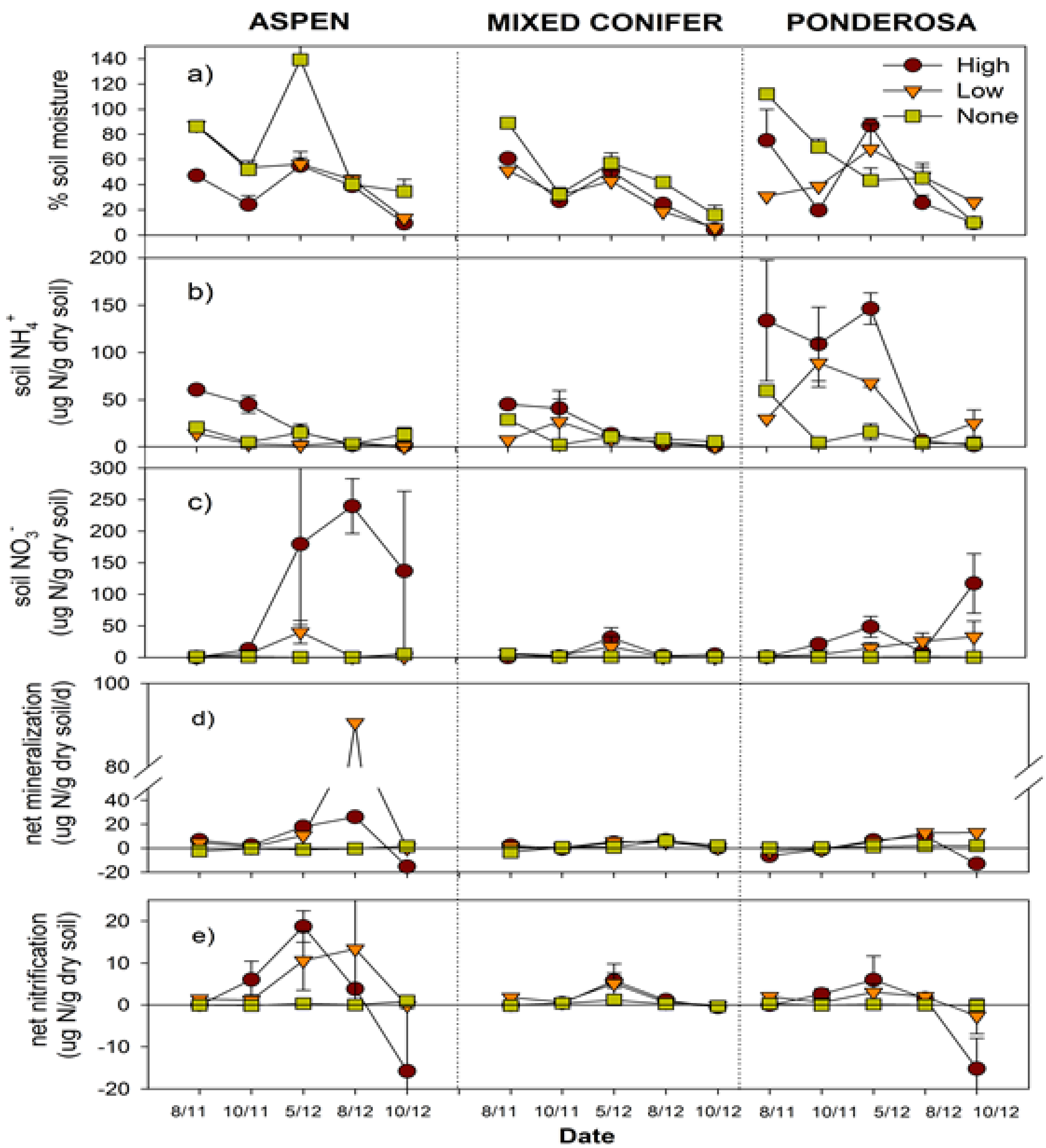

Figure 14. a) Soil moisture, b) soil ammonium pools, c) soil nitrate pools, d) rates of net mineralization, and e) net nitrification in the organic horizon of no burn, low, and high burn severity stands of aspen, mixed conifer, and ponderosa pine.

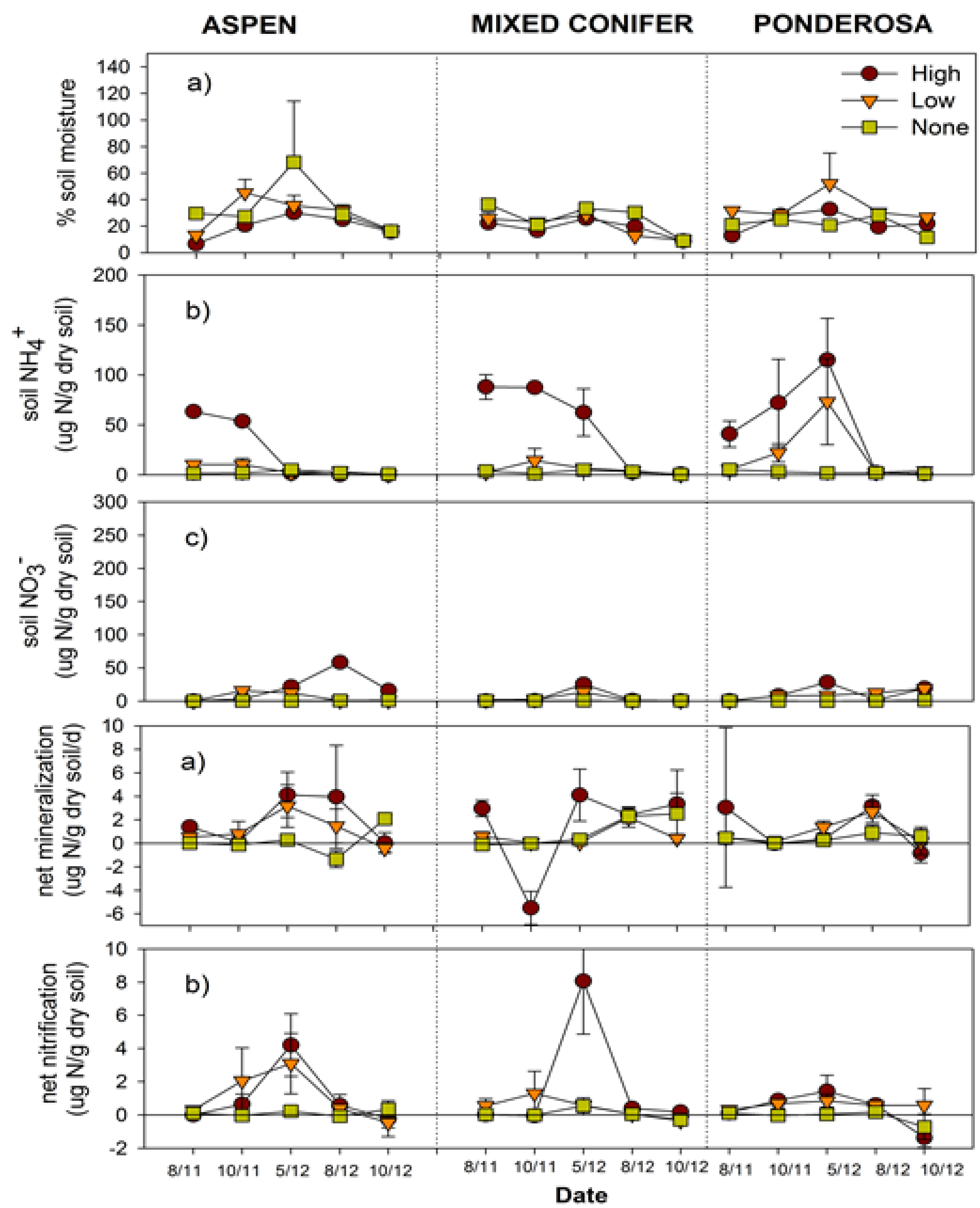

Figure 15. a) Soil moisture, b) soil ammonium pools, c) soil nitrate pools, d) rates of net mineralization, and e) net nitrification in the mineral horizon of no burn, low, and high burn severity stands of aspen, mixed conifer, and ponderosa pine.

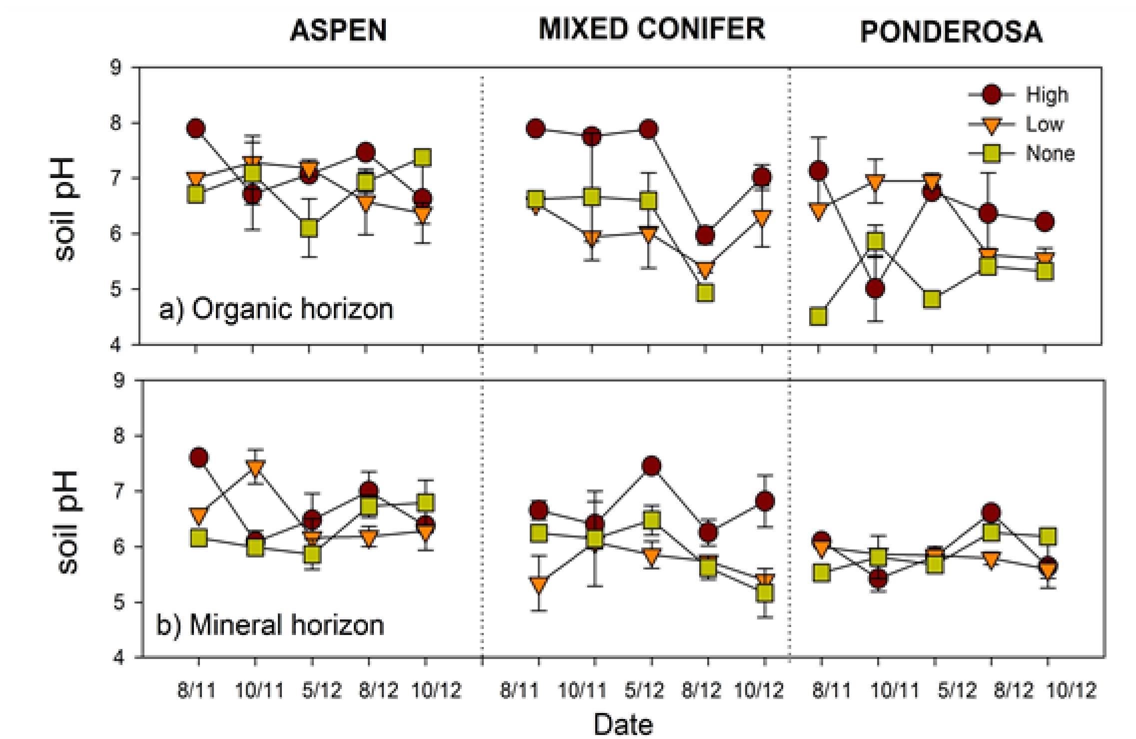

Figure 16. Soil pH in the a) organic and b) mineral horizon of no burn, low, and high burn severity stands of aspen, mixed conifer, and ponderosa pine.

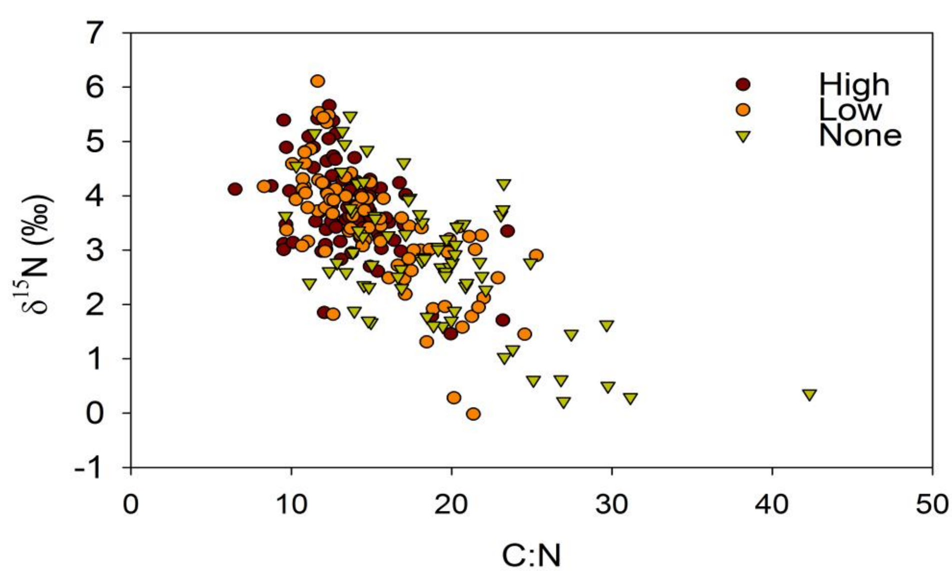

Figure 17. $\partial^{15}N$ values vary inversely with soil C:N ratios in no, low, and high burn stands.

• **Soil microbial communities 3 months following fire:** Soil microbial communities influence the rate and trajectory of ecosystem recovery after wildfire, but how their composition varies across soils from different vegetation types exposed to different burn severities is largely unknown. Lockart et al. (in review) utilized high throughput amplicon sequencing of a bacterial 16S rRNA gene fragment to determine the bacterial community composition in soils that were unburned, moderately burned ("low burn") and severely burned ("high burn") in ponderosa pine ('P') and mixed conifer ('M') forests, three months after the Las Conchas fire (New Mexico, USA; July 2011).

Community composition was distinct in unburned M and P soils, but it was indistinguishable in high burn soils, despite differences in M and P soil parameters (i.e. moisture, organic matter, carbon contents) known to correlate with shifts in bacterial community composition. Richness tended to be lower in the high burn M soils relative to unburned M soils, while it was similar across all P soils. Collectively, these results indicate that severe burn intensity may cause bacterial communities to shift to similar compositions even if the initial communities, soil physical and chemical properties and mechanisms by which community shifts occur are distinct.

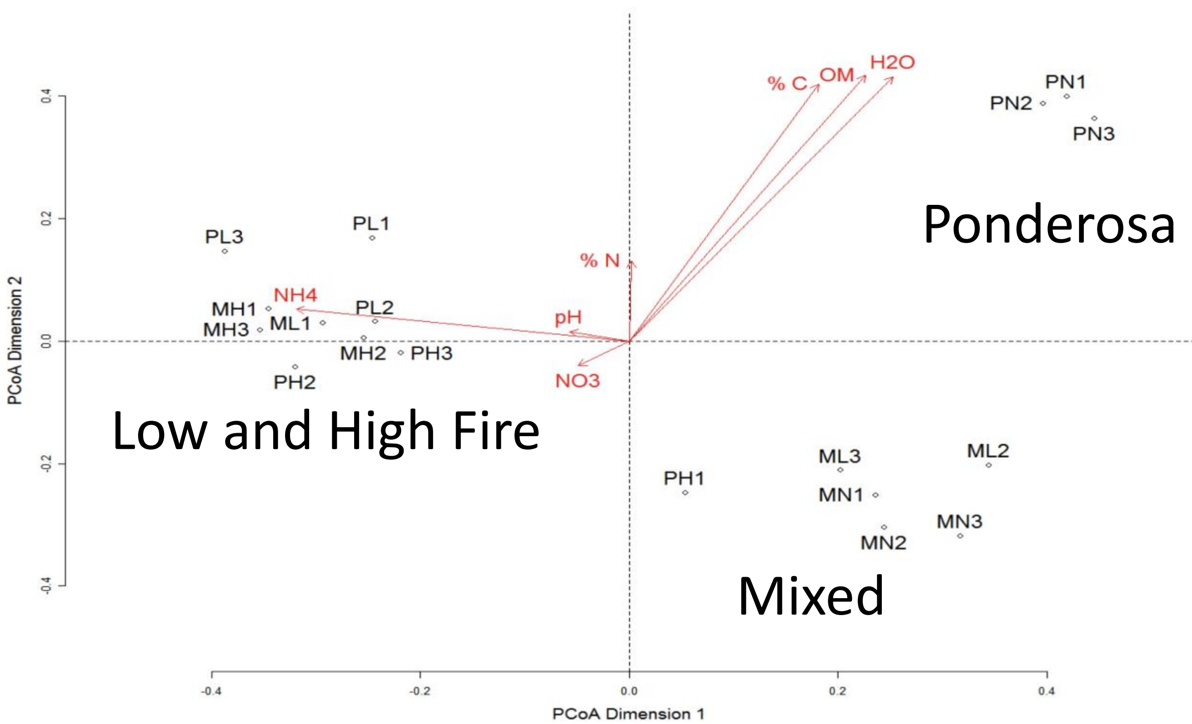

Figure 18. Principle coordinate analysis (PCoA) shows convergence of low and high burn microbial communities compared to ponderosa pine and mixed pine distinct communities. Ammonium and pH increase along the primary axis and carbon and moisture along the secondary axis.

• **Quantification and spatial modeling of soil physical and chemical properties in the JRB MC-ZOB:** Soil genesis in volcanic terrain may be controlled by complex assemblages of parent materials and local topography. The objective of this work was to quantify topographic and parent material controls on soil and catchment evolution in a mixed conifer, montane catchment in the Valles Caldera, New Mexico, as part of the JRB-CZO. The field site is a 16 ha catchment at an elevation of 3,000 m, with a frigid soil temperature regime (0-8 ^{0}C), ustic soil moisture regime with bimodal precipitation of winter snowfall and convective summer rainfall (880 mm yr^{-1}), and an overstory dominated by spruce and fir with dense grass cover in open areas. The catchment is located on the resurgent Redondo Dome that uplifted shortly after the last major eruption of the Valles Caldera 1.2 My ago. The dome includes a complex assemblage of pre-eruptive caldera materials and extant sedimentary rocks embedded within a welded, hydrothermally altered rhyolitic tuff.

We sampled a transect of seven soil profiles spanning the dominant east–west aspect of the catchment across a catena with profiles located in summit, backslope, footslope, and toeslope positions. Soil morphology was described in the field and soil samples were analyzed using a range of geochemical and mineralogical techniques including quantitative and qualitative x-ray diffraction of bulk samples and particle size fractions, elemental analysis by x-ray fluorescence, and laser particle size analysis. The data indicated strong landscape position control on soil drainage, grading from well-drained summits to poorly-drained toeslope positions based on the presence/absence of redoximorphic features. The drainage patterns were coupled with downslope thickening of dark, organic matter rich surface horizons, likely a function of both in situ organic matter production and downslope colluvial transport of carbon rich surface materials. Mineralogical and geochemical data indicated clear within profile lithologic discontinuities in backslope, footslope and toeslope positions that suggest post dome resurgence ash deposition and redistribution via physical erosion. Additionally, the majority of sites contained a modern dust signal in the upper 5 to 10 cm of the soil profile based on Ti:Zr, mica content, and particle size distribution. The dominant weathering patterns include feldspar transformation to kaolinite and alteration of volcanic glass and/or 2:1 primary minerals to smectite. Smectite is a combination of both authigenic smectite formed during hydrothermal alteration of the tuff and neogenic smectite as suggested by Si-rich soil solution and surface waters. The data indicate a sequence of dome uplift followed by periods of pedogenesis and ash input, subsequent ash redistribution via physical erosion, and modern mass input via eolian dust. The timing and magnitude of these events and impacts on chemical weathering are the subjects of ongoing model and measurement activities.

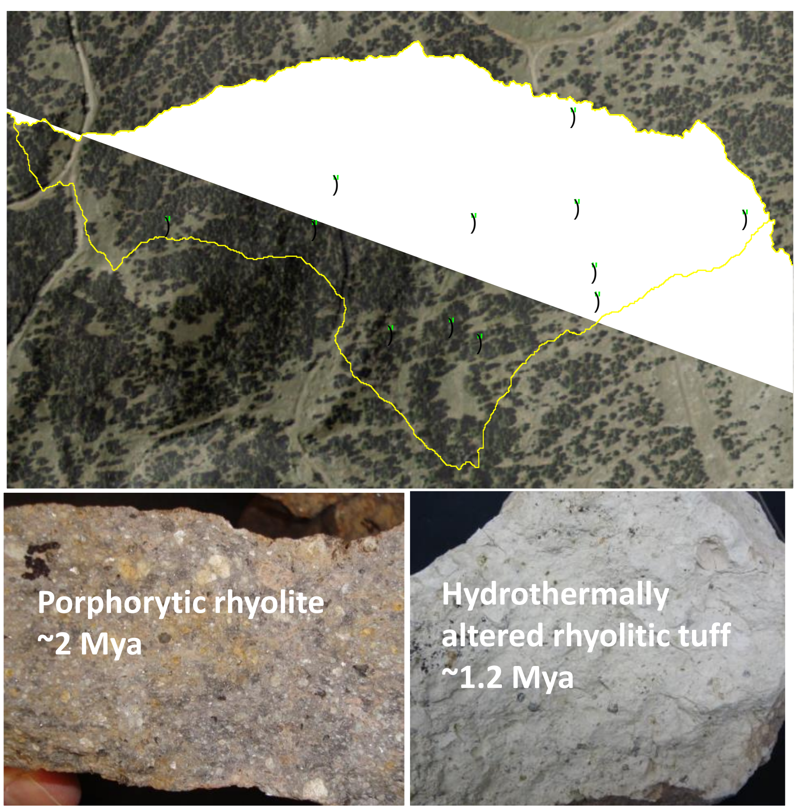

Figure 19. Locations for 12 pedons sampled in the JRB MC-ZOB that have full soil morphological, physical, chemical, and mineralogical characterization data. The pedons were grouped by landscape position across an east to west catena transect. The ZOB is underlain by two rhyolitic rock types: an older pre-caldera eruption porphorytic rhyolite, and a hydrothermally altered rhyolitic tuff formed during caldera eruption and formation. The eastern most portion of the ZOB is dominantly the porphorytic tuff.

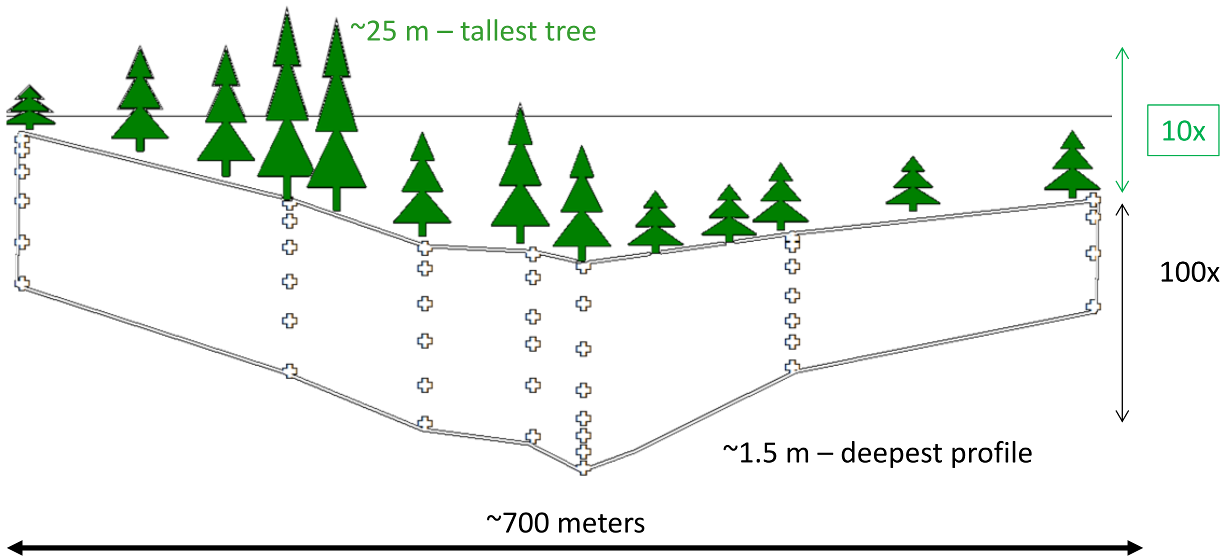

Figure 20. Figure indicating the east-west catena transect sample locations by depth and horizon (cross bars). The canopy height and soil depth data were derived from the airborne LiDAR data with vertical exaggeration of both for ease of viewing.

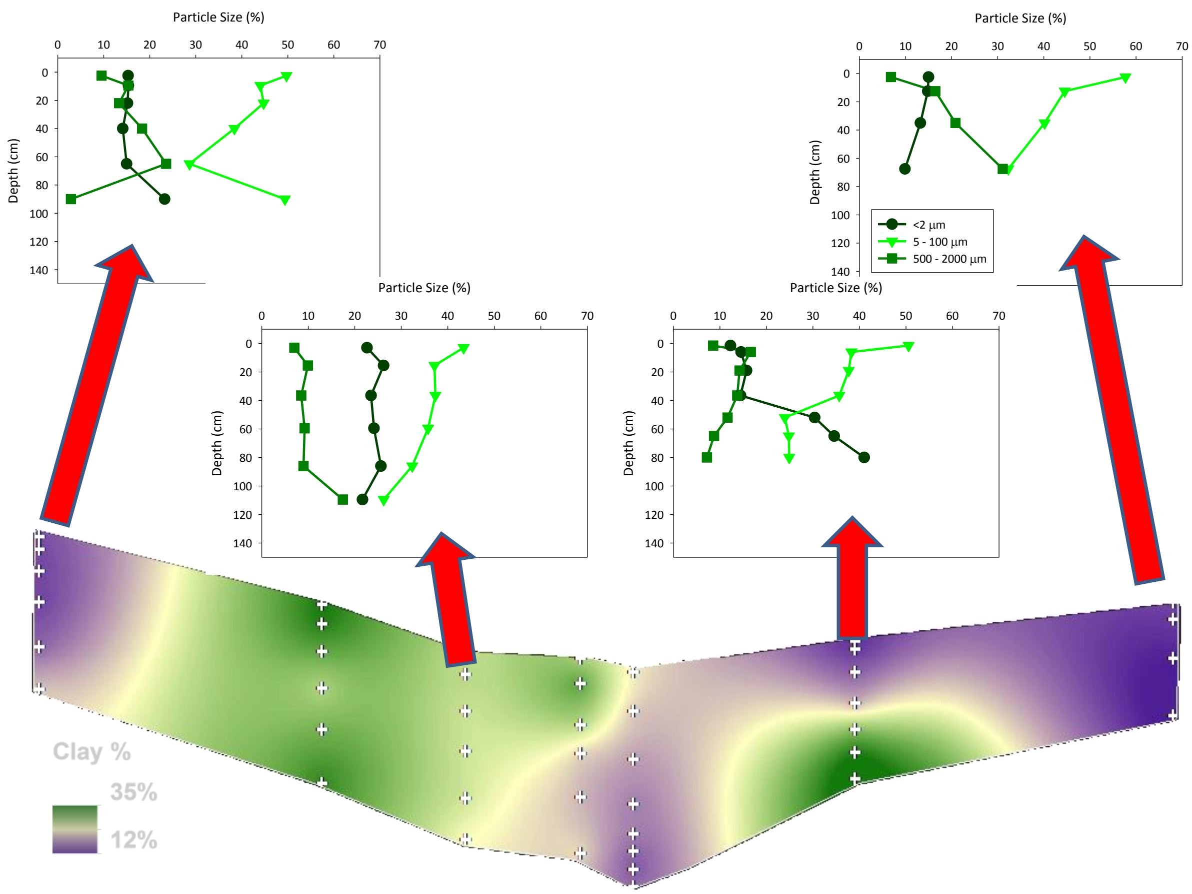

Figure 21 (prior page). Depth dependent patterns in soil particle size distribution. The eastern summit is rocky and dominated by fractured porphorytic rhyolite. This grades into a midslope position with an argillic horizon in the subsurface formed in the hydrothermally altered tuff with colluvial rhyolite in the surface. The western slope was dominated by clayey materials which occur in an area that exhibits landscape morphology similar to a solifluction event that could have occurred during the last glacial maximum.

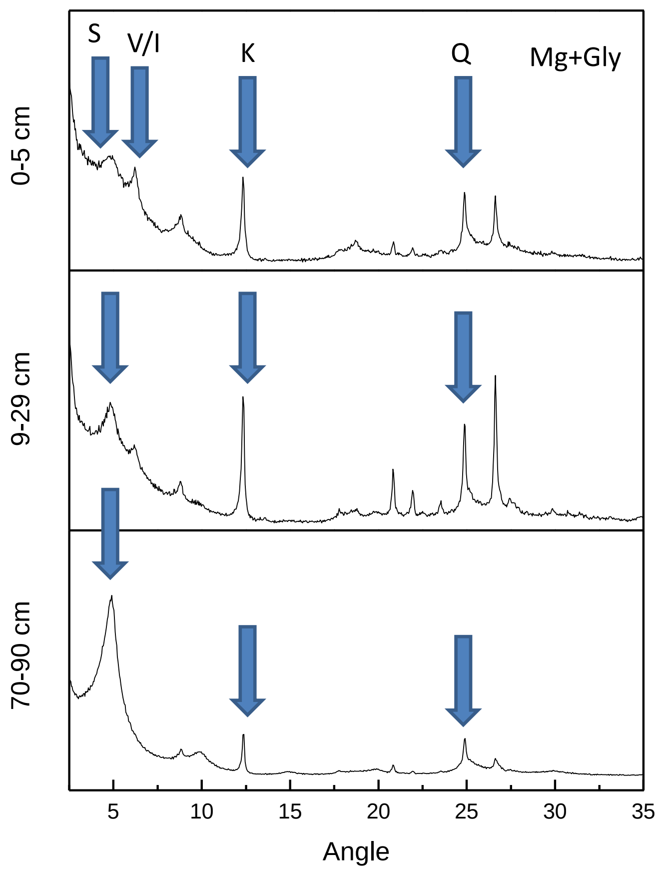

Figure 22. X-ray diffraction data of the clay fraction for the pedon in the midslope position of the eastern portion of the transect. The data indicate a clear transition in the clay mineral assemblage moving into the clay rich argillic horizon formed in the tuff that is enriched in smectite. The presence of illite/vermiculite decreases with depth suggesting a dust influence. The mineralogy and geochemistry data were used to partition out the soil material into fraction dust, tuff, and rhyolite. The data indicate clear variation in dust content with the rocky eastern portion of the transect showing higher dust contribution to the fine earth fraction.

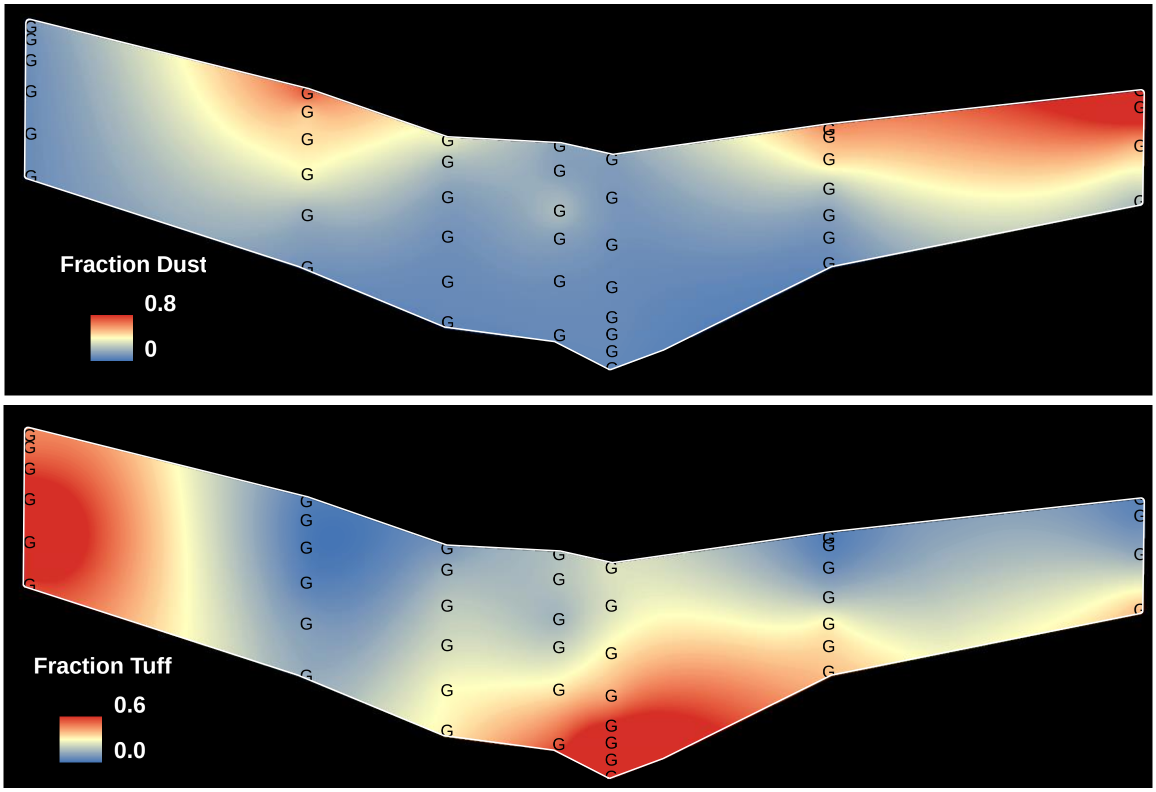

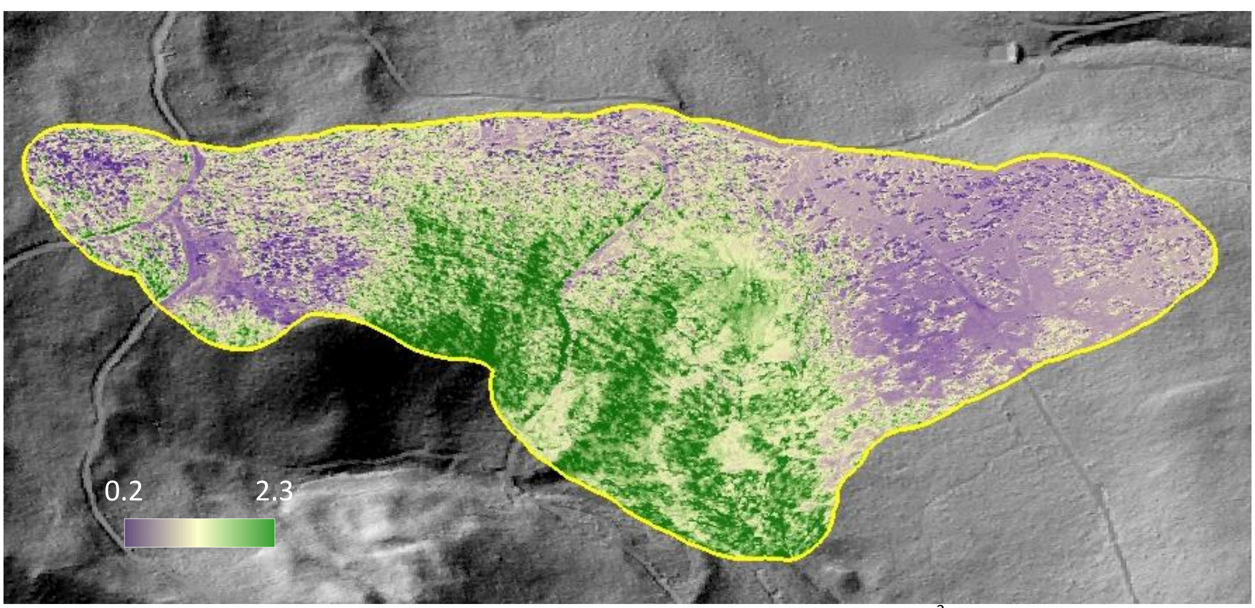

Figure 23. Modeled spatial distribution of soil organic carbon concentration (kg m^{-3}) across the entire MC-ZOB predicted using a combination of topographic and remotely sensed imagery. The clay rich western transect midslope and hollow in the center of the ZOB exhibit the highest C concentrations.

• Climate and landscape position controls on soil chemical weathering and mineral transformations: The overarching goal of this study is to address how climate and landscape position control mineral weathering and soil organic carbon storage across semiarid ecosystems. Soil pedons were sampled by genetic horizon from divergent and convergent landscape positions across distinct vegetation zones spanning the SCM-CZO (Fig. 24). The vegetation communities ranged from desert scrub to mixed conifer forest and represented significant shift in temperature (10-24°C) and precipitation (25-85 cm).

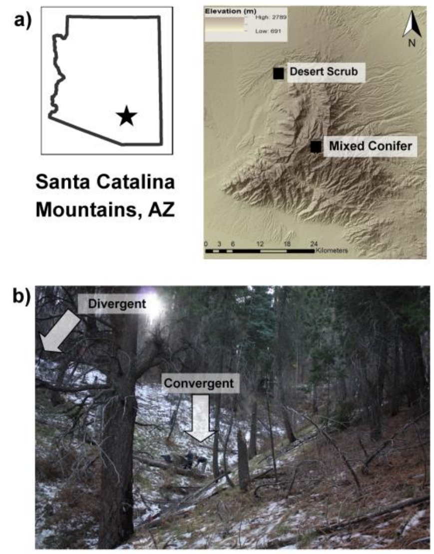

Figure 29. a) Locations of the desert scrub and mixed conifer field areas encompassed by the Santa Catalina Mountain Critical Zone Observatory. The Santa Catalina Mountains are located in southeastern Arizona as denoted on the inset map. b) An example of the two landscape positions studied in the project. The image is of an adjacent divergent-convergent landform unit pair at the mixed conifer field site.

The first objective of this research was to examine trends of elemental loss across plagioclase grains originating from natural soil systems to better understand climatic controls on soil development in semi-arid and sub-humid environments. Here, the chemical composition of plagioclase feldspar in bulk soils was coupled to the elemental changes associated with microscale mineral transformations. Bulk elemental chemistry, including major, minor, and trace elemental constituents, was determined by x-ray fluorescence (XRF) for all samples and microscale weathering patterns were quantified using electron microprobe analyses. Elemental mass-transfer percentages were calculated and normalized to the parent rock materials using Na and SiO_2 as the mobile and immobile inputs, respectively. Electron microprobe wave dispersive spectroscopy (WDS) combined with backscattered electron (BSE) imagery was used to develop a general classification scheme for characterizing the plagioclase grain-secondary mineral interface across field areas and to explore the chemical composition of external sources of altered materials (Fig. 25). Replicate grains (n=10) were examined within each soil to ensure a representative sample. Microscale studies of the feldspar-secondary mineral interface are an important step in the cross-scale investigation of the feldspar weathering sequence involving the transformation of primary to secondary minerals.

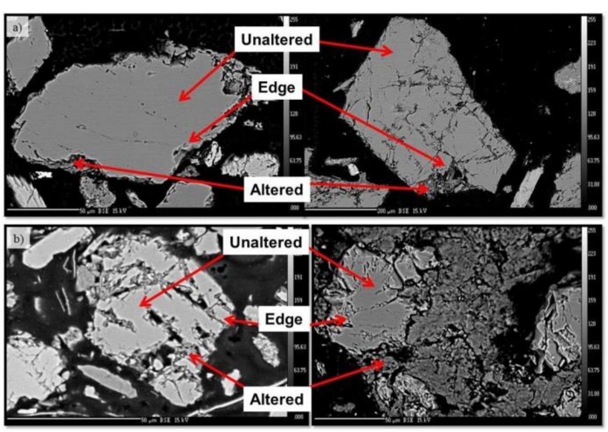

Figure 25. Backscattered electron images documenting how a) desert scrub and b) mixed conifer plagioclase feldspar grains were classified consistently across field sites.

From these data, chemical depletions of Na, a proxy for plagioclase feldspar weathering, were found across ecosystems in both bulk soil element-mass-transfer calculations and at the microscale. In the bulk soils, Na chemical loss was most consistent with depth and across soil pedons (n = 4) in the mixed conifer system where sodium depletion averaged 46% (± 5%) relative to the parent material, providing evidence for loss of plagioclase to chemical weathering (Fig. 26). Electron microprobe analyses of surface and subsurface soils at the mixed conifer site revealed a significant ($P<0.001$) decrease in sodium weight percent from the unaltered regions of the grains (Na of ~7-8%) to fully transformed areas of the grains (Na of ~0.2-0.3%) located in joint fractures and at grain edges (Figure 27). The extensive loss of Na was highly significant in both surface and saprock samples. In contrast, soils from the desert scrub site exhibited highly variable Na loss in the bulk soils with Na depletion ranging from 23 to 50%. Na (%) variability was notably high in the altered materials of both the surface and saprock samples (Figure 26). In the surface soil, the decrease of Na from 6.65% (± 0.39) in the unaltered grain section to 1.40% (± 0.93) in the altered section was highly significant ($P<0.001$) as were losses in Na from unaltered to altered grains in the saprock. Highly significant losses of Na (%) were also noted for edge to altered grain section comparisons in both surface and saprock samples.

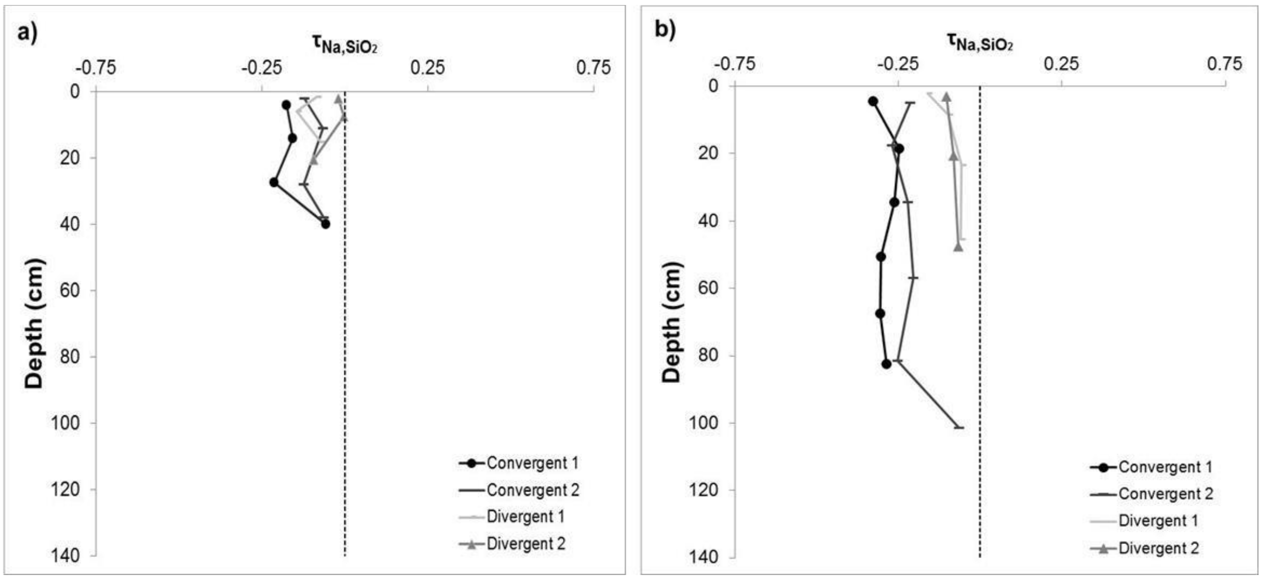

Figure 26. Na chemical depletion relative to the immobile reference quartz (SiO_2). The box plots highlight less distinction in Na depletion across landscape positions observed in a) the desert scrub field area compared to b) the mixed conifer sites which show more Na loss in the convergent landscapes.

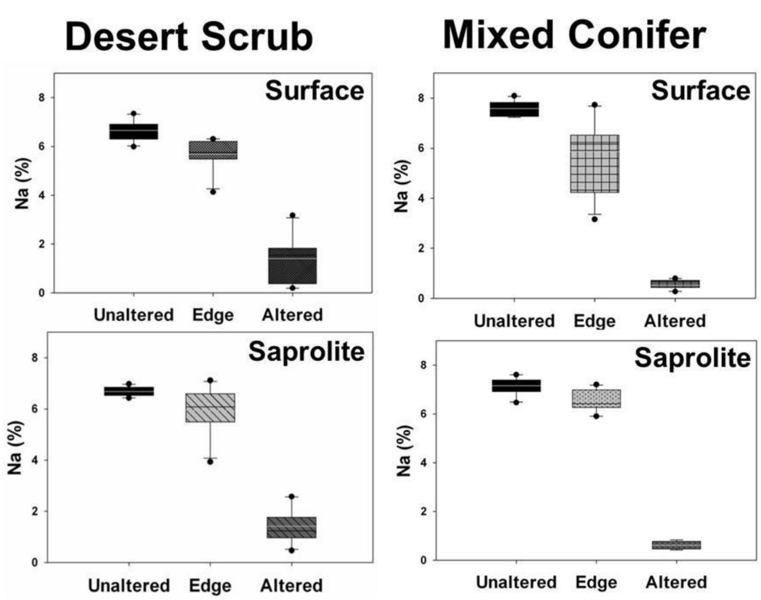

Figure 27. Box plots summarizing the weight percentages of Na for unaltered, edge, and altered sections of plagioclase feldspar grains. The figure summarizes changes in Na (%) for surface and saprock samples collected from the desert scrub and mixed conifer field areas. Each box plot is composed of 10 data points analyzed for each classification scheme (e.g. unaltered).

• Climate and landscape position controls on soil organic carbon distribution and mean residence time: The objective of this work was to identify climate and topographic controls on soil organic carbon (SOC) cycling across soils in different semiarid ecosystems of the SCM. Surface (0-10 cm) and subsurface (30-40 cm) soils from desert scrub, ponderosa pine, and mixed conifer ecosystems were collected from granitic regolith profiles across divergent and convergent landscape positions. Physical SOC distribution in the regolith was quantified using a density and sonication technique to obtain the "free" (non-mineral associated), "occluded" (SOC putatively located within aggregates), and "mineral" (SOC associated directly with mineral surfaces) C pools (Fig. 28).

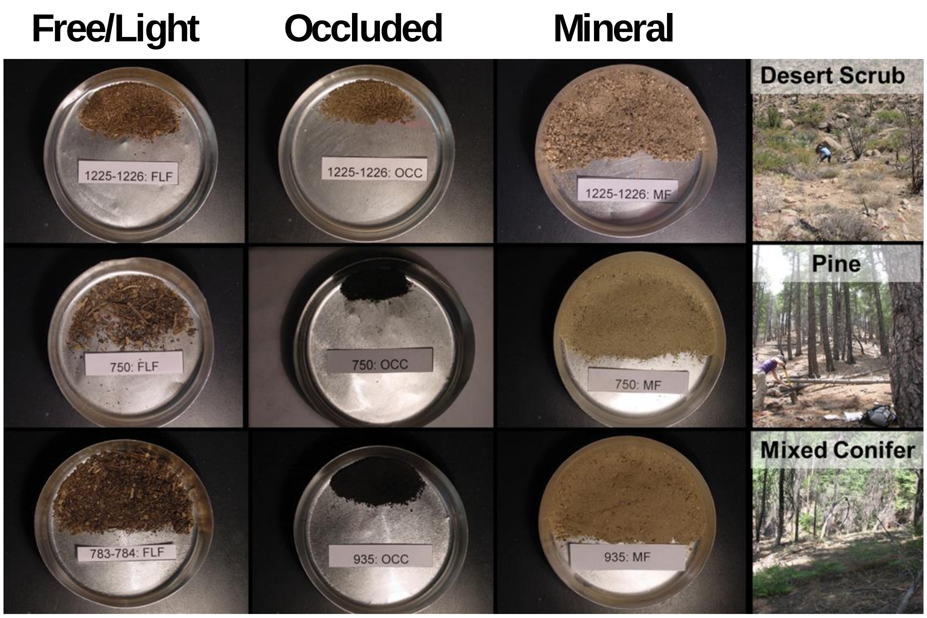

Figure 33. Photographs providing examples of the free/light, occluded, and mineral carbon fractions separated from soils in desert scrub, ponderosa pine, and mixed conifer ecosystems.

Total carbon (%) and radiocarbon analyses of the carbon fractions and bulk soil samples were used to explore soil carbon dynamics across contrasting ecosystems and landscape positions in the SCM-CZO. In terms of relative age, the free fractions were composed of the youngest SOC across all ecosystems and landscape positions considered (Fig. 29). Conversely, the mineral or occluded fractions contained the oldest SOC depending on the ecosystem. Desert scrub soils stored relatively little C (<1% SOC by weight), with all fractions dominated by fast-cycling SOC. The relatively oldest C was located in the mineral fraction, indicating organo-mineral interactions as the dominant C storage mechanism in this ecosystem (Fig. 29). In contrast, the conifer systems contained more SOC (>3%) with the oldest SOC found in the occluded fraction indicating an important role for aggregation as a SOC stabilization mechanism in these sites.

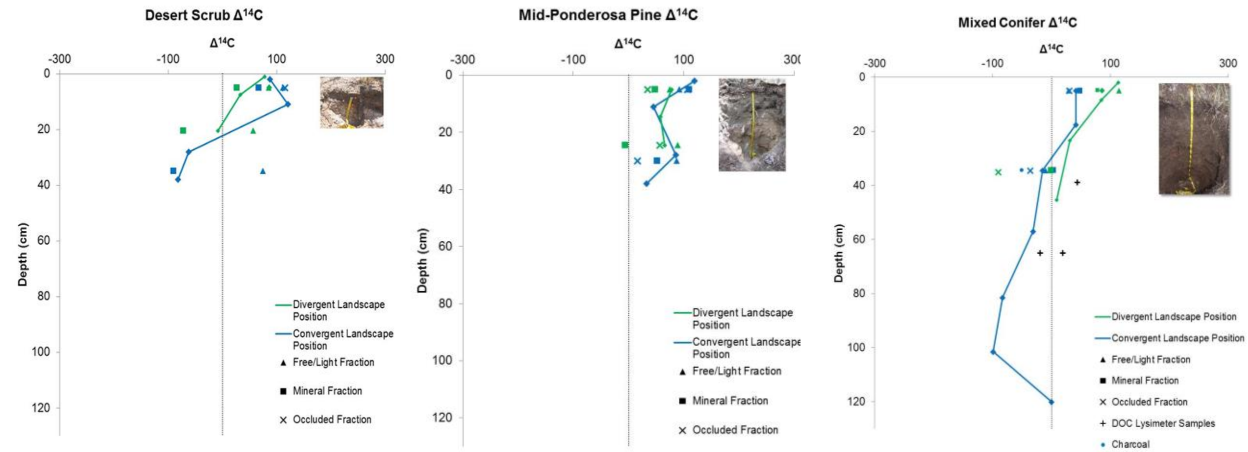

Figure 29. The figure summarizes the relationships between soil depth and the $\Delta^{14}C$ values of the carbon fractions (symbolized in legend as free/light, occluded, and mineral fractions) and bulk soil samples (solid lines) from the desert scrub, ponderosa pine, and mixed conifer ecosystems. $\Delta^{14}C$ values for DOC lysimeter samples and a charcoal sample are also represented in the mixed conifer plot.

• High resolution spatial characterization of subsurface structure, mineralogy, and chemistry of the high elevation mixed conifer ZOB in the SCM: Quantifying catchment scale regolith physicochemical variation yields insights to the evolution of the subsurface. A sample design was developed using a combination of principle component analysis (PCA) of available geospatial data and a conditioned Latin Hypercube Sampling (cLHS) scheme. Geospatial data determined by the PCA to account for 95% of landscape variance included soil depth modeled based on topography and mass transport, slope, soil wetness index, normalized difference vegetation index (NDVI) and National Agriculture Imagery Program (NAIP) bands 3/2. The cLHS scheme was derived using these geospatial data and determined 20 sample locations where soil profiles were dug to refusal, described, and sampled according to genetic horizon. Soil samples were characterized using methods of X-ray Fluorescence (XRF), X-ray Diffraction (XRD), particle size, color, pH, electrical conductivity (EC), C/N isotopes, and loss on ignition (LOI). Regression models predicting soil depth (cm), carbon (kg m^{-2}), clay (%), Na flux (kg m^{-2}), pH, and strain were developed using the 20 sample locations the six geospatial data layers determined from the PCA, and reverse step-wise multiple linear regression. Results indicated strong correlations of soil properties with the drainage systems in the MG catchment. Deeper soils, higher clay content, higher carbon content, and greater Na loss were observed and modeled within the drainages of the catchment relative to adjacent slopes and ridgelines (Fig. 29).

We argue the most highly weathered soils are found within the drainages of the catchment. We attribute deeper soils within the drainages to the flux of snowmelt and precipitation from the ephemeral drainages. A consistent flux of water through a soil profile yields more physical and chemical weathering resulting in deeper soil profiles (Yoo & Mudd, 2008; Yoo et al., 2009). We attribute a negative Na flux (Na loss, kg/m^2) within the drainages to the chemical weathering of feldspars ($NaAlSi_3O_8$) and other Na associated minerals in the granite bedrock, in contrast to adjacent slopes and ridges. High levels of clay are observed in the drainages of MG. We associate this clay accumulation with the flux and transportation of sediments and precipitation into the convergent drainages. Likewise we observe carbon (kg/m^2) accumulating in the drainages, attributed to the high flux of precipitation and the subsequent trapping of organics within the swales, generating high carbon levels. Volumetric strain is higher in the drainages, in comparison to the adjacent slopes and ridges. We associate the strain with higher physical weathering within the drainages, and therefore overall more mass loss. pH values are higher (7) in the drainages and lower (4) throughout the rest of the catchment. It's hard to determine exact environmental influences that affect pH, however with more organic matter, clay accumulation, and higher fluxes of precipitation through the drainages may lead to higher pH values.

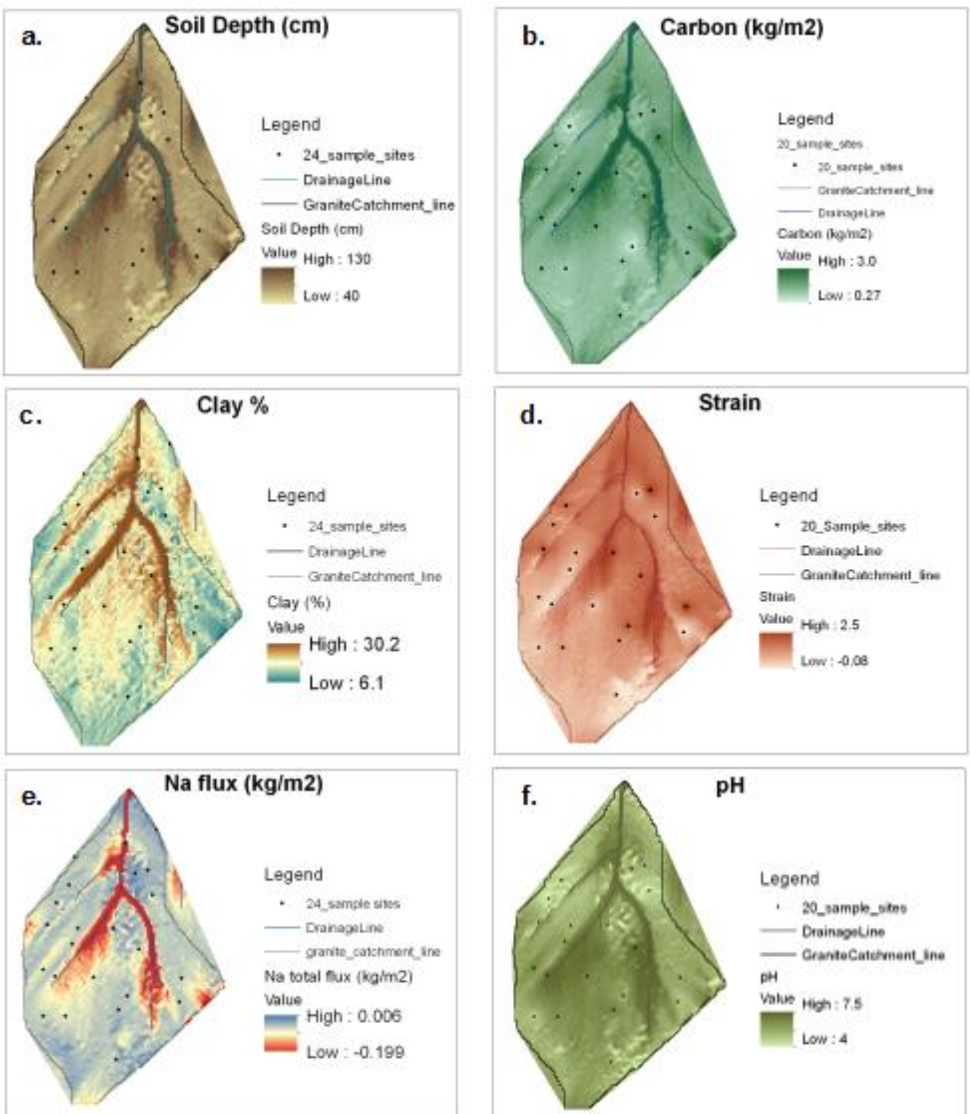

Figure 30. Final spatial predictions for target variables including soil depth (a), carbon (b), clay % (c), strain (d), Na flux (e), pH (f).

<u>3.3 *Findings*: Surface Water Dynamics (SWD) Theme</u>

• Controls on catchment mean transit times: insights from natural tracer studies

(A) Water isotopes as tracers of catchment mean transit times. Studies of water stable isotopes in the Marshall Gulch catchment, including the Schist and Granite ZOBs, in the SCM CZO found that catchment mean transit times (mTTs) are variable between seasons and different spatial patterns of mTTs emerge each year (Fig. 31) (Heidbuchel et al., re-review). For three consecutive monsoon seasons it was possible to correlate mTTs with a different physical catchment property (Fig. 32): (1) in 2007, mTTs correlated best with mean soil depth; (2) in 2008, soil hydraulic conductivity gained importance in explaining the variability of mTTs; (3) in 2009, planform curvature showed the best correlation with mTTs. Differences in meteorologic forcing between the three monsoon seasons explained the temporal variability of mTTs. In 2007, a series of precipitation events caused the storage capacity of the soils to be exceeded. As a result those catchments started producing quick runoff (overland flow and macropore flow) (Fig. 33). In 2008, precipitation events were more evenly distributed throughout the season, soils did not saturate, runoff coefficients decreased because more water left the catchment via evapotranspiration and soil hydraulic conductivity became a stronger control since matrix flow dominated. The 2009 monsoon was unusually dry, the soil storage became depleted and water flowed mainly through bedrock pathways; therefore topographic parameters gained importance in determining how quickly water arrived at the sampling location at the catchment outlet. Catchment mTTs are therefore controlled by both inherent catchment properties and external forcings and hence cannot be predicted with a single physical parameter. In order to improve our understanding of what controls mTTs we suggest a dimensionless number that helps identifying partitioning thresholds and sorts precipitation events into one of the three response modes that were observed in our catchments.

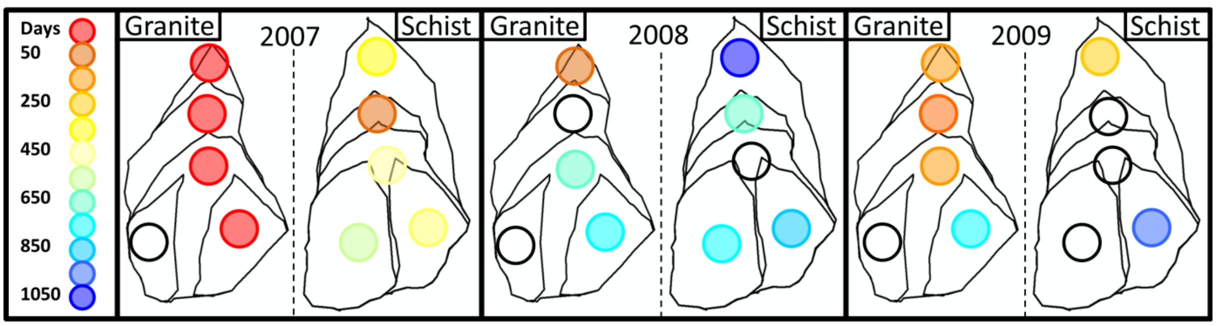

Figure 31. Catchment mean transit times vary spatially and between years for the Schist and Granite ZOBs in the Marshall Gulch catchment, SCM CZO.

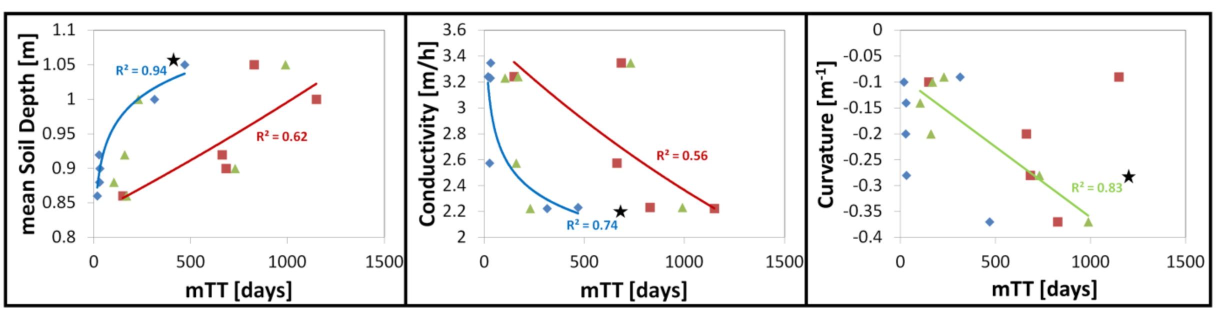

Figure 32. Relationship between catchment mean transit times (mTT) and various catchment characteristics.

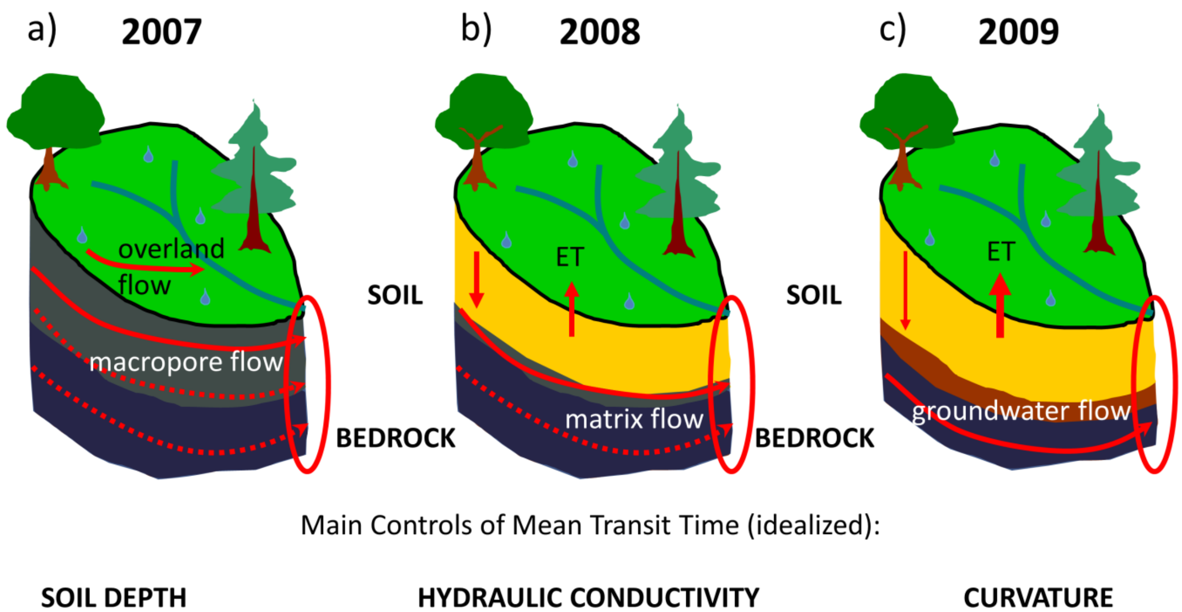

Figure 33. Conceptual model of how variability in meteorological forcing altered catchment mean transit times between years.

(B) Base cations as indirect tracers of water residence time. Base cations in water are derived predominantly as a result of water-rock interactions in the unsaturated and saturated zones. A sequential process of geochemical reactions are observed in most hydrological systems as water moves down gradient and therefore base cations may be used as indirect measures of residence times, accounting for any loss due to mineral precipitation or adsorption. Major ion concentrations, which are significantly easier and less expensive to measure than traditional age tracers have the potential to complement water dating and help us understand the dynamics of hydrologic systems. To test this hypothesis, perennial springs and first order streams draining Redondo Peak in the upper part of the JRB CZO (Fig. 34) were analyzed for major cation chemistry and age tracers, including tritium. Spring and surface water samples have similar major ion chemistries (Ca-Na-HCO_3 type waters), and winter precipitation is the main source of water to the springs and stream as indicated by water stable isotope signatures. Residence times estimated using tritium ranged from 0.69 to 13.58 years. Electrical conductivity, Na, Ca, and DIC were significantly correlated with water "age", while there was no correlation with Cl and DOC (Fig. 35). Interestingly, there was also a correlation between Na concentrations and elevation, as well as contributing area of the spring (Fig. 36). Na concentrations in surface water increases with catchment area, and mean aspect (as seen by Broxton et al., 2009, using a shorter residence time tracer, water stable isotopes). Sodium appears to be a useful, and relatively inexpensive tracer of catchment residence times.

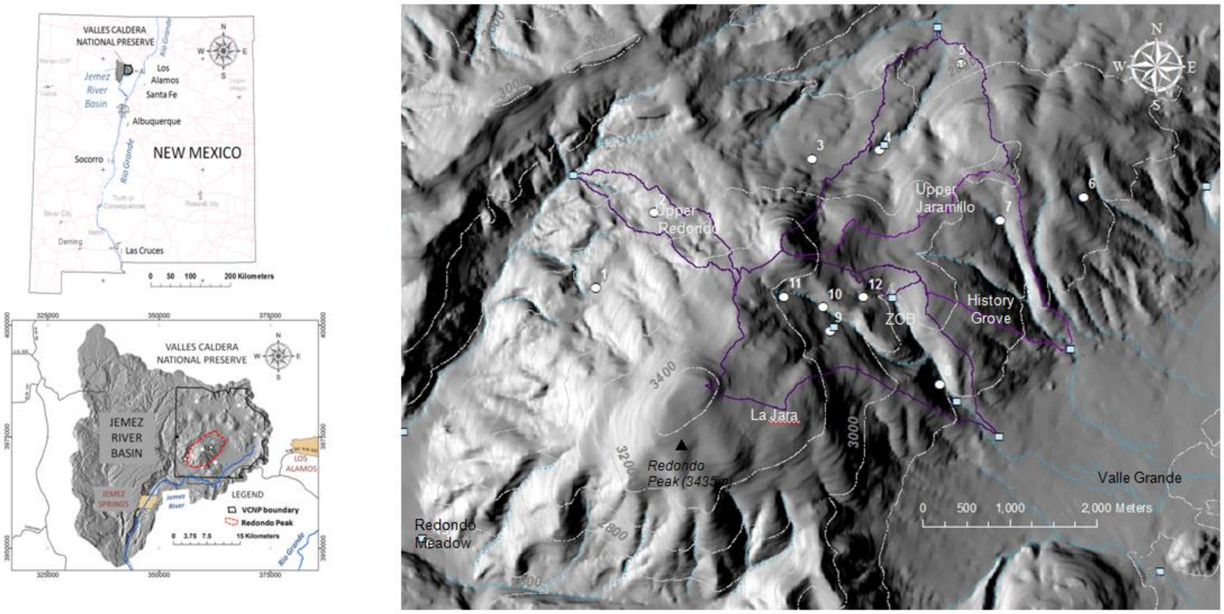

Figure 34. Location map of perennial springs and surface waters sampled around Redondo Peak to investigate relationship between residence times and solute chemistry.

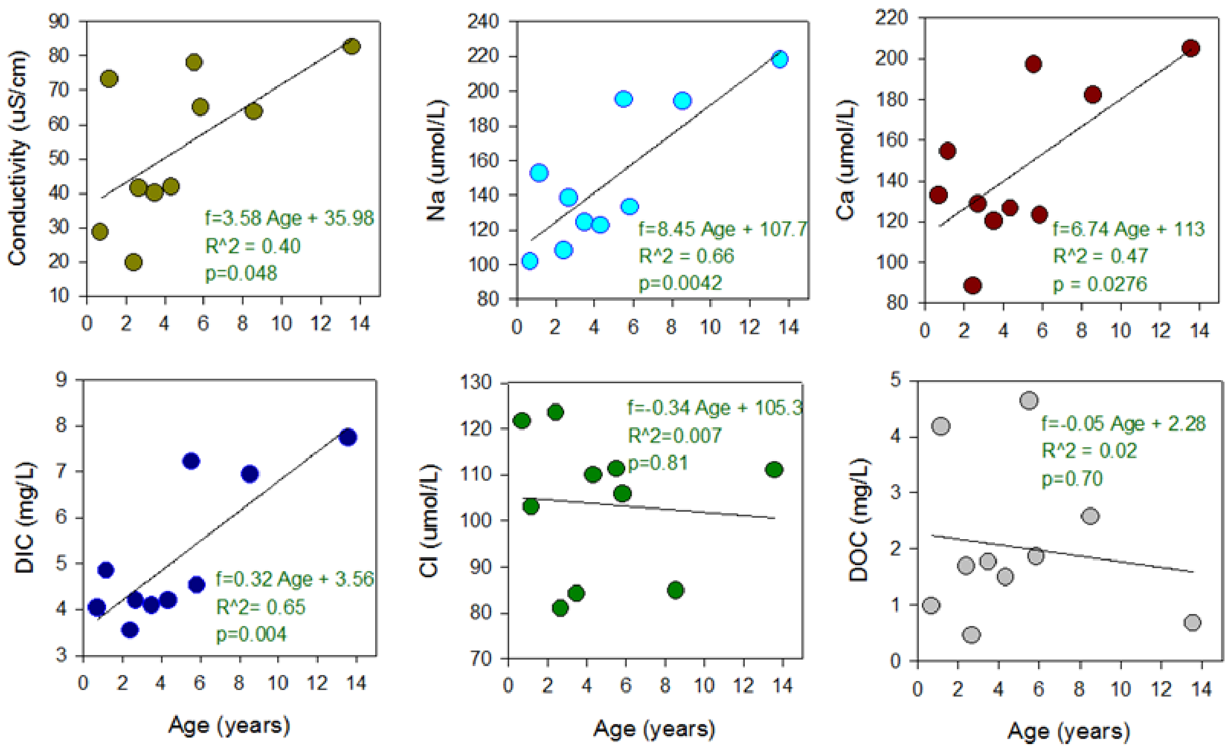

Figure 35. Correlation of electrical conductivity, DIC, DOC, Cl and base cations with apparent age.

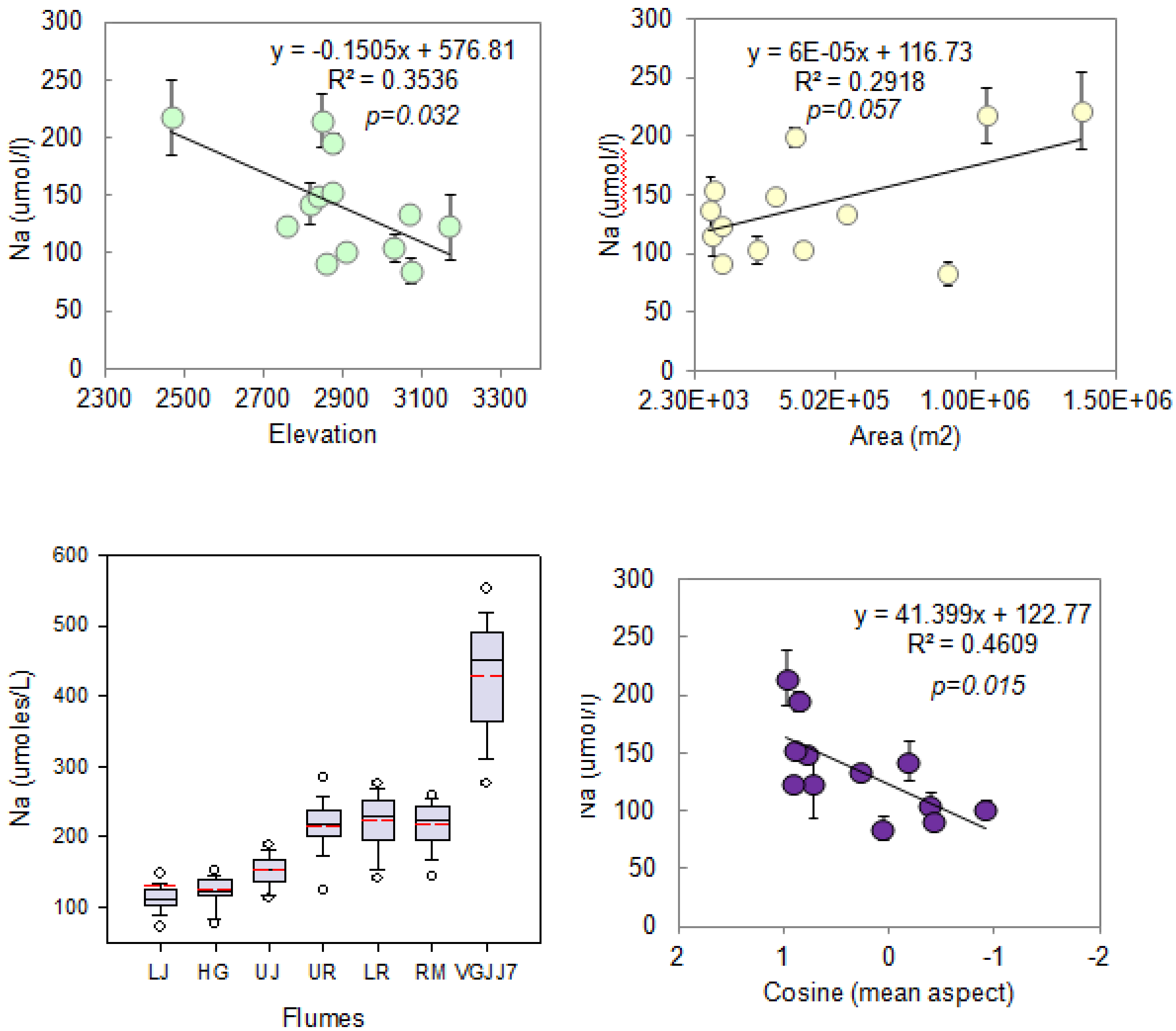

Figure 36. Relationships between sodium (Na) concentration and landscape characteristics.

(C) Uranium isotopes as indicators of catchment residence times. Surface water and stream samples in La Jara catchment show seasonal variations in contributions of deep vs. shallow groundwater, using Si and Cl mixing models, consistent with previous findings (Harpold et al., re-review). Seasonal variation was also observed in ($^{234}U/^{238}U$) in dissolved U in water samples, with decreasing ($^{234}U/^{238}U$) values in conjunction with greater contributions of deeper groundwater. ($^{234}U/^{238}U$) values in stream water decreased with increasing Si concentrations, indicating a potential relationship with residence time (Fig. 37). Increasing water residence time may result in decreasing ($^{234}U/^{238}U$) in dissolved U due to progressive depletion of easily-weathered ^{234}U in La Jara soils (Huckle et al., in prep).

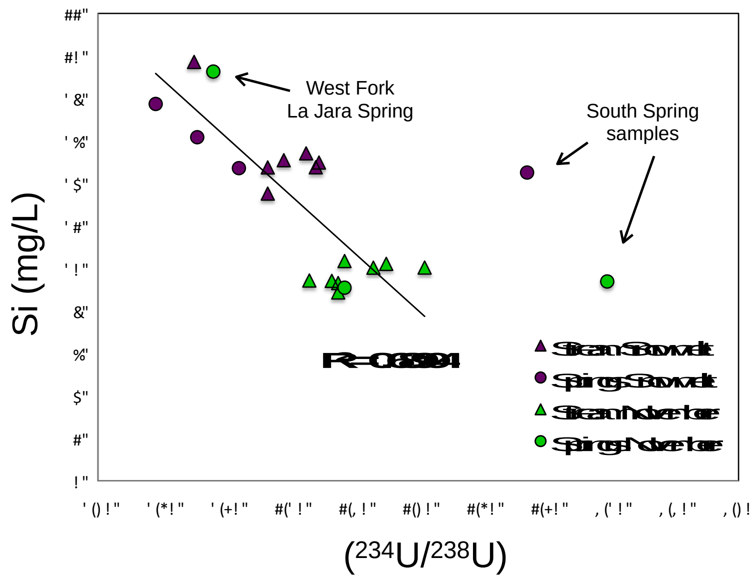

Figure 37. Si vs. ($^{234}U/^{238}U$) in La Jara spring and stream samples from both Snowmelt and dry seasons. Most samples, with the exception of the South Spring samples, plot along a trendline of decreasing ($^{234}U/^{238}U$) with increasing Si. Snowmelt season samples have higher Si and lower ($^{234}U/^{238}U$), indicating longer residence times, while dry season samples have lower Si and higher ($^{234}U/^{238}U$) indicating shorter residence times.

• Controls on dissolved and particulate fluxes of carbon and nitrogen.

(A) Hydrologic processes control the variability in C and N concentrations across JRB CZO catchments. By developing a simple end-member mixing model, Harpold et al. (in re-review) demonstrated that three catchments surrounding Redondo Peak responded differently to wet and dry winters in 2010 and 2011, respectively. Using the simple mixing model and end-member measurements they estimated the observed to predicted (O:P) ratio for stream C and N concentrations (Fig. 38). The catchment that received the largest deep groundwater (DGW) contributions (Upper Jaramillo) also had the greatest O:P ratios for DOC (Fig. 38b), suggesting that DOC concentrations increased along hydrological flowpaths between the source areas and the catchment outlet. Similarly O:P ratios for N species were highest in the catchment receiving the largest DGW contributions, however both NO_3 (Fig. 38c) and TDN (Fig. 38d) concentrations were nearly always lower than their source areas (i.e. O:P<1). The results of Harpold et al. indicate that catchment response to potential smaller and/or earlier snowmelts will likely be uneven in the JRB-CZO because of different deep groundwater recharge processes.

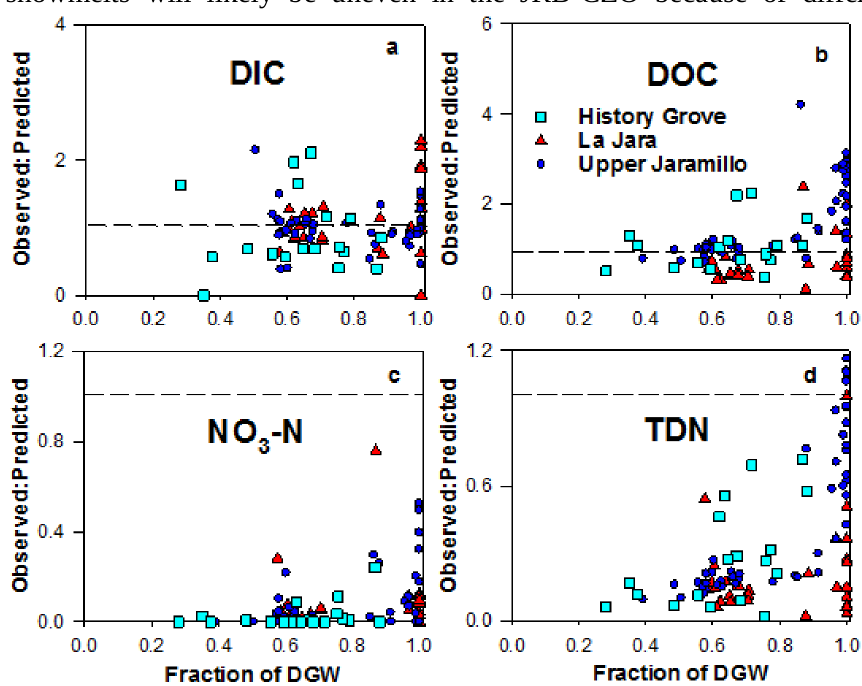

Figure 38. The ratio of observed to predicted (O:P) ratios versus the fraction of deep groundwater (DGW). Values of O:P greater than one suggest that concentrations increased during transport, whereas below one suggest reduced concentrations from the independent mixing model (from Harpold et al., in re-review).

(B) Impact of interannual variability of water fluxes, catchment aspect and seasonal processes on stream water C dynamics. Stream water carbon (C) characteristics of two different streams (draining north-facing [NF] Upper Jaramillo catchment and south-facing [SF] LaJara catchment) were analyzed for three years (2010, 2011, 2012). The objective was to elucidate the impact of: (1) changes in water fluxes by comparing wet years with a dry year; (2) catchment aspect (north-facing [NF] vs. south-facing [SF]); and (3) seasons (snowmelt vs. summer) on all forms of dissolved stream water C (DOC, DOM and DIC) in forested catchments within the JRB-CZO (Perdrial et al., accepted with revisions). A simple concept of water as *reservoir*, *transporter* and *incubator* as driver for stream water C concentration and composition was used to frame results in a conceptual context (Fig. 39). The overarching control over annual stream water C fluxes were water fluxes, likely from a well-mixed *reservoir* (groundwater) (Fig. 40). The dissolved organic matter (DOM) fluorescence signature was terrestrial year round, signaling a strong riparian and near stream soil control on DOM composition where the role of water as C *transporter* was superimposed on the reservoir control. The role as *transporter* was dominant during the snowmelt season where hillslope and riparian soil constituents were flushed into the streams (Fig. 41 a, c, f). Streams as *incubators* act as an additional control for stream water C during the warmer summer months where decreased % dissolved oxygen saturation, increased $\delta^{13}C_{DIC}$ values and microbial DOM indicated the predominance of heterotrophic respiration in the stream and riparian soils (Fig. 41 b, d, f).

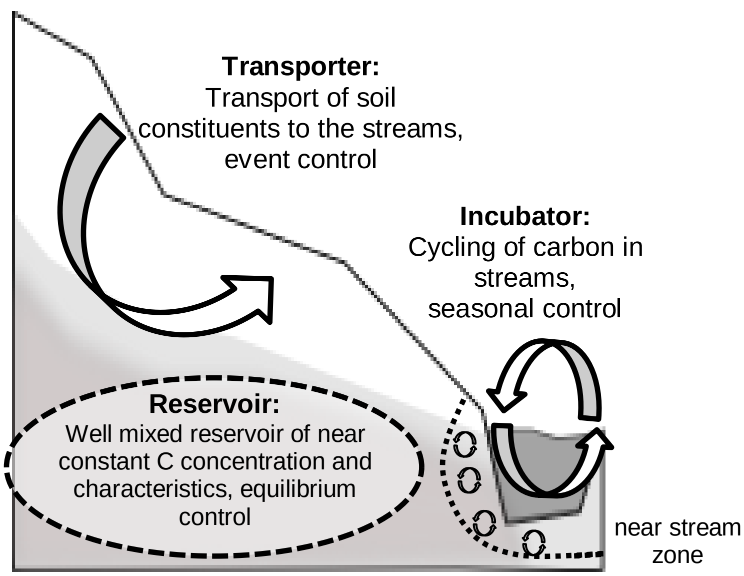

Figure 39. Simplified schematic of the role of water in controlling stream water carbon: water as "transporter" accumulates carbon along the flow path, water as "incubator" as place for microbial cycling and water as "reservoir" as large and well-mixed source of near-constant composition (ground water) that intersects near stream hotspot zones before entering the streams.

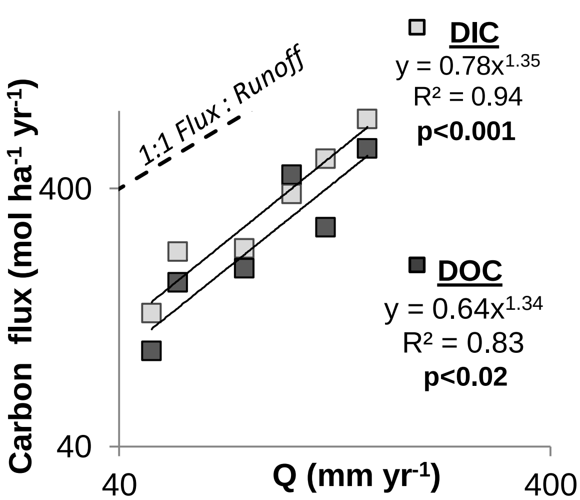

Figure 40. Annual carbon fluxes as a function of specific discharge for all years and both catchments. Dashed line indicates the 1:1 relationship between carbon fluxes and discharge indicative of constant composition.

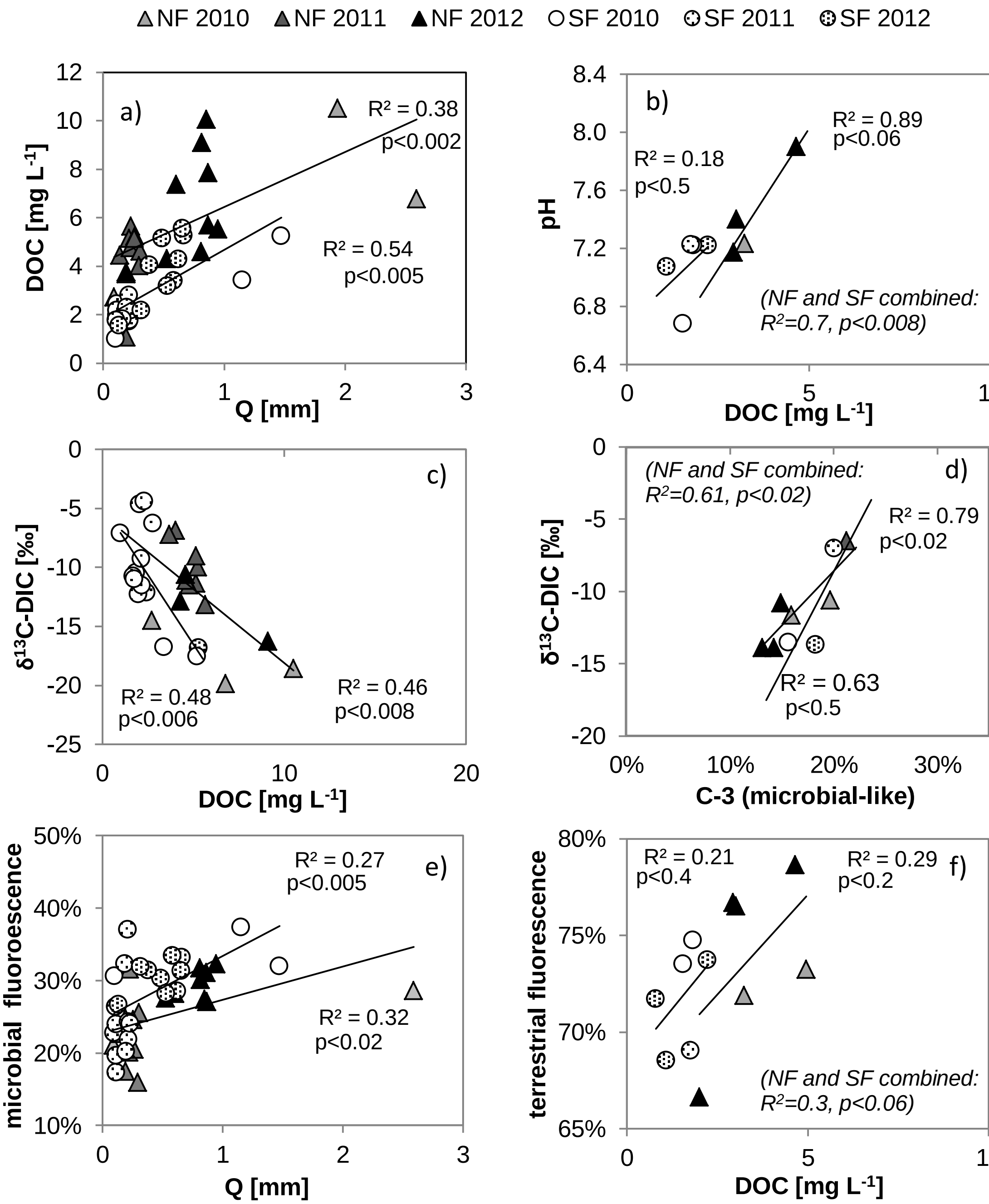

Figure 41. Correlations on controls over stream water carbon during snowmelt (plots on the left side) and the dry season (lots on the right side).

<u>3.4 *Findings:* Landscape Evolution (LSE) Theme</u>

• Quantifying how post-fire sediment yields are controlled by burn severity, slope, and drainage area. The amount of erosion that has occurred in one year following the fire is orders of magnitude larger than the "background" erosion rate of non-fire-affected catchments. This raises the possibility that the vast majority of all the erosion that occurs in forested landscapes occurs in the few years following a high severity fire. In 2013 Ph.D. student Caitlin Orem collected and analyzed ^{10}Be cosmogenic samples from stream sediments. This work will enable placing constraints on erosion rates over millennial time scales. Data collected and analyzed in previous years provided erosion rates in fire-affected and non-fire-affected drainage basins at time scales of ~1yr and ~ 10^6 yr.

We are acquiring terrestrial laser scans (ground-based LiDAR) over time in order to quantify how sediment yields change through time as the landscape "recovers." Conceptual models for the landscape adjustment to fire predict that landscapes return to a state similar to pre-burn conditions following an exponential decrease from an initial post-fire peak to a new quasi-equilibrium condition over a time scale of several years to decades. Our CZO project aims to calibrate that recovery graph and its ecologic, hydrologic, and geomorphic controls. Ground-based LiDAR will play an important role in that effort but it is important to emphasize that ground-based LiDAR cannot possibly measure geomorphic change in even a fraction of the total fire-affected area. As such, airborne LiDAR data is needed. NSF generously funded an airborne LiDAR survey of the burned area in May 2012.

We used these airborne LiDAR data to construct a precise map of all of the erosion that occurred within every 1 m^2 pixel within the 197 km^2 study area in the year following the Las Conchas fire. This map, in turn, was used to develop a new empirical model that quantifies the role of terrain slope and burn severity in post-fire erosion. We differenced the precisely co-registered bare-earth DEMs to derive a map of elevation changes, also known as a DEM of Difference (DoD). Threshold filtering of the DoD is important for this type of change-detection analysis because ground-surface elevation changes in the centimeter to low-decimeter range can result from positional errors within the point cloud and/or from errors associated with processing of the point cloud to a bare-earth DEM. We filtered the DoD in two ways: (1) by setting equal to zero all values in the DoD in which the magnitude of change was < 0.3 m, and (2) filtering out all changes < 0.3 m and filtering out all changes occurring in zones with a contributing area, A, less than 0.001 km^2. The 0.3 m value was chosen because we found that we could confidently verify, using aerial orthophotographs acquired on May 5, 2012, that erosion/deposition took place in valley bottoms where > 0.3 m was measured in the DoD. Changes < 0.3 m often could not be verified in aerial photographs, especially where they occurred on hillslopes. Since filtering scheme (1) includes sediment derived from hillslopes and valley bottoms while scheme (2) is limited to valley bottoms (based on the criterion $A > 0.001$ km^2), a comparison of the sediment yield maps obtained with these two alternative filtering schemes provides an estimate of how much sediment was derived from hillslopes versus valley bottoms. We also repeated the analysis with no filtering to determine the sensitivity of the results to the presence/absence of filtering (Fig. 42). The average decrease in ground-surface elevation upslope of every pixel was computed by summing the threshold-filtered DoD values (to compute the net change, with erosion counted as positive and deposition as negative) along overland and channel flow pathways downstream, then dividing each pixel by the upslope contributing area and retaining only the positive values. The resulting map is both the net surface elevation decrease upslope from each pixel and the sediment yield Y (expressed as volume per unit area, i.e. units of length) transported through each pixel. Fig. 42 shows the results using the most conservative filtering scheme, i.e. the one that retains only verifiable changes (> 0.3 m) in valley bottoms ($A > 0.001$ km^2).

Average sediment yields mapped in Fig. 42D increase steadily and nonlinearly with average slope and soil burn severity class (SBSC) within a drainage basin (Fig. 43A). SBSC is a standard measure of burn severity produced by the Department of the Interior Burned Area Emergency Response (BAER) team using multispectral satellite imagery as described in U.S. Forest Service (1995). The map of SBSC for the Las Conchas fire is shown in Fig. 42B. The effect of average slope and SBSC on sediment yields can be quantified using

$$Y = aS^b B^c \quad , \tag{1}$$

where Y is the sediment yield (mm), S is the average slope (m/m), B is the average SBSC, and a (mm), b, and c are coefficients equal to 8 mm, 1.5, and 1.0 (Fig. 43A) for the case of the Las Conchas fire.

We constructed sediment yield maps using the raw, unfiltered DoD data for comparison. The sediment yield map in the unfiltered case (Fig. 42F) has clear artifacts associated with flight lines. As such, we do not recommend using unfiltered data but it is nonetheless useful as it provides an upper bound on sediment yields from hillslopes and low-order valleys (Fig. 43B). Fig. 43E shows the sediment yield map obtained using the DoD filtered only for the magnitude of change. This DoD includes sediment derived from hillslopes in addition to low-order valleys but it may overestimate yields because some areas of change > 0.3 m on hillslopes cannot be verified in the aerial photographs. Average sediment yields obtained by filtering the DoD by the magnitude of change only are approximately 3 times greater than those obtained using the DoD filtered by using both the magnitude of change and contributing area (Fig. 43B), indicating that most of the sediment yield is derived from hillslopes rather than from valley bottoms.

We also compared our measurements with Tillery et al. (2011a), who predicted the volumes of post-fire sediment, V (m^3), excavated by debris-flow scour and exported from drainage basins following the 2011 Las Conchas fire using an empirical equation developed by Gartner et al. (2008) and Cannon et al. (2010a):

$$\ln V = 7.2 + 0.6\ln(SG30) + 0.7(AB)^{0.5} + 0.2(T)^{0.5} + 0.3, \qquad (2)$$

where SG30 (km^2) is the area of the basin above 30% slope, AB (km^2) is the area classified with moderate or high soil burn severity, and T (mm) is the total storm precipitation. Sediment yield is obtained by dividing the V predicted in eqn. (2) by basin area, A, i.e. $Y = V/A$. We found that eqn. (2) predicts sediment yields that match measured yields quite well for relatively large drainage basins (> 0.1 km^2) (Fig. 43B). For small drainage basins, however, eqn. (2) overpredicts yields by up to a factor of 50, with the largest discrepancies occurring for relatively small (< 0.01 km^2) drainage basins (Fig. 43B). Eqn. (2) predicts a systematic decrease in sediment yield with increasing drainage basin area, while measured yields are, to first order, independent of drainage basin area (Fig. 43B). These results are currently being prepared for submission as a peer-reviewed journal article.

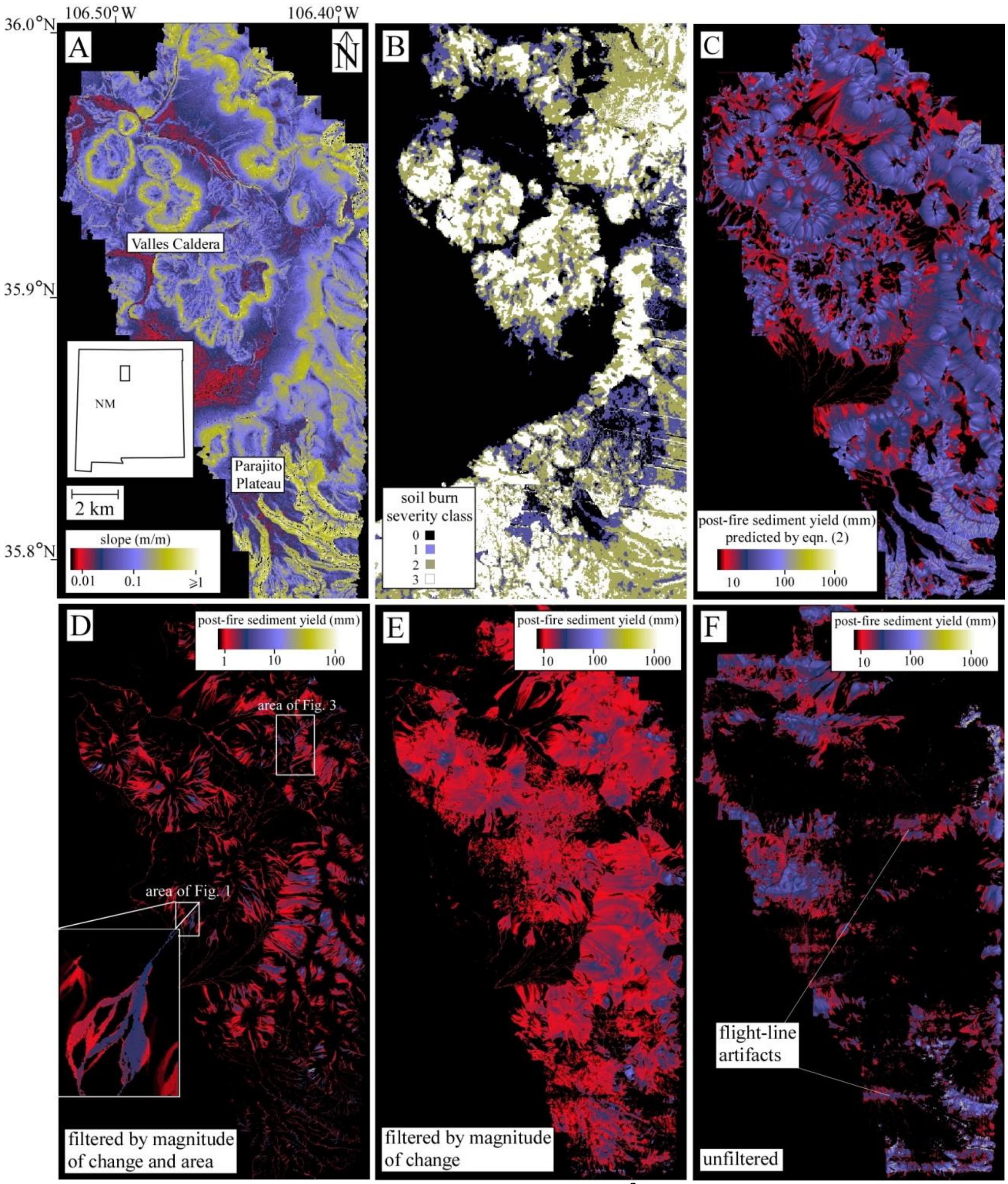

Figure 42. Maps of sediment yield and its controlling variables in 197 km^2 of the area burned by the Las Conchas fire, along with predictions of the model of Gartner et al. (2008) and Cannon et al. (2010a). Color maps of (A) terrain slope, (B) soil burn severity class (SBSC) (U.S. Forest Service, 2011), (C) post-fire sediment yield predicted by the Gartner et al. (2008) and Cannon et al. (2010a) model (eqn. (2)), (D)-(F) post-fire sediment yield measured from airborne lidar using (D) filtering by magnitude of change and contributing area, (E) filtering by magnitude of change only, and (F) no filtering. Note that color scale for (D) differs from that of (C), (E), & (F).

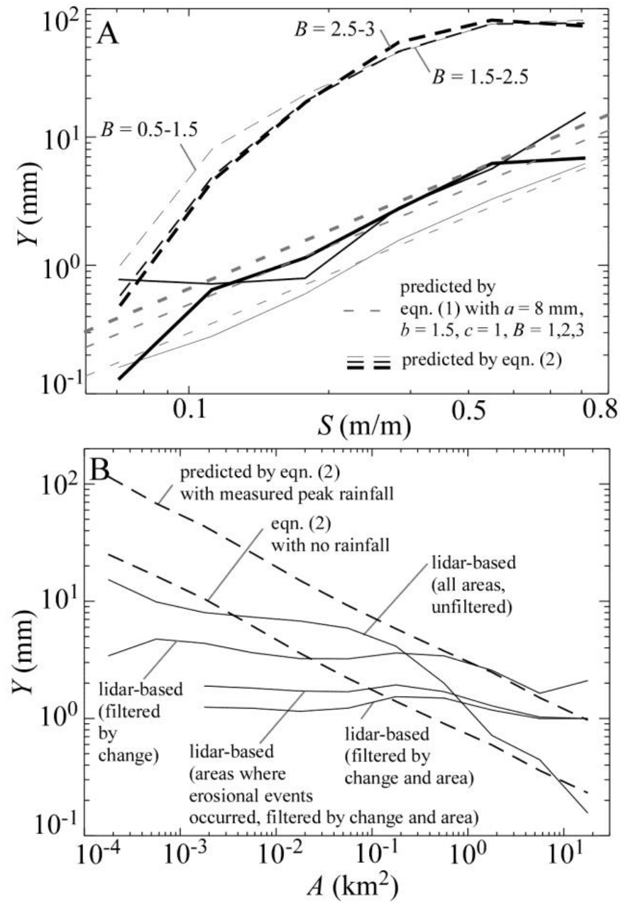

Figure 43. Dependence of average post-fire sediment yields on average terrain slope, SBSC, and contributing area in drainage basins (average of all drainage basins with contributing areas greater than 0.001 km^2), and comparison of the measurements to the predictions of empirical models (eqns. (1) and (2)). Bolder line styles indicate data from more severely burned areas. Average slope is denoted as S, contributing area as A, and average burn severity class as B. (A) Relationships among measured and predicted average sediment yields, average terrain slope, and average SBSC. Dashed black curves show predictions of eqn. (2), dashed gray lines show predictions of eqn. (1). Measured data are shown using solid (i.e. un-dashed) curves. Note logarithmic scales on both axes. Averaging was performed in seven logarithmically spaced bins of slope from 0.1 to 1 and three bins of average SBSC (B = 0.5-1.5, 1.5-2.5 and 2.5-3). (B) Plots of average sediment yield as a function of drainage basin area. Dashed lines indicate predictions of Gartner (2008) and Cannon et al. (2010a) model (i.e. eqn. (2)). Four lidar-based measured curves are presented corresponding to yields computed using (1) an unfiltered DoD, (2) a DoD filtered by the magnitude of change only, (3) a DoD filtered by the magnitude of change and contributing area (all areas included) and (4) a DoD filtered by the magnitude of change and contributing area with only the areas where debris flows actually occurred included in the analysis. Yields were averaged in 10 logarithmically spaced bins from 0.0001 to 20 km^2 (only 8 bins from 0.001 to 20 km^2 for the case of the DoD map filtered by area).

● **Quantifying the export of C and N in fire-affected drainage basins.** As a compliment to the work of Orem and Pelletier, graduate student Kate Condon and Prof. Paul Brooks quantified post-fire organic carbon and nitrogen fluxes in four zobs (approximately 0.1 km^2) and two larger catchments (approximately 1.3 km^2) debris following the Las Conchas fire and compared these amounts to background fluxes from three, undisturbed catchments. They found that particulate carbon and nitrogen fluxes from burned forested catchments are approximately two orders of magnitude higher than annual background POM fluxes from unburned sites. These fluxes from burned sites are equal to 1-3 years of net carbon uptake in adjacent sites and consequently do not represent a major storage or loss of carbon. In contrast, particulate nitrogen fluxes following fire are a significant loss of nutrients in these nitrogen-limited forests, equal to 50 – 100 years of net N deposition. The ultimate fate of this nitrogen is unknown, but the majority is deposited in a comparatively small area adjacent to the stream channel and riparian zone with the potential to leach to surface or groundwater during subsequent flow events. These results are currently being prepared for submission as a peer-reviewed journal article.

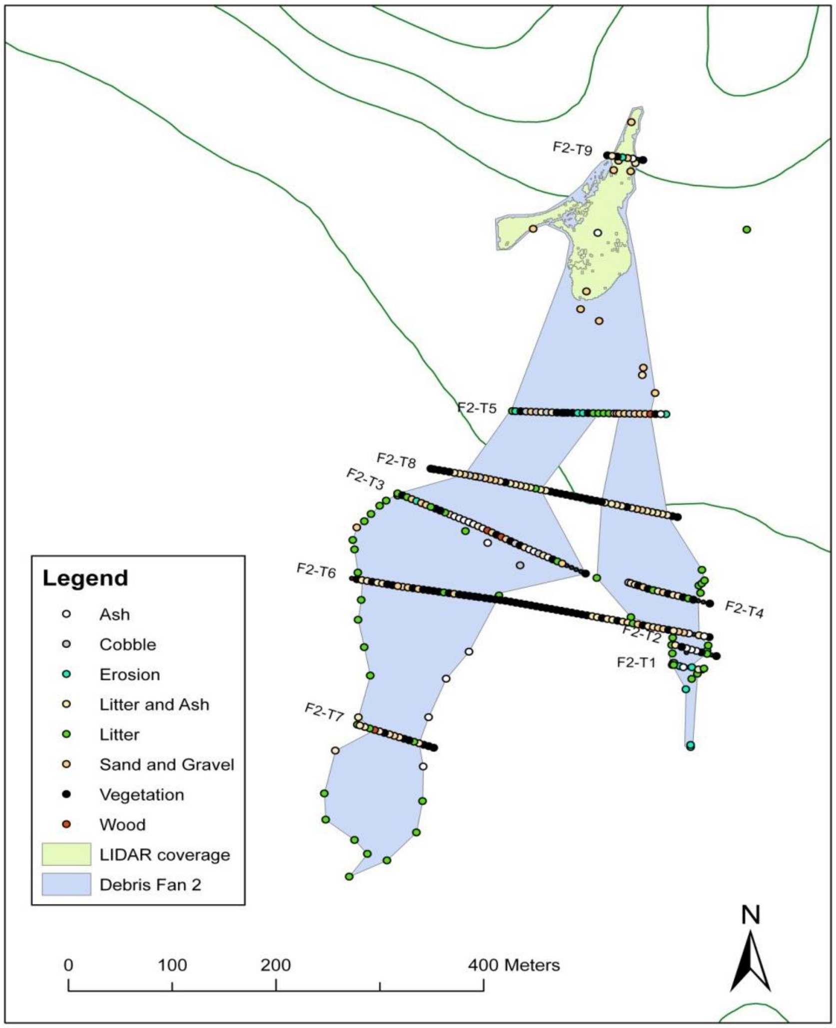

Figure 44. Example outline of debris fan in the JRB CZO site along with sampling locations for particulate organic matter (POM) content.

● **Seismic refraction mapping of soil thickness.** Regolith in the JRB site is commonly 3-5 m in some places, making traditional methods of measuring regolith thickness above bedrock difficult to use. Over 8 days in 2012, a team consisting of Pelletier, Johnson, and 5 students worked to acquire seismic reflection/refraction data along 7 seismic lines with 2.5 m horizontal resolution (e.g., Fig. 45). We acquired 2 cross-valley profiles each in La Jara, History Grove, and Upper Jaramillo, plus 1 in Banco Bonito for calibration (because many soil pits have been dug there coinciding with the seismic transects).
Seismic data were processed using ProMAX® (Halliburton Corp.) and SeisImager/2D (OYO Corporation/Geometrics) software. Survey geometries for each transect were entered into ProMAX® and

first breaks were picked for each shot record. First-break picks were exported as ASCII files from ProMAX® and used in a time-term inversion approach (using the Plotrefa module of SeisImager) in which three-layer velocity-depth profiles were generated by distinguishing the depths of prominent refractions; these time-term inversions constituted the starting models for further processing.

Network ray tracing and turning-ray tomography were performed through each starting model in order to distinguish lateral heterogeneities that the starting models alone could not properly represent (Sheehan et al., 2005). For our tomographic models, each velocity-depth cross-section was discretized into a grid of cells 2.5 meters wide by 0.2 meters high at the surface, increasing in grid height to 1.0 meters at the lower boundary. A total of 10-20 iterations of the inversion process for each model were completed with the goal of yielding a root-mean-square error of less than 3 ms, which is consistent with the 1- to 3-ms uncertainty associated with manually assigning first-break arrival times (Befus et al., 2011). A three-term, weighted moving-average smoothing filter was used in order to remove small-scale velocity artifacts that may otherwise have been interpreted as real. No vertical smoothing was applied within the inversion.

Our seismic work reveals variable depths to bedrock (defined as >= 3000 m/s) for each transect. The average depth of low-velocity material (< 600 m/s) is 0-2 meters for non-north-facing slopes, while low-velocity zones for north-facing slopes are greater, on the average of 4-5 meters. However, the Upper Lajara and Upper History Grove transects show much broader medium-velocity zones (> 600 and < 2500 m/s) than for corresponding north-facing drainages. The zones of increased soil thickness (< 600 m/s) for north-facing slopes confirms the hypothesis that north-facing slopes contain soils that are systematically deeper, with lower radiant forces causing the differences. Our results also confirm that soil development is influenced by mean water-transit time, which is a function of slope aspect. The steeper slopes in the Lower Lajara and Lower History Grove both contain thinner soils. These results are currently being prepared for submission as a peer-reviewed journal article.

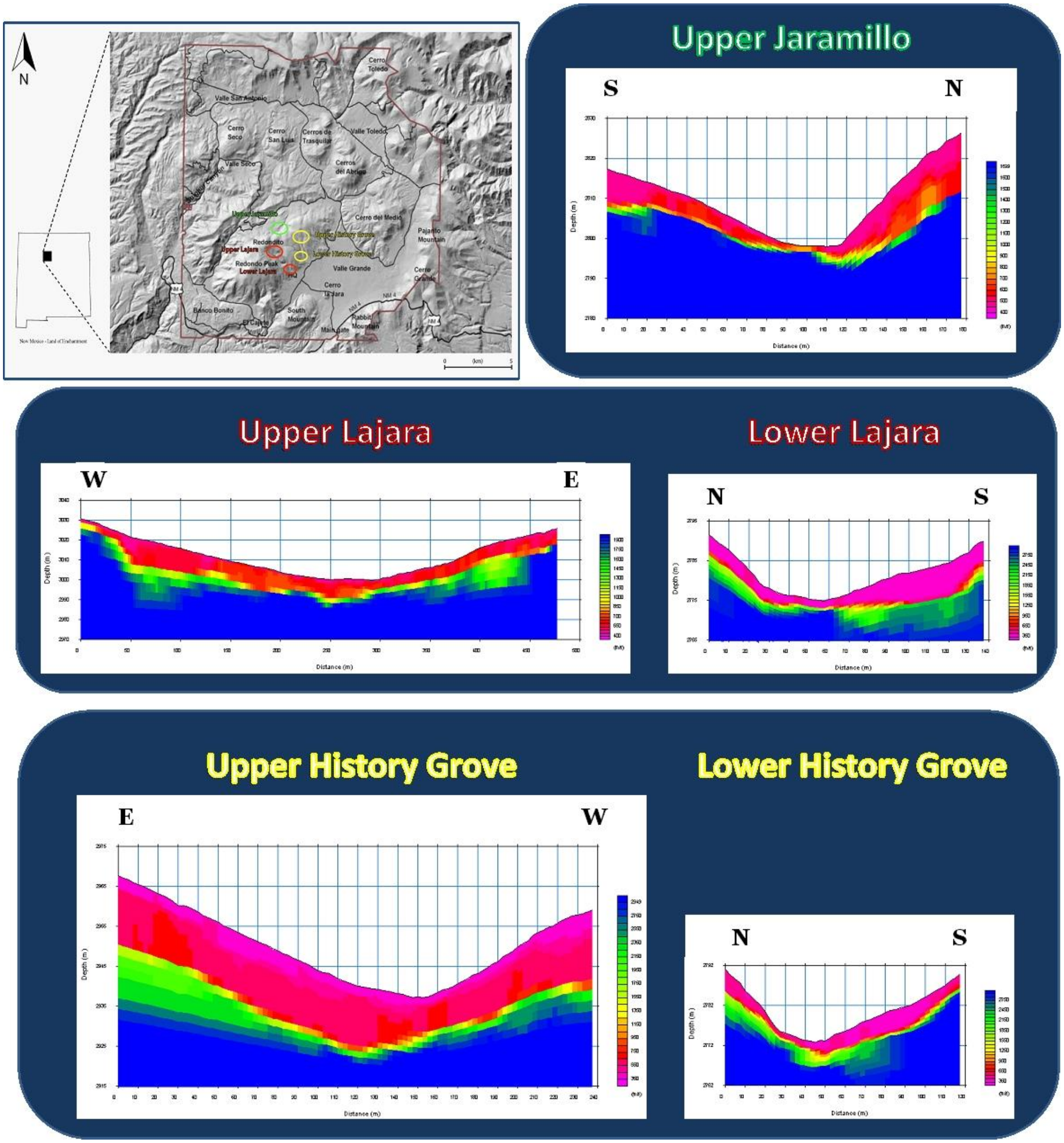

Figure 45. Best-fit P-wave velocity models from the seismic refraction surveys in the JRB. These data consistently show thicker regolith on south-facing slopes (in valleys, these are the northern slopes denoted by N). These data also provide crucial constraints on mathematical models of regolith production at the JRB site.

4. Data Management Activities

The JRB-SCM CZO data manager, Matej Durcik, participated in conference calls with other CZO data managers to design and test the national CZO website. After creating and entering the content of web pages, the JRB-SCM CZO website was switched to the new CZO website (http://criticalzone.org/jemez-catalina/) on April 18, 2013. Between August 1, 2012 and April 18, 2013, the old CZO web site had 1284 visits (5 visits per day on average) by 722 unique visitors from 45 different countries. The new CZO website had 3033 unique page views (22 unique page views per day) during the transition period (12/4/2012 – 4/18/2013) and 5006 unique page views (47 unique page views per day) after switching to the new website (4/18/2013 – 8/1/2013).

The JRB-SCM CZO data manager and investigators have actively participated in the development of the Integrated CZO Data System (CZOData) for the CZO network together with the CZO data development team (led by Anthony Aufdenkampe, Stroud Water Research Center) and data managers with the other CZOs. The main goal of CZOData is to integrate data between CZ disciplines and across the observatories (X-CZO). This approach should enable seamless data discovery and distribution across all CZOs for the entire scientific community. As a first step we designed and implemented data presentation and publication via the CZO website (http://criticalzone.org/jemez-catalina/data/) and these data pages were launched on May 31, 2013. Currently, we have published 35 datasets which are formatted in the CZO data and metadata formats. The data and metadata published on the CZO website will be harvested and stored in the CZO Central Database hosted by the SDSC and available for download via the CZO Central portal and CUAHSI Water Data Center (http://wdc.cuahsi.org/). Until now, more than 5 million data values out of more than 25 million values stored in the CZO ODM database have been harvested from the JRB-SCM CZO to the CZO Central Database. More new data are currently quality controlled and formatted to be published on the CZO website and harvested in upcoming year.

Additionally, our data manager participated in the ODM2 Design Workshop in the Lamont-Doherty Earth Observatory, Columbia University on July 30-31, 2013. Observation Data Model version 2 (ODM2) has been designed to better support additional data types, including water quality, solid earth, and geochemical samples. The development of ODM2 is supported by the NSF and CZO data management will benefit from this model in the way of storing, publishing and discovering data.

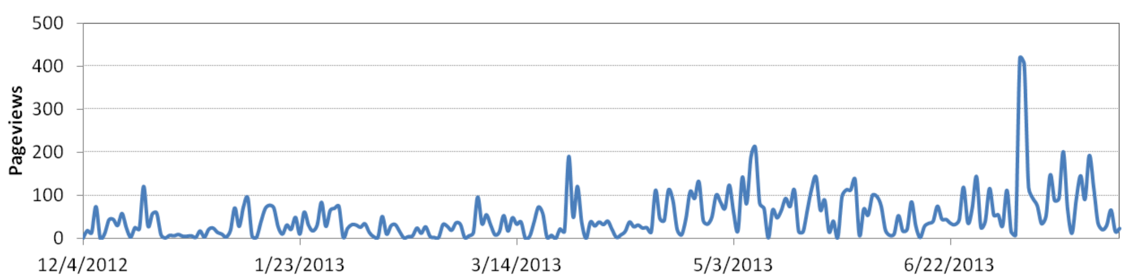

Figure 46. The number of daily page visits for the new CZO website.

5. Opportunities for Training, Development, and Mentoring Provided by the Project

The multiple graduate and undergraduate students involved in this project have gained invaluable field and laboratory skills, and research experience working as part of a large interdisciplinary team. In addition, funding of an REU site proposal at Biosphere 2 (B2) has provided excellent opportunities for collaboration with that program via undergraduate research experiences associated with the JRB-SCM CZO. Several B2 REU students were involved in CZO research during summers of 2010, 2011, 2012 and 2013 as described in "Personnel" section of this report. In addition to graduate and undergraduate training described in the activities and findings above, five postdoctoral scientists (Dr. Julia Perdrial, Dr. Adrian Harpold, Dr. Ciaran Harman, Dr. Bhaskar Mitra, and Dr. Jason Field) have also received training and mentorship experience as part of this grant.

Several undergraduate students have been employed on the CZO project to conduct a wide range of environmental, isotopic and geochemical analyses.

A summer intern and Northwestern University Undergraduate Earth Sciences major, Jessica Prescott-Smith, joined the CZO program for the summer 2012 (June 18th-August 24th) and focused on developing an independent research project in collaboration with Julia Perdrial, Michael Pohlmann and Jon Chorover entitled "Impact of storm events on stream water particulate and colloidal matter: resolving variation by colloid size fractionation." This summer project resulted in submission of an AGU fall 2012 meeting abstract.

The HWR 696G course entitled "Water-Rock-Microbial Interactions" taught by J. McIntosh utilized results from CZO research in integration of course topics.

Student research grants and awards that were leveraged by the JRB-SCM CZO include:
David Huckle - University of Arizona GPSC Travel Grant (2012) to present at AGU
Angelica Vasquez-Ortega – University of Arizona Institute of Environment Award for AGU travel
Rebecca Lybrand - University of Arizona Space Grant Scholarship for her CZO research

6. Outreach Activities Undertaken by the Project

The CZO project is developing a collaboration with the Biosphere 2 (B2), where CZO science and related findings will be displayed in conjunction with the B2-led "Landscape Evolution Observatory" (LEO) that involves conjunctive study of hydrologic, biogeochemical, and geomorphic process couplings in three replicated zero order basin hillslope models subjected to controlled environment inputs (http://leo.b2science.org/). The public display pertaining to LEO is going to focus on both LEO related activities and also complementary research occurring in CZO field sites. A large display at B2 currently presents a description of the National CZO program. Public displays at Biosphere 2 provide unique opportunites to reach a very large number of public visitors each year.

A wide array of information, including data, personnel and interpretive media are being uploaded regularly at the Jemez-Santa Catalina CZO website (http://criticalzone.org/jemez-catalina/).

7. Publications Resulting From Research

Published, Submitted and In Prep. Papers (since last report):

Adams H.A., Germino M.J., Breshears D.D., Barron-Gafford G.A., Guardiola-Claramonte M., Zou C.B., and Huxman T.E. (2013) Nonstructural leaf carbohydrate dynamics of Pinus edulis during drought-induced tree mortality reveal role for carbon metabolism in mortality mechanism. New Phytologist 197: 1142–1151. DOI: 10.1111/nph.12102.

Adams H.D., Luce C.H., Breshears D.D., Allen C.D., Weiler M., Hale V.C., Smith A.M.S., and Huxman T.E. (2012) Ecohydrological consequences of drought- and infestation- triggered tree die-off: insights and hypotheses. Ecohydrology 5: 145-159. DOI: 10.1002/eco.233.

Breshears D. D., Adams H. D., Eamus D., McDowell, N. G., Law D. J., Will R. E., and Zou C. B. (2013) The critical amplifying role of increasing atmospheric moisture demand on tree mortality and associated regional die-off. Frontiers in Plant Science 4:266.

Breshears D.D., Kirchner T.B., Whicker J.J., Field J.P., and Allen C.D. (2012): Modeling aeolian transport in response to succession, disturbance and future climate: Dynamic long-term risk assessment for contaminant redistribution . Aeolian Research, 3(4): 445-457. DOI: 10.1016/j.aeolia.2011.03.012.

Clifford M. J., Royer P. D., Cobb N. S., Breshears D. D., and Ford P. L. (2013) Precipitation thresholds and drought -induced tree die-off: Insights from patterns of Pinus edulis mortality along an environmental stress gradient. New Phytologist, doi: 10.1111/npn.12362.

Harpold, A.A., Biederman, J. A., Condon, K., Merino, M., Korgaondar, Y., Nan, T., Sloat, L., Ross, M., and Brooks, P.D. (2012) Changes in Snow Accumulation and Ablation Following the Las Conchas Forest Fire, New Mexico. USA Ecohydrology doi: 10.1002/eco.1363.

Harpold, A.A., Brooks, P.D., Perdrial, J., McIntosh, J., Meixner, T., Lohse, K.A., Zapata-Rios, X., Rios-Vasquez, A., and Chorover, J. (In Revision) Quantifying Variation in Solute Sources and Nutrient Cycling in Montane Headwater Catchments. Water Resour. Res.

Harpold, A.A., Brooks, P.D., Rajagopal, S., Heidüechel, I., Jardine, A., and Stielstra, C. (2012) Changes in Snowpack Accumulation and Ablation in the Intermountain West. Water Resources Research VOL. 48, W11501, doi:10.1029/2012WR011949.

Harpold, A.A., Guo, Q., Molotch, N., Brooks, P., Bales, R., Fernandez-Diaz, J.C., Musselman, K.N., Swetnam, T., Kirchner, P., Meadows, M., Flannagan, J., and Lucas, R. (in review) A LiDAR derived snowpack dataset from mixed conifer forests in the Western U.S. Water Resour. Res.

Heckman, K., Grandy, A.S., Gao, X., Keiluweit, M., Wickings, K., Carpenter, K., Chorover, J., and Rasmussen C. (2013) Sorptive fractionation of organic matter and formation of organo-hydroxy-aluminum complexes during litter biodegradation in the presence of gibbsite. Geochimica et Cosmochimica Acta. http://dx.doi.org/10.1016/j.gca.2013.07.043.

Heidbüchel, I., Troch, P.A., and Lyon, S.W. (re-review) Separating physical and meteorological controls on variable transit times in zero-order catchments. Water Resour. Res.

Heidbüchel, I., Troch, P.A., Lyon, S.W., and Weiler, M. (2012) The master transit time distribution of variable flow systems. Water Resour. Res., 48(6): W06520, doi: 10.1029/2011WR011293.

Huckle, D., Ma, L., McIntosh, J., Chorover, J., and Rasmussen, C. (in prep) Characterizing U-series isotope signatures in soils and headwater streams in a complex volcanic terrain: Valles Caldera, New Mexico. To be submitted to Chem. Geol.

Lockhart, J.S., Weber, C.F., Charaska, E., and Lohse, K.A. In review. Composition of distinct soil bacterial communities converges in initial response to wildfire. Soil Biology and Biochemistry.

Law D.J., Breshears D.D., Ebinger M.H., Meyer C.W., and Allen C.D. (2012) Soil C and N patterns in a semiarid pinon-juniper woodland: Topography of slope and ephemeral channels add to canopy-intercanopy heterogeneity. Journal of Arid Environments, 79: 20-24,. DOI: 10.1016/j.jaridenv.2011.11.029.

Lohse, K.A., Charaska, E., Brooks, P.D., and Chorover, J., (in prep) Influence of burn intensity and vegetation type on temporal dynamics of soil nitrogen pools and processes following wildfire. Ecosystems.

Lybrand, R.A. and Rasmussen, C. (in prep) Linking soil element-mass-transfer to microscale mineral weathering in the Santa Catalina Critical Zone Observatory. To be submitted to Chem. Geol.

Michelotti E.A., Whicker J.J., Eisele W.F., Breshears D.D., Kirchner T.B. (2013) Modeling aeolian transport of soil-bound plutonium: considering infrequent but normal environmental disturbances is critical in estimating future dose. Journal of Environmental Radioactivity 120: 73-80. DOI: 10.1016/j.jenvrad.2013.01.011.

Nelson, K., Kurc, S. A., John, G., Minor, R. and Barron-Gafford, G. A. (2013) Influence of snow cover duration on soil evaporation and respiration efflux in mixed-conifer ecosystems. Ecohydrol. doi: 10.1002/eco.1425.

Pelletier J. D. (2013) A robust, two-parameter method for the extraction of drainage networks from high-resolution Digital Elevation Models (DEMs): Evaluation using synthetic and real-world DEMs. Water Resources Research 49(1): 75–89. DOI: 10.1029/2012WR012452.

Pelletier J.D. and Perron J.T. (2012) Analytic solution for the morphology of a soil-mantled valley undergoing steady headward growth: Validation using case studies in southeastern Arizona. Journal of Geophysical Research, 117: F02018. DOI: 10.1029/2011JF002281.

Pelletier, J., Barron-Gafford, G., Breshears, D., Brooks, P., Chorover, J., Durcik, M., Harman, C., Huxman, T., Lohse, K., Lybrand, R., Meixner, T., McIntosh, J., Papuga, S., Rasmussen, C., Schaap, M., Swetnam, T., and Troch, P. (2013) Coevolution of nonlinear trends in vegetation, soils, and topography with elevation and slope aspect: A case study in the sky islands of southern Arizona. Journal of Geophysical Research: Earth Surface 118(2): 741-758. doi: 10.1002/jgrf.20046

Perdrial, J., McIntosh, J., Harpold, A., Brooks, P.D., Zapata-Rios, X., Porter, C., Ray, J., Troch, P., and Chorover, J. (In Revision) Impact of winter climate change and catchment aspect on carbon dynamics in snow-dominated headwater streams. Biogeochemistry.

Perdrial, J., McIntosh, J., Harpold, A., Brooks, P., Zapata-Rios, X., Ray, J., Meixner, T., Kanduc, T., Litvak, M., Troch, P., and Chorover, J. (accepted with revisions) Stream water carbon controls in seasonally snow-covered mountain catchments: impact of interannual variability of water fluxes, catchment aspect and seasonal processes. Biogeochemistry.

Perdrial J.N., Perdrial N., Harpold A., Gao X., Gabor R., LaSharr K., and Chorover J. (2012) Impacts of Sampling Dissolved Organic Matter with Passive Capillary Wicks Versus Aqueous Soil Extraction. Soil Science Society of America Journal, 76: 2019–2030. DOI: 10.2136/sssaj2012.0061.

Rasmussen C. and Gallo E.L. (2013) Technical Note: A comparison of model and empirical measures of catchment scale effective energy and mass transfer. Hydrology and Earth System Sciences Discussions, 10 (3), 3027-3044.

Rasmussen C. (2012): Thermodynamic constraints on effective energy and mass transfer and catchment function. Hydrology and Earth System Sciences 16(3): 725-739,. DOI: doi:10.5194/hessd-8-7319-2011.

Sankey J.B., Law, D.J., Breshears, D.D.,. Munson, S.M, and. Webb, R.H. (2013) Employing lidar to detail vegetation canopy architecture for prediction of aeolian transport. Geophysical Research Letters 40: 1724–1728. DOI: 10.1002/grl.50356.

Stielstra, C.M., Lohse, K.A., Chorover, J., McIntosh, J.C., Barron-Gafford, G., and Brooks, P.D. (in review) Climatic controls on soil carbon efflux in seasonally snow-covered forest ecosystems. Biogeochemistry.

Troch P.A., Carrillo, G., Sivapalan, M., Wagener, T., and Sawicz, K. (2013) Climate-vegetation-soil interactions and long-term hydrologic partitioning: signatures of catchment co-evolution. Hydrology and Earth System Sciences 17: 2209–2217. DOI: 10.5194/hess-17-2209-2013.

Vazquez-Ortega, A., Hernandez-Ruiz, S., Amistadi, M.K., and Chorover, J. (in review) Fractionation of dissolved organic matter by (oxy)hydroxide-coated quartz sands: Competitive sorbate displacement during reactive transport. Submitted to a special issue of Vadose Zone Journal.

Vazquez-Ortega, A., Perdrial, J., Harpold, A., Zapata, X., Rasmussen, C., McIntosh, J., Schaap, M., Pelletier, J.D., Amistadi, M.K., and Chorover, J. (in prep) Rare earth elements as reactive tracers of biogeochemical weathering in forested rhyolitic terrain. To be submitted to Geochim. Cosmochim. Acta.

Vazquez-Ortega, A., Perdrial, J., Huckle, D., Rasmussen, C., Amistadi, M.K., McIntosh, J., and Chorover, J. (in prep) Redistribution of rare earth elements and yttrium (REY) in topographically distinct, rhyolite-derived pedons. To be submitted to Geoderma.

Zapata-Rios, X., Troch, P., McIntosh, J., Broxton, P., Harpold, A., Litvak, M., Brooks, P. (in review) Hydrological response of semi-arid mountain catchments to changes in winter precipitation. Hydrol. Process.

<u>Masters and Ph.D. Theses:</u>

Condon, K. 2013. "Quantifying Catchment-Scale Particulate Organic Matter (Pom) Loss Following Fire, Relative To Background Pom Fluxes", MS Thesis, Hydrology and Water Resources, University of Arizona.

Jardine, A. 2011. "Aqueous phase tracers of chemical weathering in a semi-arid critical zone", MS Thesis, Hydrology and Water Resources, University of Arizona.

Heidbüchel, I. 2013. "On the Variability of Hydrologic Catchment Response: Inherent and External Controls", Ph.D. Dissertation, Hydrology and Water Resources, University of Arizona.

Holleran, M. 2013. "Quantifying catchment scale soil variability in Marshall Gulch, Santa Catalina Mountains Critical Zone Observatory", MS Thesis, Soil, Water and Environmental Science, University of Arizona.

Huckle, D. 2013. "Characterizing U-series isotope signatures in soils and headwater streams in a complex volcanic terrain: Jemez River Critical Zone Observatory, Valles Caldera, NM", MS Thesis, Hydrology and Water Resources, University of Arizona.

Mahmood T.H. 2012. "Hillslope Scale Hydrologic Spatial Patterns in a Patchy Ponderosa Pine Landscape: Insights from Distributed Hydrologic Modeling", PhD Thesis, School of Earth and Space Exploration, Arizona State University.

Nelson, K. 2011. "The Influence of Snow Cover Duration on Evaporation and Soil Respiration in Mixed-Conifer Ecosystems", MS Thesis, School of Natural Resources and Environment, University of Arizona.

Porter, C. 2012. "Solute inputs to soil and stream waters in a seasonally snow-covered mountain catchment determined using Ge/Si, 87Sr/86Sr and major ion chemistry: Valles Caldera, New Mexico", MS Thesis, Hydrology and Water Resources, University of Arizona.

Stielstra C.M. 2012. "Quantifying the role of hydrologic variability in soil carbon flux", MS Thesis, Hydrology and Water Resources, University of Arizona.

Vazquez-Ortega, A. 2013. "Coupled transport, fractionation and stabilization of dissolved organic matter and rare earth elements in the critical zone". Ph.D. Dissertation, Soil, Water and Environmental Science, University of Arizona.

<u>Presentations:</u>

Barron-Gafford, G.A., R.L. Minor, Z. Braun, and D.L. Potts, Ecohydrological responses of a model semiarid system to precipitation pulses after a global change type dry-down depend on growth-form, event size, and time since establishment. Annual Conference of the American Geophysical Union, Dec. 4-10, 2012, San Francisco, CA.

Biederman J.A., A.A. Harpold, P.D. Broxton, P.D. Brooks (2012) The shifting nature of vegetation controls on peak snowpack with varying slope and aspect. Abstract C33D-0685 presented at 2012 Fall Meeting, AGU, San Francisco, Calif., 3-7 Dec.

Braun, Z., R.L. Minor, Potts, D.L., and G.A. Barron-Gafford, Quantifying thermal constraints on carbon and water fluxes in a mixed-conifer Sky Island ecosystem. Annual Conference of the American Geophysical Union, Dec. 4-10, 2012, San Francisco, CA.

Breshears D. D., Drought-induced tree die-off: An overview and update on patterns, mechanisms, and consequences. The University of Arizona SWES Colloquium, Nov. 5, 2012, The University of Arizona, Tucson, AZ.

Brooks, P.D., A. Harpold, J. A. Biederman, M. Litvak, D. Gocis, P. Broxton, E. Gutmann, N. Molotch, P. Troch, and B. Ewers, Plenary Speaker, Climate change and forest disturbance effects on western forests. Utah State University Spring Runoff Symposium, April 8-10, 2013, Logan, UT.

Brooks, P.D., A. Harpold, J.A. Biederman, M. Litvak, D. Gocis, P. Broxton, E. Gutmann, N. Molotch, P. Troch, and B. Ewers, Insects, Fires, and Climate Change: Implications for Snow Cover, Water Resources and Ecosystem Recovery in Western North America. Conference of the American Geophysical Union, Dec. 4-10, 2012, San Francisco, CA.

Charaska, E., K.A. Lohse, C. Weber, P. Brooks, and J. Chorover. Nitrogen cycling in post-fire soils across a burn intensity gradient. Rocky Mountain Geological Society of America, May 7-10 2012, Albuquerque, NM.

Charaska, E., K. Lohse, C. Strielstra, P. Brooks, and J. Chorover, Controls of EEMT on DOC and nutrient losses from the Jemez River Basin. NSF CZO All Hands Meeting, May 8-10, 2011, Biosphere 2, Oracle, AZ.

Chorover, J., Anderson, S.P., Bales, R.C., Duffy, C., Scatena, F.N., Sparks, D.L., and White, T. (2012): Critical Zone Observatories (CZOs): Integrating measurements and models of Earth surface processes to improve prediction of landscape structure, function and evolution (Invited). Abstract GC54A-05 presented at 2012 Fall Meeting, AGU, San Francisco, Calif., 3-7 Dec.

Chorover, J., P. Brooks, A. Harpold, M. Litvak, J. McIntosh, J. Pelletier, J. Perdrial, P. Troch, C. Rasmussen. 2013. Critical zone evolution by jerks (Keynote). Presented at the 2013 Goldschmidt Geochemistry Conference, Florence, Italy, 24-30 August.

Driscoll, J.M., A. Harpold, J.C. McIntosh, T. Meixner, X.E. Zapata-Rios, C.M. Porter, R. Lybrand, D. Zaharescu, and D. Huckle, Chemical weathering and solute flux in the critical zone: catchment-scale hydrology in the Jemez River Basin at the Valles Caldera, NM. 2012 GSA Rocky Mountain Regional Meeting, May 9-11, 2012, Albuquerque, NM.

Driscoll J.M., N.P. Molotch, S.M. Jepsen, T. Meixner, M.W. Williams, J.O. Sickman (2012) Hydrologic response to modeled snowmelt input in alpine catchments in the Southwestern United States. Abstract H51B-1336 presented at 2012 Fall Meeting, AGU, San Francisco, Calif., 3-7 Dec.

Harpold, A., P. Brooks, J. Perdrial, J. McIntosh, T. Meixner, X. Zapata, and J. Chorover, Quantifying variation in solute sources and nutrient cycling in montane headwater catchments. Conference of the American Geophysical Union, Dec. 4-10, 2012, San Francisco, CA.

Harpold, A.A., P.D. Brooks, J.N. Perdrial, J.C. McIntosh, T. Meixner, X. Zapata, and J. Chorover, Quantifying variation in solute sources in montane headwater catchments. Conference of the American Geophysical Union, Dec. 4-10, 2012, San Francisco, CA.

Harpold, A.A., P.D. Brooks, J.A. Biederman, and D. Gochis, Snowpack following forest disturbance: Implications for negative feedbacks on water availability. MTNCLIM Conference, Oct. 1-4, 2012, Estes Park, CO.

Harpold, A.A., P.D. Brooks and J.A. Biederman, Changes in snow accumulation and ablation following the Las Conchas forest fire, NM. CUASHI Biennial Meeting, July 16-18, 2012, Boulder, CO.

Harpold, A.A., N.P. Molotch, and D.R. Gochis. Doing Big Science With Big Data: Preliminary Ecohydrologic Investigations at the Western CZO Sites. EarthCUBE Meeting, Jan. 23, 2013, Newark, DE.

Heidbuechel I., P. A. Troch (2012) What controls the shape of transit time distributions? Abstract H31B-1117 presented at 2012 Fall Meeting, AGU, San Francisco, Calif., 3-7 Dec.

Holleran, M. and C. Rasmussen, Quantifying Catchment Scale Soil Variability in Marshall Gulch, Santa Catalina Mountains Critical Zone Observatory. Annual Conference of the Soil Science Society of America, Oct. 21-24, 2012, Cincinnati, OH.

Holleran, M. and C. Rasmussen, Quantifying catchment scale soil variability in Marshall Gulch, Santa Catalina Mountains Critical Zone Observatory. Annual Conference of the American Geophysical Union, Dec. 4-10, 2012, San Francisco, CA.

Huckle, D., L. Ma, J. McIntosh, C. Rasmussen, and J. Chorover, Using uranium-series isotopes to trace water sources to streamflow and estimate soil formation rates in a semiarid montane catchment. Annual Conference of the American Geophysical Union, Dec. 4-10, 2012, San Francisco, CA.

Huxman T. E., R.L Scott, G.A. Barron-Gafford, E.P. Hamerlynck, D. Jenerette, D.T. Tissue, D.D. Breshears, and S.R. Saleska, Understanding the biological underpinnings of ecohydrological processes. Annual Conference of the American Geophysical Union, Dec. 4-10, 2012, San Francisco, CA.

Lohse, K.A. E. Charaska, P. Brooks, and J. Chorover, Influence of burn intensity and vegetation type on recovery of soil nitrogen cycling. Ecological Society of America, Aug 4-9, 2013, Minneapolis, MN.

Lohse, K.A., E. Charaska, P. Brooks, C. Rasmussen, and J. Chorover, Soil carbon and nitrogen cycling in the Valles Caldera, NM: Initial responses to the Las Conchas fire. Tri-State EPSCoR Annual Meeting, April 2-6, 2012, Sun Valley, ID.

Lybrand, R.A. and C. Rasmussen, Quantifying Mineral Transformations in Granitic Terrain Across the Santa Catalina Mountain Environmental Gradient. Annual Conference of the Soil Science Society of America, Oct. 21-24, 2012, Cincinnati, OH.

Lybrand, R. and C. Rasmussen, Soils of the Santa Catalina Mountains. University of Arizona's Institute of the Environment Grad Blitz Program, Nov. 8, 2012, Tucson, AZ.

Lybrand, R. and C. Rasmussen. Soils of the Santa Catalina Mountains of southern Arizona. University of Arizona's Graduate and Professional Student Council (GPSC) Student Showcase, Nov. 9, 2012, Tucson, AZ.

Lybrand, R.A. and C. Rasmussen, Linking soil element-mass-transfer to microscale mineral weathering in the Santa Catalina Critical Zone Observatory. Annual Conference of the American Geophysical Union, Dec. 4-10, 2012, San Francisco, CA.

Lybrand, R., and C. Rasmussen, Soil development along an environmental gradient in the Santa Catalina Mountains, AZ. In Abstracts, International Annual Meeting, ASA-CSSA-SSSA, Nov. 3-6, 2013, Tampa, FL.

Lybrand, R., K. Heckman, and C. Rasmussen, Climate and topographic controls on soil organic carbon cycling in southern Arizona, USA. In Abstracts, Goldschmidt 2013, Aug. 25-30, 2013, Florence, Italy.

Lybrand, R., K. Heckman, and C. Rasmussen. Soil carbon cycling along the Santa Catalina Mountain Critical Zone Observatory. In Abstracts, Western Society of Soil Science Meeting, July 22-23 2013, Tucson, AZ.

Lybrand, R., K. Heckman, and C. Rasmussen. The interactive effects of climate and landscape position on soil organic carbon cycling in southern Arizona. In Abstracts, University of Arizona's EarthWeek Conference, April 11, 2013, Tucson, AZ.

Meixner, T., How water, carbon and energy drive evolution of the Critical Zone: The Jemez-Santa Catalina Critical Zone Observatory. Johns Hopkins University, Sept. 26, 2012, Baltimore MD.

Meixner, T., How water, carbon and energy drive evolution of the Critical Zone: The Jemez-Santa Catalina Critical Zone Observatory. University of Delaware Department of Plant and Soil Sciences, Oct. 5, 2012, Newark, DE.

Meixner, T., How water, carbon and energy drive evolution of the Critical Zone: The Jemez-Santa Catalina Critical Zone Observatory. Cary Institute of Ecosystem Studies, Oct. 8, 2012, Millbrook, NY.

Meixner, T., How water, carbon and energy drive evolution of the Critical Zone: The Jemez-Santa Catalina Critical Zone Observatory. Pennsylvania State University CZO group, Oct. 25, 2012, University Park, PA.

Mitra, B. and S.A. Papuga, Toward an improved understanding of the role of transpiration in critical zone dynamics. Annual Conference of the American Geophysical Union, Dec. 4-10, 2012, San Francisco, CA.

Molotch, N.P., Musselman, K.N., Kirchner, P.B., Bales, R.C., and Brooks, P.D. (2012): Effects of forest structure on snow accumulation and melt derived from ecohydrological instrument clusters across the Western US Abstract C33D-0684. Annual Conference of the American Geophysical Union, Dec. 4-10, 2012, San Francisco, CA.

Niu G., P.A. Troch, C. Paniconi, X. Zeng, R.L. Scott, T.E. Huxman, J.D. Pelletier (2012) An Integrated Model Framework of Catchment-Scale Ecohydrological Processes. Abstract H33F-1385 presented at 2012 Fall Meeting, AGU, San Francisco, Calif., 3-7 Dec.

Ochoa, M. B., C. Logie, E. D. Reynoso, D.J. Law, J.P. Field, D.D. Breshears, and S.Archer, Determining a new dryland decomposition input term: Rainfall simulated fluvial redistribution of sediment to litter surfaces. The University of Arizona, Latin America Summer Research Program, Organized Oral Session, Aug. 2, 2013, The University of Arizona, Tucson, AZ.

Ochoa, M. B., C. Logie, E.D. Reynoso, D.J. Law, J.P. Field, D.D. Breshears, and S. Archer, Determining a new dryland decomposition input term: Rainfall simulated fluvial redistribution of sediment to litter surfaces. The University of Arizona, Latin America Summer Research Program, Organized Poster Session, Aug. 6, 2013, The University of Arizona, Tucson, AZ.

Perdrial, J.N., C. Rasmussen, J.C. McIntosh, X. Zapata-Rios, A. Harpold, A. Vazquez-Ortega, C. Porter, P.D. Brooks, T. Meixner, B. Mitra, P.A. Troch, and J. Chorover, Carbon and water, the energy for weathering and chemical denudation. Annual Conference of the American Geophysical Union, Dec. 4-10, 2012, San Francisco, CA.

Pohlmann M. A., J. N. Perdrial, J. Prescott-Smith, M. Amistadi, P. A. Troch, J. Chorover (2012) Resolving dissolved versus colloidal and particulate weathering product forms across the storm hydrograph. Abstract EP43A-0867 presented at 2012 Fall Meeting, AGU, San Francisco, Calif., 3-7 Dec.

Porter, C., J. McIntosh, L. Derry, T. Meixner, J. Chorover, P. Brooks, C. Rasmussen, and J. Perdrial, Determining solute inputs to soil and stream waters in a seasonally snow-covered mountain catchment in northern New Mexico using Ge/Si, 87Sr/86Sr and ion chemistry. Annual Conference of the American Geophysical Union, Dec. 4-10, 2012, San Francisco, CA.

Potts, D.L., R.L. Minor, Z. Braun, and G.A. Barron-Gafford, Species-specific and seasonal differences in chlorophyll fluorescence and photosynthetic light response among three evergreen species in a Madrean sky island mixed conifer forest. Annual Conference of the American Geophysical Union, Dec. 4-10, 2012, San Francisco, CA.

Prescott-Smith J., M. A. Pohlmann, J. N. Perdrial, N. Perdrial, P. A. Troch, J. Chorover (2012) Does the composition of streamwater colloidal and particulate matter change during monsoon storms? Abstract EP43A-0866 presented at 2012 Fall Meeting, AGU, San Francisco, Calif., 3-7 Dec.

Rasmussen, C., Quantifying the Energetics of Pedogenesis Using Thermal Analysis. Annual Conference of the Soil Science Society of America, Oct. 21-24, 2012, Cincinnati, OH.

Rasmussen C., S.M. Meding, A. Vazquez, and J. Chorover, EP42D-04, Domes, Ash and Dust – Controls on soil genesis in a montane catchment of the Valles Caldera, New Mexico. Annual Conference of the American Geophysical Union, Dec. 4-10, 2012, San Francisco, CA.

Reynoso E. D., C. Logie, M. B. Ochoa, D. J. Law, J.P. Field, D.D. Breshears and S. Archer, Determining a new dryland decomposition input term: Natural events of aeolian and fluvial redistribution of sediment to litter surfaces. Organized Poster session, Research Experience for Undergraduates, Biosphere 2 REU Program, Aug. 6, 2013, The University of Arizona, Tucson, AZ.

Smettem K., D.D. Breshears, and M. Waddington, Observations on the development of ecohydrology as a discipline: History and future opportunities. European Geophysical Union, Apr. 25, 2012, Vienna, Austria.

Stielstra, C., P.D. Brooks, J. Chorover, and K. Lohse. 2011. Monitoring carbon fluxes from shallow surface soils in the critical zone, Abstract B33G-0556. Conference of the American Geophysical Union, Dec. 5-9, 2011, San Francisco, CA.

Swetish, J., S.A. Papuga, M. Litvak, G. Barron-Gafford, and B. Mitra. Influence of understory greenness on trace gas and energy exchange in forested ecosystems. Annual Conference of the American Geophysical Union, Dec. 4-10, 2012, San Francisco, CA.

Vazquez A., J. N. Perdrial, A. A. Harpold, X. Zapata, C. Rasmussen, J. C. McIntosh, M. G. Schaap, J. D. Pelletier, M. Amistadi, J. Chorover (2012) Rare earth elements as reactive tracers of biogeochemical weathering in the Jemez River Basin Critical Zone Observatory. Abstract H53I-1651 presented at 2012 Fall Meeting, AGU, San Francisco, Calif., 3-7 Dec.

Zapata, X., P. Troch, J. McIntosh, P. Broxton, and P. Brooks, The effect of terrain aspect on interannual variability of hydrologic response in mountainous catchments in New Mexico. Annual Conference of the American Geophysical Union, Dec. 4-10, 2012, San Francisco, CA.

Zapata, X., J.C. McIntosh, A. Sorooshian, K.A. Lohse, P.D. Brooks, P.A. Troch, J. Chorover, and I. Heidbuechel, Sources and amounts of nitrogen deposited in sky-island ecosystems, Abstract B13G-0652. Conference of the American Geophysical Union, Dec. 5-9, 2011, San Francisco, CA.

Other:

Harpold, A.A. and T.S. White, Exploring the Critical Zone with LiDAR. American Geosciences Institute handout for K-12 teachers. Available at: http://criticalzone.org/national/publications/pub/harpold-agi-lidar-handout/

8. Contributions to within Discipline

As described in detail above, ongoing research in multiple coordinated projects is resulting in substantive, peer-reviewed contributions within the fields of ecology, geochemistry, hydrology, and geomorphology. These disciplinary contributions are strengthened by the inter-disciplinary linkages that are being made to allied disciplines via cross-cutting CZO science themes. Within field contributions include:

- Quantifying vegetation-topography interactions at hillslope scales
- Understanding winter-to-summer transitional periods in forested regions
- Quantifying the role of forest disturbance on snow water balance
- Understanding vegetation demography across complex terrain in the critical zone
- Relating contemporaneous fluxes of carbon and water to geochemical weathering extent
- Measuring the impacts of major disturbance (wildfire) on landscape evolution
- Using a variety of stable and radiogenic isotopes and solutes to measure water transit time

9. Contributions to Resources for Research and Education

In so far as the principal intent of the CZOs is to establish natural laboratories for use by the broader earth sciences community, we have made significant progress in this respect through installations of sampling equipment and sensors in the SCM at low, intermediate and high elevation sites, and intensive instrumentation array in the JRB at high elevation (mixed conifer) burned and unburned sites.

The JRB-SCM CZO is coordinating with the Biosphere 2 REU/RET site to provide an exciting venue for their earth system sciences summer research program. Several of the CZO investigators hosted REU/RET students in their lab groups during summers of 2011-2013 focusing on CZO research.